

**FAILURE ANALYSIS REPORT:
SULPHUR MINES SALT DOME
CAVERN NO. 006 & NO. 007 AS OF
MARCH 23, 2023
OPERATOR: EAGLE US 2, LLC**

Author: Lonquist Field Service, LLC (LA Firm License No. EF5853)

Friday, May 5, 2023

SULPHUR MINES PPG CAVERN NO. 007**FAILURE ANALYSIS REPORT****TABLE OF CONTENTS**

1	Introduction	1
2	Sulphur Dome History & Introduction to Caverns.....	2
3	Cavern Integrity Failure Mechanisms	14
3.1	Introduction & Definitions.....	14
3.2	Cavern Integrity Failure Mechanisms.....	14
3.2.1	Roof Fall / Rock Fall / Cavern Breach	14
3.2.2	Hydraulic Connection / Cavern Coalescence	14
3.2.3	Wellbore or Wellhead Leak.....	15
3.2.4	Surface Expression / Sinkhole	15
4	Cavern Integrity Evaluation Variables	16
4.1	Injection / Withdrawal Operations.....	16
4.2	Cavern Creep Closure	16
4.3	Brine Thermal Expansion / Contraction and Ground Temperature Variations	16
4.4	Dissolution / Crystallization.....	17
4.5	Micro-permeation	17
4.6	Wellbore or Cavern Leak	17
4.7	Earth Tides Effects and Barometric Pressure Variations.....	17
5	Examples of Cavern Integrity Failure Incidents	18
5.1	Louisiana Offshore Oil Platform (LOOP) Cavern No. 14	18
5.2	Starks PPG No. 008	18
5.3	Bayou Corne/Oxy-Geismar Cavern No. 003	19
6	Cavern 7 History and Geologic Structure	20
6.1	Historical Timeline (Major Events)	20
6.2	Distance to Salt Dome Flank.....	20
6.3	Notable Workover, Inspection, and Sonar History	22
6.4	Wellbore Diagrams.....	23
7	Cavern No. 007 Integrity Failure Pressure Analysis.....	26
7.1	Cavern No. 007 Acute Pressure Loss Event	26
7.2	Cavern No. 007 Pressure History.....	27
7.2.1	Cavern Compressibility Determination	28
7.2.2	Cavern Build Rate Determination	29
7.2.3	Oil Withdrawals.....	30
7.3	Fluid Loss Calculations.....	31
7.3.1	Estimated Fluid Loss.....	31
7.3.1.1	September 1, 2021 – May 18, 2022.....	32
7.3.1.2	May 18, 2022 – August 22, 2022	35

7.3.1.3	August 23, 2022 – March 23, 2023	37
7.4	Summary of Cavern 7 Pressure Loss Event and Estimated Fluid Loss.....	44
8	Cavern 6 History & Geologic Structure.....	46
8.1	Historical Timeline (Major Events)	46
8.2	Distance to Salt Dome Flank.....	47
8.3	Cavern 6 Distance to Cavern 7	48
8.4	Notable Workover, Inspection, and Sonar History	51
8.5	Wellbore Diagrams.....	52
9	Cavern 6 Integrity Failure Pressure Analysis	55
9.1	Pressure History.....	55
9.2	Fluid Loss Calculation	56
10	Post-Failure Evaluation & Monitoring.....	58
10.1	Monitoring.....	58
10.1.1	Surface Observations/Monitoring	58
10.1.2	Wellhead & Downhole Pressure Monitoring.....	58
10.1.3	Surface Seismic Monitoring Stations / Downhole Seismic Geophones.....	58
10.1.3.1	Phase 1: Temporary Surface Seismic Array	58
10.1.3.2	Phase 2: Semi-Permanent Surface Seismic Array.....	59
10.1.3.3	Phase 3: Borehole Seismic Network	60
10.1.4	InSAR Enhanced Monitoring	66
10.1.4.1	Methodology.....	66
10.1.4.2	Data Properties	66
10.1.4.3	Data Frequency	67
10.1.4.4	Subsidence Monitoring Areas of Interest (AOIs)	70
10.1.4.5	Continuous Monitoring and Evaluation Plan.....	71
10.1.5	Periodic Sonar Surveys.....	72
10.1.6	Sampling of Groundwater, Surface Water, Oil & Gas, Bubbles	73
10.1.6.1	Groundwater.....	73
10.1.6.2	Surface Water	76
10.1.6.3	Oil and Gas	78
10.1.7	Aerial Thermal Imaging	80
10.1.7.1	Data Collection.....	80
10.1.7.2	Data Processing.....	80
10.2	Evaluation	81
10.2.1	Current Geologic Understanding and Further Evaluation	81
10.2.2	Vertical Seismic Profile.....	83
10.2.3	Magnetometer Survey	84
10.2.4	Geomechanics Modeling.....	84
10.2.4.1	Background	85
10.2.4.2	Methodology.....	85
10.2.4.3	Reporting.....	87
11	Theoretical Failure Mechanisms & Associated Impacts.....	88

11.1	Continued Loss of Brine to Adjacent Formation	88
11.1.1	Geomechanical Stresses.....	88
11.1.2	Adjacent Mineral Production Impacted.....	89
11.1.3	Impact to USDW	89
11.2	Cavern Coalescence.....	90
11.3	Cavern-To-Flank Pillar Failure with Associated Surface Expression.....	91
11.3.1	Geomechanical Stresses.....	91
11.3.2	Adjacent Mineral Production Impacted.....	92
11.3.3	Impact to USDW	93
11.3.4	Offset Wellbore Damage / Blowout.....	93
11.3.5	Surface Environmental Impact.....	93
11.3.6	Surface Expression Impact Zone Estimate	94
12	Concluding Remarks	98
13	References	101

Figures

Figure 1	– Regional Landmarks Map.....	3
Figure 2	– Satellite Image of Sulphur Mines Dome Contours and Proximal Landmarks	4
Figure 3	– Satellite Image of Sulphur Mines Dome Contours and All Salt Caverns	5
Figure 4	– Plan View Color Coded Image of All Salt Caverns in Sulphur Mines Dome	6
Figure 5	– Side View Color Coded Image of All Salt Caverns in Sulphur Mines Dome	7
Figure 6	– Cross Section Through Fee 1012 and PPG 6 & 7	9
Figure 7	– Aerial View of Seismic Cross Section Through Fee 1012 and PPG 6 & 7	10
Figure 8	– Perspective View of Caverns 6 and 7 from South and East	11
Figure 9	– Side View of Caverns 6 and 7 from East-Southeast	11
Figure 10	– Perspective View of Caverns 6 and 7 from East-Southeast	12
Figure 11	– Perspective View of Caverns 6 and 7 from North	13
Figure 12	– Cavern No. 007 Timeline (Major Events)	20
Figure 13	– Cavern 7 Minimum 3D Distance to Salt Dome Flank	21
Figure 14	– As-Built Wellbore Diagram of PPG 007A.....	23
Figure 15	– As-Built Wellbore Diagram of PPG 007B.....	24
Figure 16	– As-Built Wellbore Diagram of PPG 007C.....	25
Figure 17	– Cavern 7 Recorded Pressure During Acute Pressure Loss Event	26
Figure 18	– Cavern 7 Cumulative Pressure Loss Recorded During Acute Pressure Loss Event	27
Figure 19	– Cavern 7 Pressure History, November 15, 2020, Forward.....	28
Figure 20	– Cavern 7 Compressibility Determination Trendline.....	29
Figure 21	– Cavern 7 Build Rate Calculation Against Measured Historical Pressures	30
Figure 22	– Example Leak Volume Calculation	32
Figure 23	– Cavern 7 Historical Pressure from September 1, 2021, to June 1, 2022	33
Figure 24	– Cavern 7 Estimated Leak Rate from September 1, 2021, to May 18, 2022.....	35
Figure 25	– Cavern 7 Historical Pressure and Oil Withdrawals from May 18, 2022, to August 22, 2022	36

Figure 26 – Cavern 7 Estimated Leak Rate from May 18, 2022, to August 22, 202237

Figure 27 – Cavern 7 Historical Pressure and Oil Withdrawals from August 23, 2022, to March 23, 2023.....38

Figure 28 – Cavern 7 Historical and Estimated Pressures with Periodic Injection from August 23, 2022, to January 5, 202338

Figure 29 – Cavern 7 Historical and Estimated Pressures and Periodic Injection from August 23, 2022, to January 5, 202340

Figure 30 – Cavern 7 Historical and Estimated Pressures with Periodic and Continuous Injection from January 5, 2023, to March 23, 2023.....41

Figure 31 – Cavern 7 Estimated Leak Rate from August 23, 2022, to March 23, 202343

Figure 32 – Cavern No. 007 Cumulative Leak Volume from September 1, 2021, to March 23, 202345

Figure 33 – Cavern 6 Timeline (Major Events)46

Figure 34 – Cavern 6 Minimum 3D Distance to Salt Dome Flank47

Figure 35 – Plan view of Cavern 6 and Cavern 748

Figure 36 – Perspective view of Cavern 6 and Cavern 7 showing minimum web thickness49

Figure 37 – Side view of Cavern 6 and Cavern 750

Figure 38 – As-Built Wellbore Diagram of PPG 006X52

Figure 39 – As-Built Wellbore Diagram of PPG 006Y53

Figure 40 – As-Built Wellbore Diagram of PPG 006Z54

Figure 41 – Measured Tubing Pressure History for Cavern 6 & Cavern 755

Figure 42 – Cavern 6 Estimated Leak Rate from September 1,2021 to March 23, 202357

Figure 43 – Temporary Seismic Recording Station Locations at Sulphur Mines Salt Dome. Station Locations as Of Feb 27, 2023 As Provided By Eagle.....59

Figure 44 – Example of a JDS Pole-Mounted Seismic Station.....60

Figure 45 – Proposed Geophone Locations62

Figure 46 – Proposed Geophone Location East-West Cross-Section Uncertainty Modeling63

Figure 47 – Proposed Geophone Location North-South Cross-Section Uncertainty Modeling64

Figure 48 – Proposed Geophone Location East-West Cross-Section Magnitude Sensitivity Modeling65

Figure 49 – Proposed Geophone Location North-South Cross-Section Magnitude Sensitivity Modeling65

Figure 50 – InSAR Image Collection Frequency, Satellite Data Parameters and Orbit Visualization 69

Figure 51 – SNT and TSX InSAR Measurement Points.....70

Figure 52 – InSAR Areas of Interest (AOIs).....71

Figure 53 – Known Active Water Well Locations74

Figure 54 – Surface Water Sampling Locations.....77

Figure 55 – Sulphur Mines Fee #1016 VSP Salt Proximity Survey.....84

Figure 56 – Known Active Water Well Locations Adjacent to PPG Cavern No. 00790

Figure 57 – Example of Cavern Collapse Surface Features94

Figure 58 – Side View of Oxy 395

Figure 59 – Top View of Oxy 3.....96

Figure 60 – Side View of Cavern 7.....97

Figure 61 – Top View of Cavern 7 w/ Theoretical Sink Hole Projection98

Tables

Table 1 – All Salt Caverns in Sulphur Mines Dome8
 Table 2 – Workover, Inspection, & Sonar History of Cavern No. 007.....22
 Table 3 – Value of Coefficients in Cavern Build Rate Estimation Equation29
 Table 4 – Cavern 7 Fluid Loss Calculations from September 1, 2021, to May 18, 2022.....34
 Table 5 – Cavern 7 Non-Metered Injection and Withdrawal Volumes from August 23, 2022, to January 5, 202339
 Table 6 – Cavern 7 Metered Injection and Withdrawal Volumes from January 5, 2023, to March 23, 2023.....41
 Table 7 – Cavern 7 Fluid Loss Calculations from August 23, 2022, to March 23, 202342
 Table 8 – Fluid Loss Calculations from September 1, 2021, to March 23, 2023.....44
 Table 9 – Workover, Inspection, & Sonar History of Cavern No. 006.....51
 Table 10 – Groundwater Data Summary75
 Table 11 – Surface Water Data Summary78

Equations

Equation 1 – Cavern Build Rate Estimation.....29
 Equation 2 – Pressure Balance Equation31
 Equation 3 – Fluid Loss Equation31
 Equation 4 – Example Fluid Loss Equation.....32



Certified By: Lonquist Field Service, LLC
 Louisiana Registration No. EF5853

Ben H. Bergman P.E.

Ben H. Bergman P.E.
 Senior Engineer
 Louisiana Registration No. 40184
 Date Signed: May 5th, 2023



Teresa H. Rougon P.G.
 Teresa H. Rougon P.G.
 Principal Geologist
 Louisiana Registration No. 330
 Date Signed: May 5th, 2023

1 Introduction

PPG Cavern No. 007, located within the Sulphur Mines Salt Dome near the city of Sulphur, Louisiana, is an inactive solution mined salt cavern with three wellbore entries (PPG No. 007A [SN 67269], 007B [SN 67270], and 007C [SN 971288]). Cavern No. 007 solution mining operations began in 1957 and were temporarily paused in 1977 when the cavern was transferred to and utilized by the U.S. Department of Energy for strategic crude oil storage until 1992. Solution mining operations then continued under different ownership (PPG Industries) until 2005 at which time the cavern and three wellbore entries remained in a monitoring status. In 2013 the cavern transferred ownership to Axiall Corporation, and in 2016 transferred ownership to the current operator of record Eagle US 2, LLC. PPG No.'s 007A and 007C were plugged and abandoned in October 2018 and monitoring of Cavern No. 007 is currently maintained via the PPG No. 007B wellbore entry.

An acute pressure loss event was observed on Cavern No. 007 on December 29, 2021, and subsequently the Cavern pressure appeared to stabilize until late 2022 when it became definitively apparent that the pressure began to decline again. Twenty-four hour a day brine injection operations have been under way since late 2022 to maintain cavern pressure slightly above a brine pressure gradient.

PPG Cavern No. 006, located within the Sulphur Mines Salt Dome near the city of Sulphur, Louisiana, is an inactive solution mined salt cavern with three wellbore entries (PPG No. 006X [SN 57788], 006Y [SN 58711], and 006Z [SN 971287]). Cavern No. 006 solution mining operations began in 1955 and were temporarily paused in 1977 when the cavern was transferred to and utilized by the U.S. Department of Energy for strategic crude oil storage until 1992. Solution mining operations then continued under different ownership (PPG Industries) until 2012 at which time the cavern and three wellbore entries remained in a monitoring status. In 2013 the cavern transferred ownership to Axiall Corporation, and in 2016 transferred ownership to the current operator of record Eagle US 2, LLC. PPG No.'s 006Y and 006Z were plugged and abandoned in July 2017, and monitoring of Cavern No. 006 is currently maintained via the PPG No. 006X wellbore entry.

Cavern No. 006 responded to the acute pressure loss event of Cavern No. 007, with a pressure decline of less magnitude. Cavern No. 006 pressure appears to be influenced by variations in Cavern No. 007 pressure.

Lonquist Field Service, LLC ("LFS") was contracted by Eagle US 2, LLC ("Eagle") to develop a "failure analysis report" by way of Order No. IMD 2022-027 of the Injection and Mining Division ("IMD") of the Louisiana Department of Natural Resources ("LDNR"). The format and contents of this failure analysis report were a novel development and document the history of the Sulphur Mines Salt Dome, Cavern No. 007 and Cavern No. 006, the acute and continued pressure/integrity failure loss, the evaluation and investigation efforts implemented and underway, and an assessment of theoretical failure mechanisms that may explain the integrity failure. LFS and Eagle have jointly contracted additional subject matter experts and services to support the efforts discussed in this report.

2 Sulphur Dome History & Introduction to Caverns

Significant events throughout the history of Sulphur Dome are summarized as follows:

- 1868 Sulfur deposits located in the caprock of the Sulphur Mines salt dome were discovered by the Louisiana Petroleum and Coal Company while drilling in the area in search of oil which had been observed at surface in the surrounding marshes via oil seeps. Historical notes indicate that “caprock” was struck at a depth of 333 feet and over 100 feet of pure sulfur was encountered at 551 feet.
- 1868-1892 Multiple attempts to conventionally mine sulfur were unsuccessful.
- 1892-1902 Herman Frasch conceived the idea of using hot water to melt the sulfur in situ and pump it out as a sulfur saturated liquid. Ten years of experimentation followed before commercial production of sulfur began.
- 1902-1924 Sulfur was economically produced using the Frasch hot water injection process. 9.4 million long tons of Sulphur were removed. Over 700 wells were drilled into the caprock for sulfur production.
- 1910-1924 Surface subsidence occurred due to extensive sulfur mining. A catastrophic example of collapse was the formation of a 100 foot diameter sink hole in 1914 which eventually engulfed a drilling rig.
- 1927 Oil and gas production development begins. Over 130 wells were drilled by 1940, and over 180 wells by 1950. Oil and gas production and development activity continues currently.
- 1957 Cavern 7 entry wellbores 7A and 7B were drilled by Pittsburg Plate Glass (PPG). Cavern 7 solution mining commenced soon thereafter. The third cavern entry wellbore 7C was drilled later in 1979.
- 1965 Drilling for sulfur (65 wells) production resumed. This venture proved unprofitable and was abandoned. Solution mining of the salt from the Sulphur Mines Dome has continued to present, and some of the caverns are currently utilized for hydrocarbon storage.

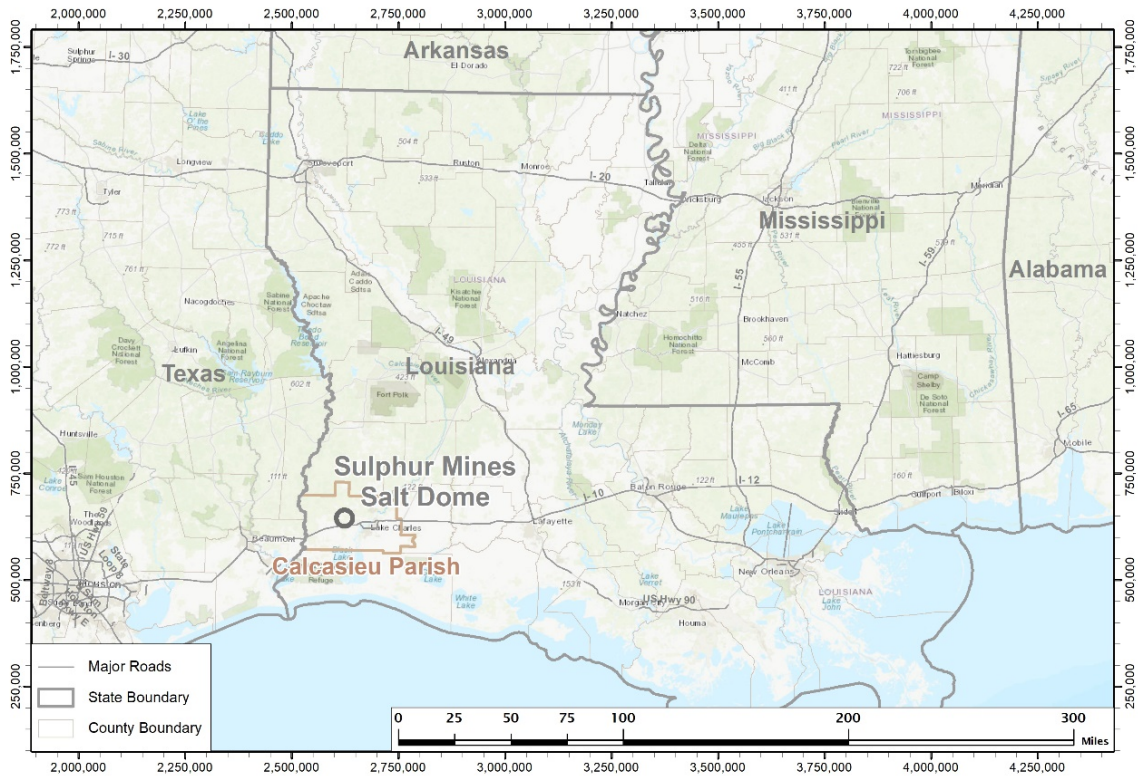


Figure 1 – Regional Landmarks Map

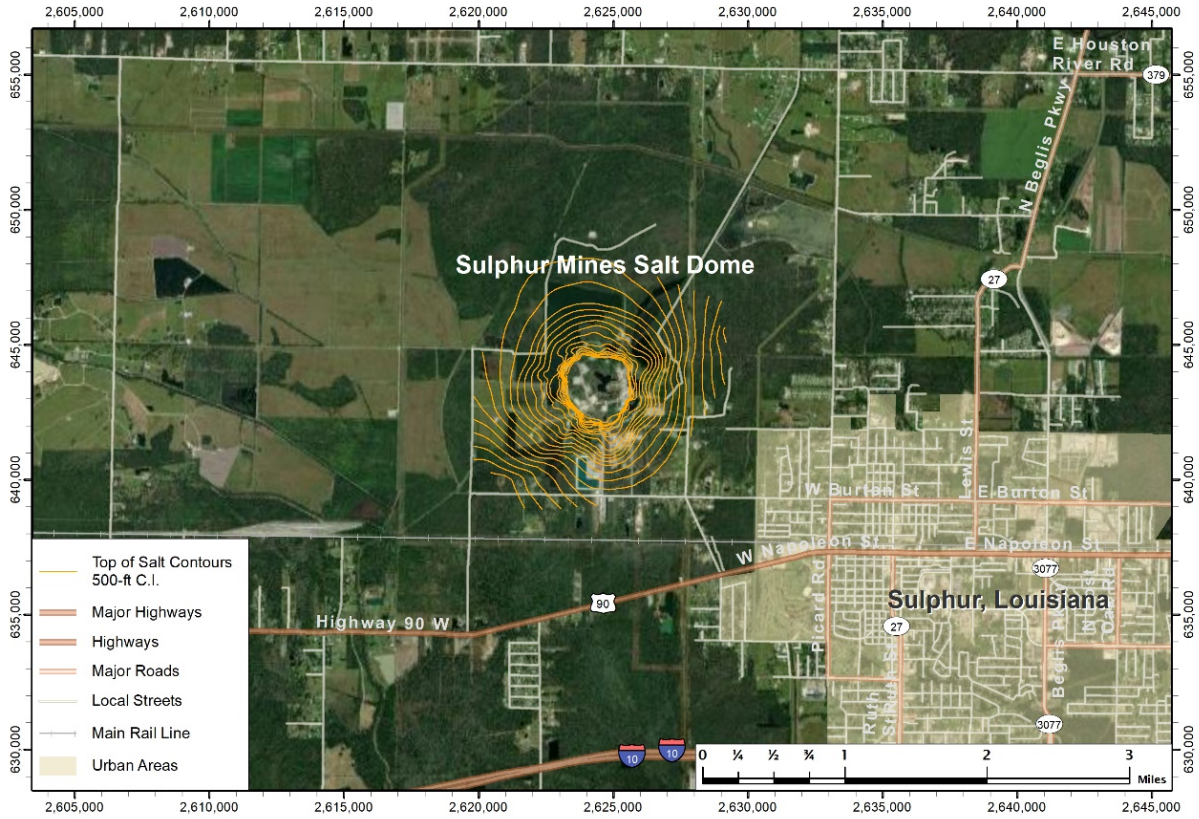


Figure 2 – Satellite Image of Sulphur Mines Dome Contours and Proximal Landmarks

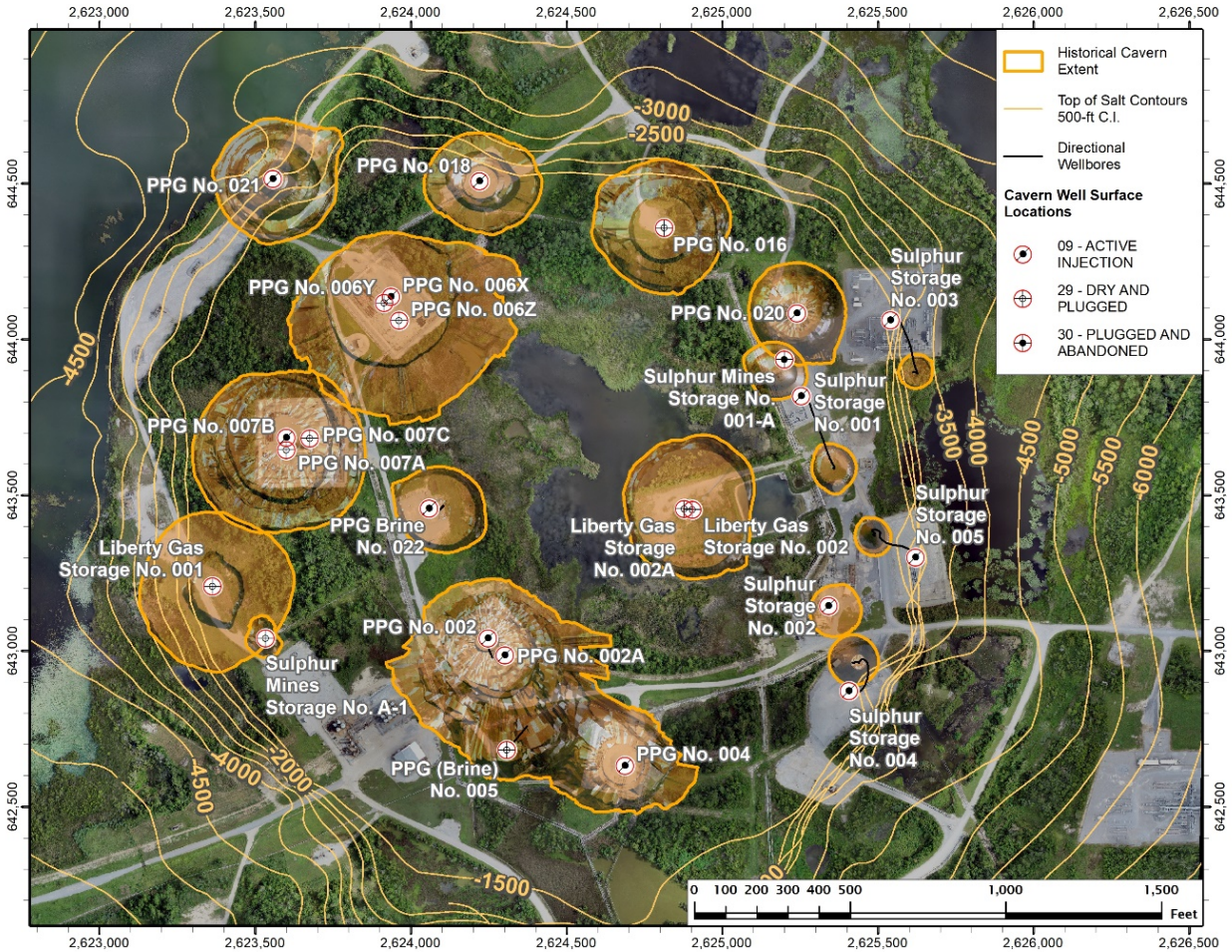


Figure 3 – Satellite Image of Sulphur Mines Dome Contours and All Salt Caverns



Figure 4 – Plan View Color Coded Image of All Salt Caverns in Sulphur Mines Dome

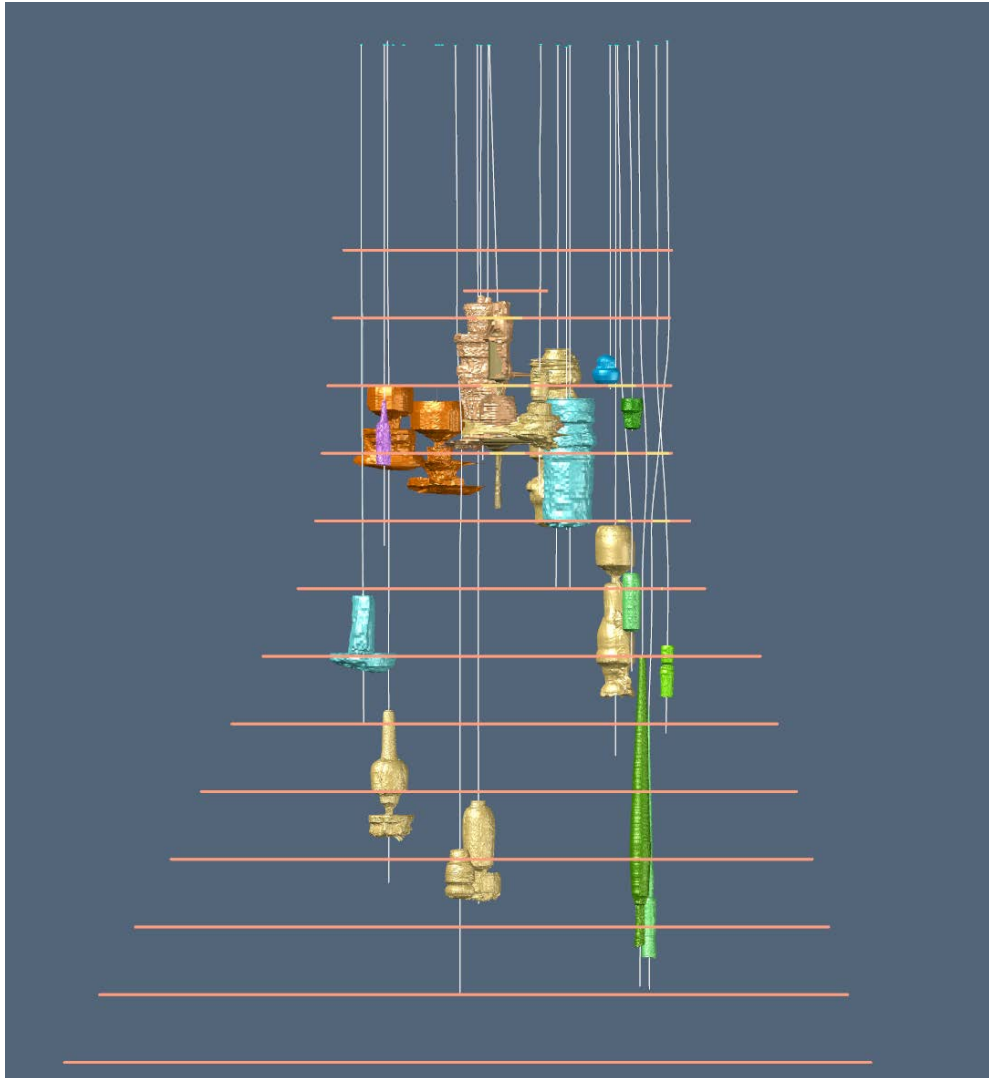


Figure 5 – Side View Color Coded Image of All Salt Caverns in Sulphur Mines Dome

Table 1 – All Salt Caverns in Sulphur Mines Dome

Cavern	Operator	Status
Liberty Gas Storage No. 001	Liberty Gas Storage, LLC	Plugged & Abandoned
Liberty Gas Storage No. 002	Liberty Gas Storage, LLC	Plugged & Abandoned
PPG No. 002	Eagle US 2, LLC	In-Active
PPG No. 004	Eagle US 2, LLC	In-Active
PPG Brine No. 005	Eagle US 2, LLC	Plugged & Abandoned
PPG No. 006	Eagle US 2, LLC	In-Active
PPG No. 007	Eagle US 2, LLC	In-Active
PPG No. 016	Eagle US 2, LLC	Plugged & Abandoned
PPG No. 018	Eagle US 2, LLC	Active (Solution Mining)
PPG No. 020	Eagle US 2, LLC	Active (Solution Mining)
PPG No. 021	Eagle US 2, LLC	Active (Solution Mining)
PPG Brine No. 022	Eagle US 2, LLC	Active (Solution Mining)
Sulphur Mines Storage No. 001-A	Union Texas Petroleum	Plugged & Abandoned
Sulphur Mines Storage No. A-1	Boardwalk Louisiana Midstream, LLC	Plugged & Abandoned
Sulphur Storage No. 001	Boardwalk Louisiana Midstream, LLC	Active (Hydrocarbon Storage)
Sulphur Storage No. 002	Boardwalk Louisiana Midstream, LLC	Active (Hydrocarbon Storage)
Sulphur Storage No. 003	Boardwalk Louisiana Midstream, LLC	Active (Hydrocarbon Storage)
Sulphur Storage No. 004	Boardwalk Louisiana Midstream, LLC	Active (Hydrocarbon Storage)
Sulphur Storage No. 005	Boardwalk Louisiana Midstream, LLC	Active (Hydrocarbon Storage)

Section 10.2.1 provides a detailed geologic discussion, however, the below serves as an introductory illustration to the reader about the geologic setting. There exist stratified formations adjacent to the salt dome. Figure 6 below is a cross-section of the salt dome and adjacent formations with visual representation of Cavern 6 and 7, an adjacent oil production well Fee 1012 (operated by Yellowrock), seismic profile visualization, and well log from Fee 1012. All sonars for which digital files were available for Caverns 6 and 7 were overlaid and positioned to display the caverns as hollow cavities with the combined extent of the historical sonars. Caprock geometry was drawn along the cross-section path from the caprock structure map contours. All perforated intervals are indicated along the directional survey for Fee 1012. A seismic profile was created from the PSTM (“pre-stack time migration”) 3D seismic data that intersects Cavern 7 and Fee 1012. This seismic cross-section provided the framework for the salt dome interpretation and productive sands interpretation (current completion intervals) relative to Fee 1012 to create the Figure. The cross-section is not to be considered final work product, but more so a tool to help the reader visualize the relationship between the salt dome and adjacent formations.

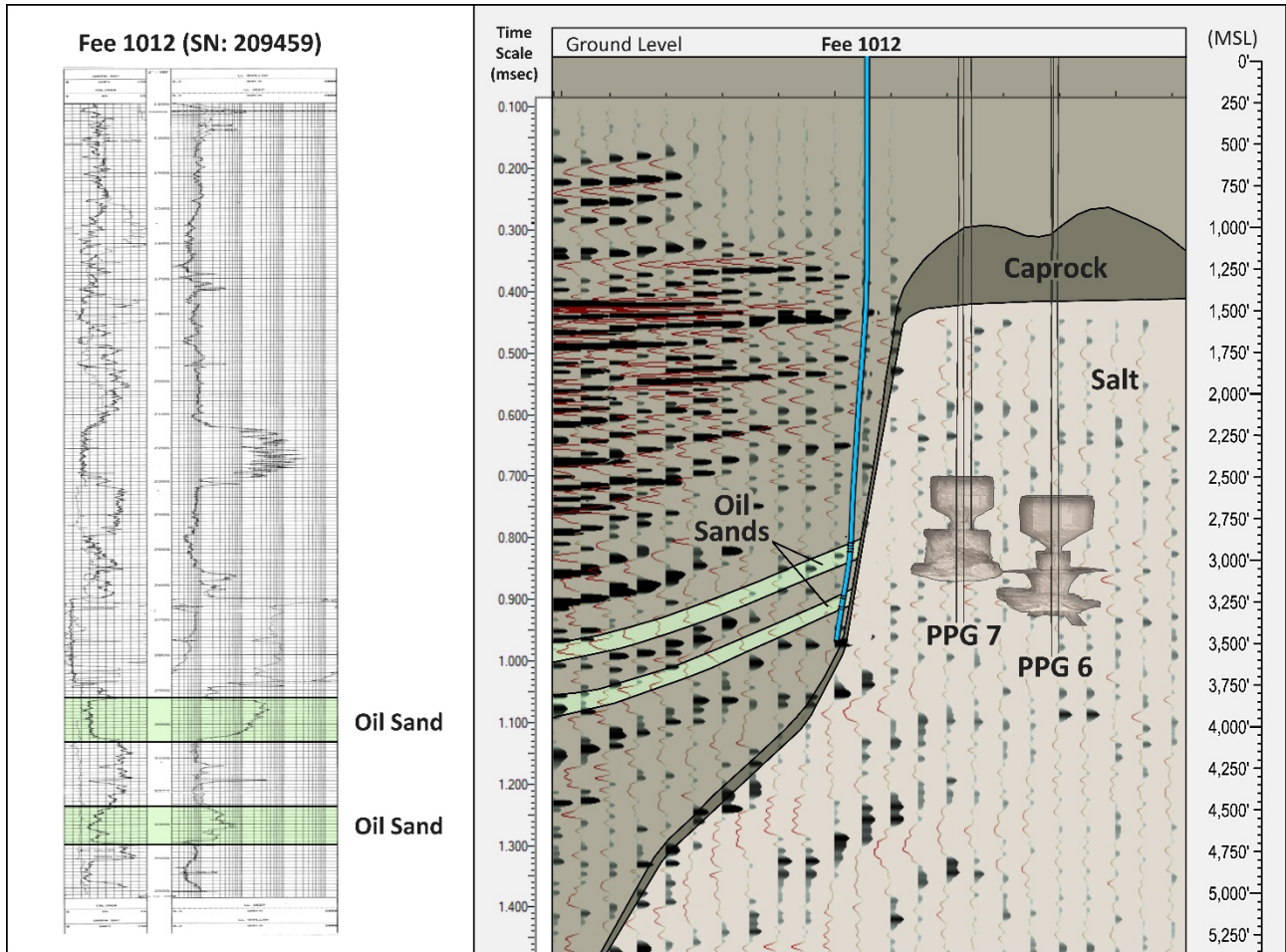


Figure 6 – Cross Section Through Fee 1012 and PPG 6 & 7

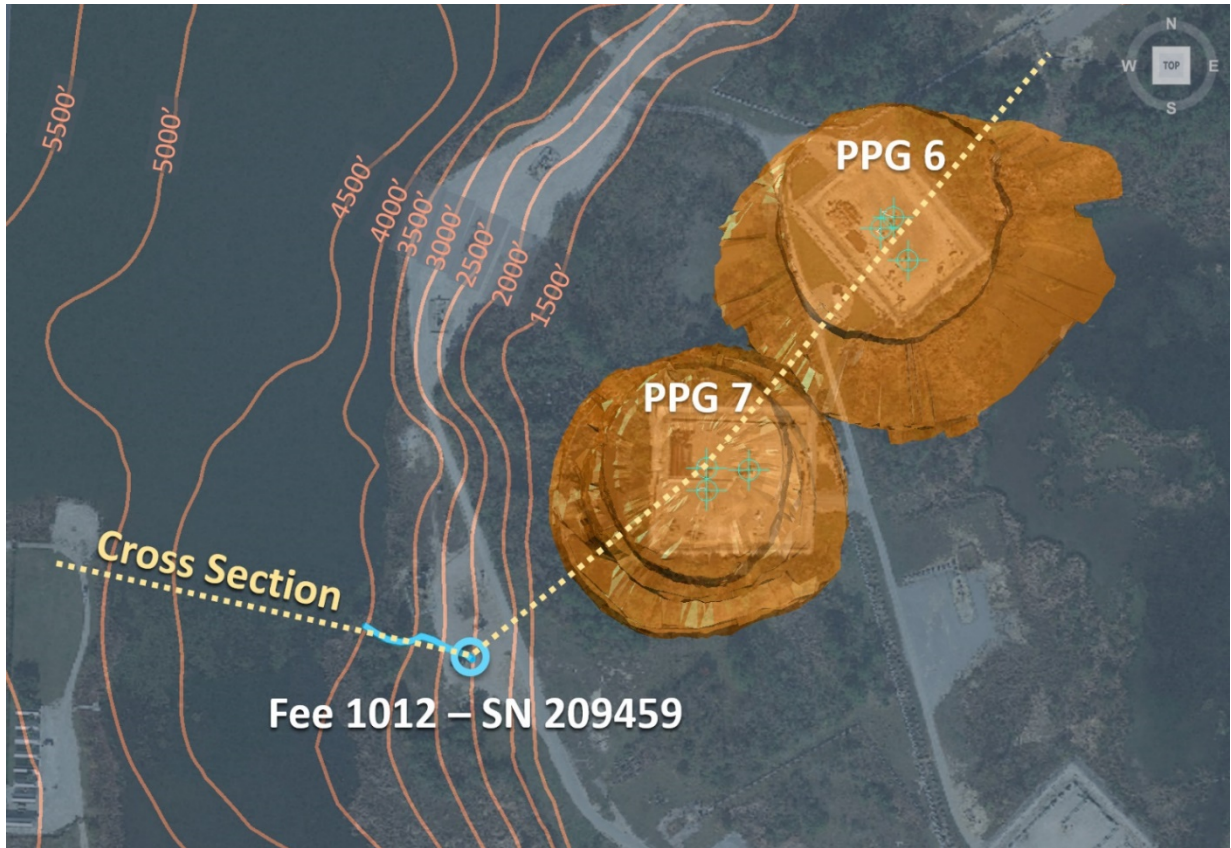


Figure 7 – Aerial View of Seismic Cross Section Through Fee 1012 and PPG 6 & 7

AUSTIN · HOUSTON · WICHITA · DENVER · BATON ROUGE · COLLEGE STATION · CALGARY · EDMONTON

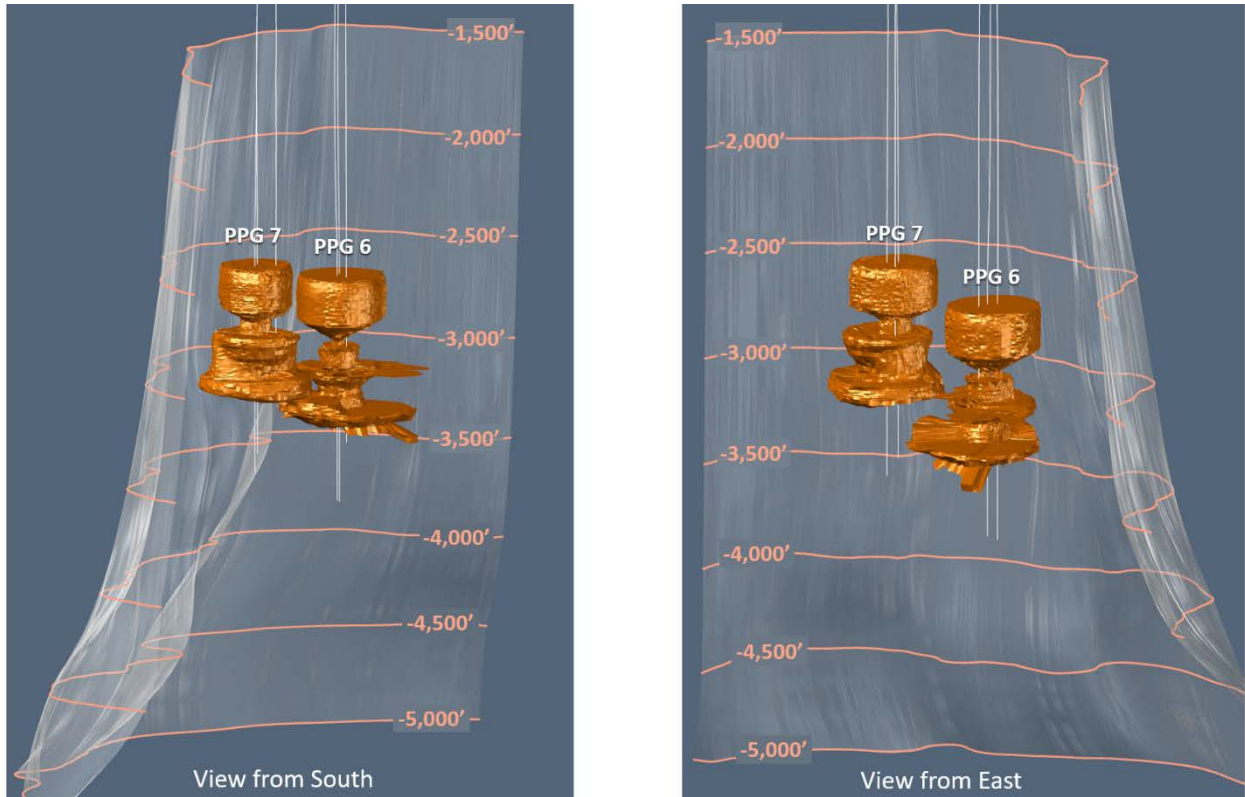


Figure 8 – Perspective View of Caverns 6 and 7 from South and East



Figure 9 – Side View of Caverns 6 and 7 from East-Southeast

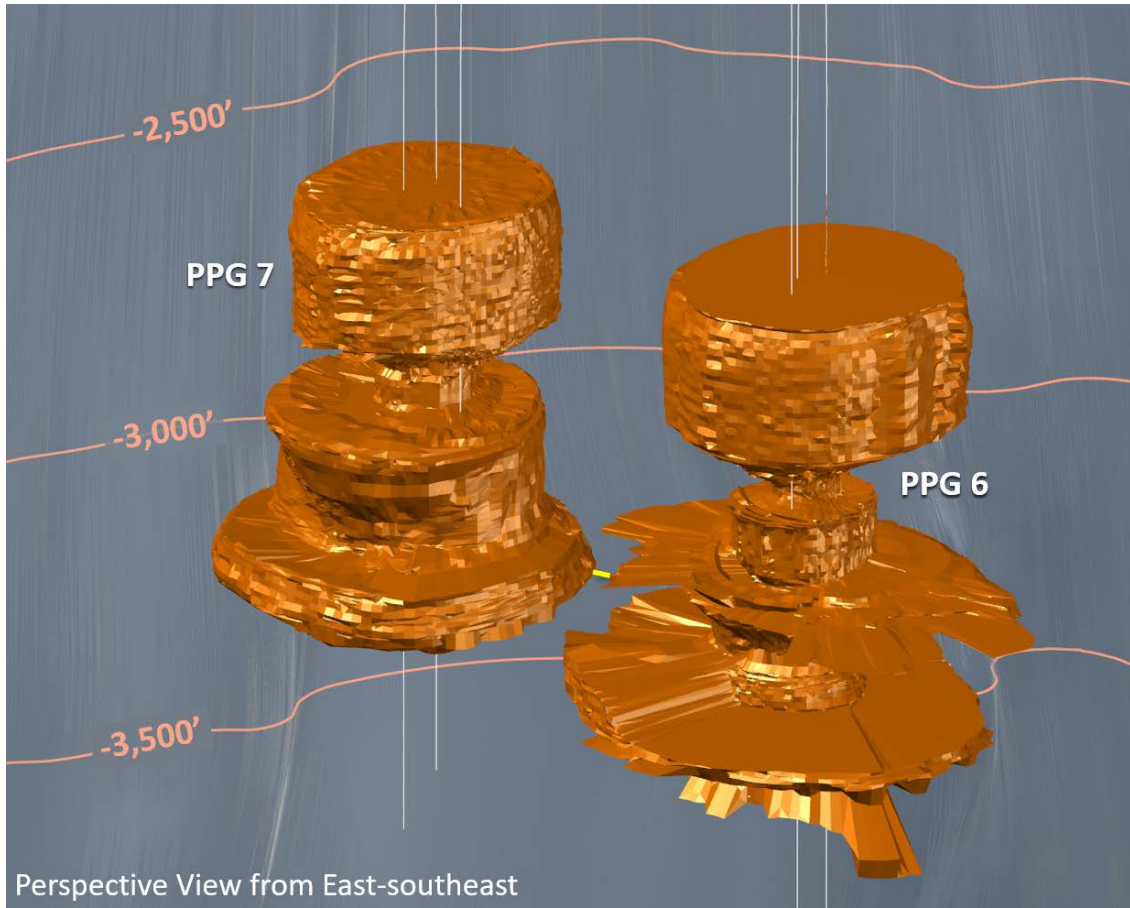


Figure 10 – Perspective View of Caverns 6 and 7 from East-Southeast

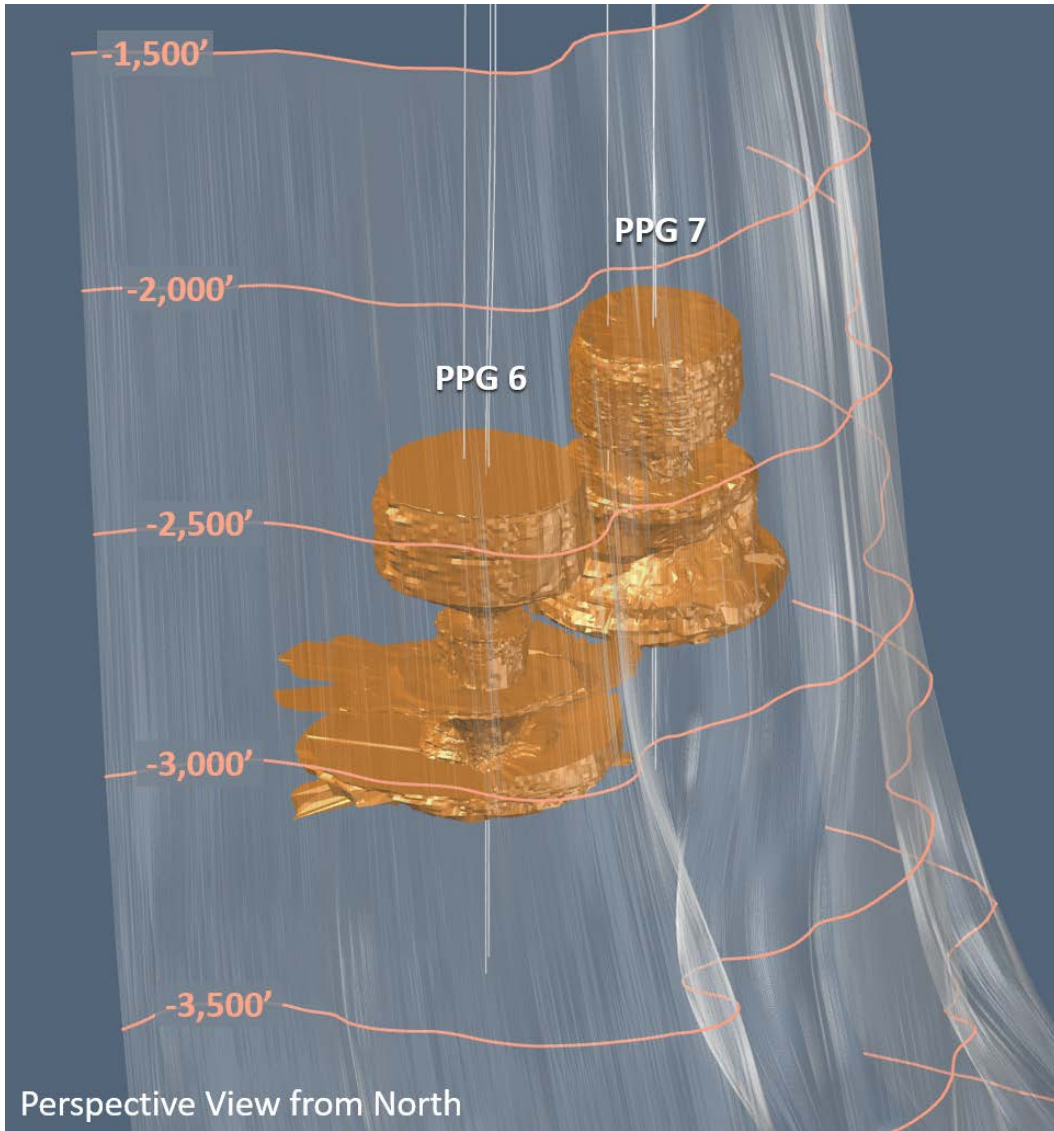


Figure 11 – Perspective View of Caverns 6 and 7 from North

3 Cavern Integrity Failure Mechanisms

3.1 Introduction & Definitions

In the simplest form and in the context of this report, cavern failure is defined as the loss of mechanical integrity of an individual cavern. The consequences of cavern failure can include loss of stored products/fluids, salt/rock/cavern collapses, contamination of formations outside of the salt, inter-cavern communication/coalescence, surface environment contamination, and potentially additional or interconnected consequences. The integrity failure mechanisms outlined in this section focus primarily on domal salt structures, and it is not intended to be an exhaustive list.

3.2 Cavern Integrity Failure Mechanisms

3.2.1 Roof Fall / Rock Fall / Cavern Breach

A cavern roof fall, or rock fall, is commonly defined as a loss of material from the cavern roof, cavern walls, or underside of an exposed shelf in a cavern that falls to the floor of the cavern. These falls are generally an unavoidable phenomenon throughout the life of a salt cavern, however, can be caused by solution mining activity, pressure fluctuation regimes, geologic variation, and salt/rock stresses.

In many cases, these falls remain unobserved until a sonar survey identifies a change in geometry of the cavern roof and/or walls and a rise in the cavern floor. Roof/Rock falls can create operational issues such as a damaged hanging string(s) (which can typically be easily remediated) or can create cavern integrity failures by, in simple terms, creating a conduit for stored product/fluid to migrate out of the cavern system.

In severe cases, a rock/salt fall may produce a breach of the cavern. This is defined as penetration of the cavern through the surface or the side of the salt dome. Cavern breaching occurs if the existing salt back between the top of the cavern and the caprock base, or the salt pillar between the side of the cavern and sediments adjacent to the salt dome structurally fail causing collapse of those units into the cavern, and therefore likely causing loss of cavern fluids into an adjacent formation. This type of severe case could lead to additional integrity failure mechanisms.

3.2.2 Hydraulic Connection / Cavern Coalescence

One form of cavern hydraulic connection is when adjacent caverns communicate through the salt pillar separating the two independent cavern geometries. Typically, a hydraulic connection between caverns is identified by observing an interconnected pressure influence and/or interconnected volumetric influence. In more severe cases, cavern coalescence can also occur if the salt between adjacent caverns is completely dissolved or structurally fails, creating a direct connection from cavern to cavern that can be identified clearly by sonar survey. In either instance the affected caverns can be referred to as a gallery.

Another form of hydraulic connection is between a salt cavern and a formation adjacent to the salt dome. The connection conduit could be caused by a geologic inconsistency within the salt dome like

a non-salt stringer, spine, or fault, or by uncharacteristically weak/impure salt. The cavern could maintain its structural integrity, or it could structurally fail, dissolve, or erode to the point where it leads to an additional integrity failure mechanism.

3.2.3 Wellbore or Wellhead Leak

Most commonly cavern integrity failures are due to mechanical integrity failure of the “man-made” components of a cavern system being the cased wellbore and the wellhead. The failure points are most commonly; 1) a casing shoe leak where the bond between a cemented casing string and the formation and/or other casing string does not have the integrity to support the cavern storage/mining operation or to support a successful mechanical integrity test, 2) a casing connection leak where the stored fluid or test fluid leaks through a failed threaded or welded casing connection or remedial patch, 3) a wellhead leak where the stored fluid or test fluid leaks through a sealing element within the wellhead assembly, 4) a combination of these.

The integrity failure is typically identified due to pressure loss when the system is observed during shut-in, a stored fluids inventory discrepancy, and/or during a mechanical integrity test of the system.

3.2.4 Surface Expression / Sinkhole

Surface expressions can occur in the form of relatively minor ground-level subsidence from long term cavern development/operation and as large sinkholes following the structural collapse of a cavern which could be related to one of the previously mentioned mechanisms.

4 Cavern Integrity Evaluation Variables

Various factors can affect the evaluation of cavern integrity during operation or monitoring. There are various methods to evaluate the integrity of a cavern system (wellhead, wellbore, and cavern). For example; a hydrostatic pressure observation test, a mass-balance interface test method, or a mass-balance inventory variance test method. These methods, among others, share a common component which is monitoring the pressure of the shut-in cavern. The following non-exhaustive list explains a few of the variables that would impact the evaluation of shut-in or operational cavern pressure as it pertains to an assessment of cavern integrity.

4.1 Injection / Withdrawal Operations

Normal cavern operations, namely fluid injection and withdrawal, have a profound effect on cavern behavior. The amount of influence on cavern pressure from injection/withdrawal operations depends on many factors, including but not limited to injection/withdrawal rate (or simultaneous), characteristics of fluid injected/withdrawn, wellbore geometry, casing/tubing depths, cavern geometry, and system temperatures. While the cavern is undergoing injection/withdrawal operations, it may be hard to identify cavern integrity issues, and therefore it is most common to shut-in a cavern when trying to evaluate cavern integrity.

4.2 Cavern Creep Closure

Salt creep is a natural phenomenon that always occurs in salt formations (bedded or domal) in which the salt around a cavern continuously moves toward the cavern void primarily due to differential pressure and stress that has been created in the salt member. The result of salt creep on a cavern is also known as cavern creep closure and typically presents itself as a cavern pressure increase on a shut-in cavern and can also be identified by changes in cavern geometry via sonar survey. The rate of salt creep is pressure differential dependent, and therefore gradually decreases as the internal cavern pressure increases to achieve an equilibrium with the pressure/stress in the surrounding salt. The cavern geometry and cavern pressure, along with the geomechanical properties of the salt member can affect salt creep rate and associated cavern geometric closure rate.

4.3 Brine Thermal Expansion / Contraction and Ground Temperature Variations

Brine thermal expansion and contraction in a salt cavern occurs due to cavern temperatures attempting to equalize with the natural geothermal gradient of the Earth, and due to the natural variability in the geothermal gradient of the Earth. Commonly solution mining and storage operations in salt caverns produce an internal cavern brine temperature that is cooler than the surrounding native salt/formation geothermal temperature. Consequently, the brine in a shut-in salt cavern will typically increase in temperature over time, which will produce a cavern pressure increase. The rate of pressure change and magnitude over time is dependent on a number of variables.

Additionally, ambient temperature at surface will show day-to-day surface instrumentation monitoring variations. This effect could also be induced by large injection or withdrawal volumes at temperatures different than the equilibrium temperature of the fluid in the cavern.

4.4 Dissolution / Crystallization

Salt dissolution and crystallization in a salt cavern occur due to chemical reactions between the brine fluid and surrounding salt. The reaction will follow Le Chatelier's Principle which states that changes in temperature, pressure, volume, or salt concentration of a system will result in changes to drive the system towards equilibrium for the new conditions. Any rapid changes in these parameters, such as fluid injection or withdrawal, will affect the behavior of the cavern dramatically at first, but taper off over time as the system gets closer to equilibrium.

4.5 Micro-permeation

Micro-permeation of fluid in a cavern can be defined as the process of fluid loss through the solid salt matrix surrounding the cavern. The permeation process only occurs when the pressure within the cavern is greater than the overburden formation pressure, and the extent of fluid loss is a direct correlation of the geomechanical and physical characteristics of the surrounding salt.

4.6 Wellbore or Cavern Leak

A wellbore penetrating a cavern and/or the cavern itself that has lost mechanical integrity will exhibit a cavern pressure decrease. In some cases, the pressure loss rate due to a leak can be matched or outpaced by the associated pressure increase rate due to one or more of the above variables. This can make leak identification complex.

4.7 Earth Tides Effects and Barometric Pressure Variations

Much like water on the surface of the Earth, the fluid and rock in and around a cavern will be affected by the position of the sun and moon relative to Earth. These movements will cause barometric induced pressure changes, but the overall effects are usually so small in magnitude that they go unnoticed. Similarly, natural variations in the atmospheric pressure at the location of a salt cavern will also cause induced pressure changes with overall effects usually so small in magnitude that they go unnoticed.

5 Examples of Cavern Integrity Failure Incidents

The following are examples of cavern integrity failure incidents that generally have similar geologic and/or operational characteristics that could be considered as analogous to Cavern No. 7 and Cavern No. 6 at Sulphur Mines Dome. To be clear, the failure mechanism and long-term implications of the integrity failure of Cavern No. 7 and Cavern No. 6 are not yet understood at the time this report was written; however, monitoring, technical evaluations, and other investigatory efforts are actively being conducted in an effort to produce a confident understanding.

5.1 Louisiana Offshore Oil Platform (LOOP) Cavern No. 14

The Louisiana Offshore Oil Platform (LOOP) is a field of high-rate crude oil storage caverns located within a marsh on the Clovelly Salt Dome 18 miles from Galliano, Louisiana. In 1992, LOOP Cavern No. 14 was found to have lost integrity because it encountered a non-salt layer within the salt dome that provided a permeability conduit to formations adjacent to the dome. It was discovered that brine from Cavern 14 was migrating through the conduit and into an adjacent formation. Sonar surveys of Cavern 14 had indicated an anomalous bulge in an area of the cavern wall, and it was later identified that it was due to an inhomogeneity (a non-salt layer) within the salt dome structure with a location oriented toward the nearest distance of the cavern to the dome flank (approximately 400 feet from the cavern wall to the salt dome flank). The pressure in Cavern 14 was intentionally allowed to decrease to achieve an equilibrium pressure between the cavern and the adjacent formation (requiring the brine level in the Cavern 14 wellbores to drop to approximately 300 feet below surface). Once the equilibrium pressure was achieved the brine migration through the conduit reduced to a nominal rate, and Cavern 14 pressure remained generally static. Attempts were made to seal the cavern breach using a remote operated vehicle and a polymer gel, however, those efforts proved to be unsuccessful. Currently, Cavern 14 and the associated wellbore entries are not in active storage service and remain in monitoring status.

5.2 Starks PPG No. 008

Starks PPG No. 008 was an active solution-mining cavern in the Starks Dome, near Vinton, Louisiana. Generally, this salt cavern is positioned in the diametric center of the salt dome (many hundred feet away from the salt dome flank). In 1987, circulation was lost while solution mining the cavern and the cavern was subsequently plugged and abandoned in 1988. In the 2000's the cavern was re-entered via the original plugged entry with the intent of investigating if the cavern could be utilized for hydrocarbon storage service, however, the cavern was not found to have mechanical integrity. An investigation revealed that during the solution mining of the cavern, the expanding cavern wall likely intersected a "ghost wellbore" which led to the mechanical integrity failure. The "ghost wellbore" was likely an unmapped wellbore penetration related to historical oil and gas exploration or sulfur mining operations from the 1920's to 1960's. It became apparent that the "ghost wellbore" also did not have integrity and was acting as a fluid migration conduit to outside the salt dome to a formation(s) in which it is believed to be trying to achieve equilibrium with. The cavern is currently in a monitoring status with the fluid interface at a depth notably below ground level.

5.3 Bayou Corne/Oxy-Geismar Cavern No. 003

Bayou Corne/Oxy-Geismar Cavern No. 003 was an abandoned, solution-mined cavern within the Napoleonville Salt Dome in Assumption Parish, Louisiana. The Napoleonville Salt Dome is utilized for the development of many salt caverns solution-mined for brine and hydrocarbon storage. . The Oxy-Geismar No. 3 well was drilled in 1982 and was solution mined for brine production until a mechanical integrity test was failed in June 2011, and was subsequently plugged and abandoned. In July of 2012, methane bubbling was observed with increasing frequency and intensity within the marsh generally above Cavern No. 3 and earthquakes were felt in the local community near the cavern. On August 3, 2012, the first surface expression of what was to become a sinkhole began to develop proximal to the location of the edge of the salt dome above Cavern 3. It was discovered that the cavern had a failure of the relatively thin salt pillar (believed to be under 30 feet thick) between the edge of the salt dome structure flank near the base of Cavern No. 3. The salt pillar failure consequently caused the adjacent stratified non-salt formations to fall into the cavern void, and thereby ultimately being expressed as a sinkhole at the surface. One theory during the event investigation was that the adjacent oil and gas formations had been de-pressurized due to decades of production operations, and which created an abnormal pressure/stress differential across the salt pillar in comparison to the native/discovery pressure/stress conditions. Furthermore, it was theorized that the plugged salt cavern was also building pressure due to salt creep closure, and thereby adding additional differential pressure/stress across the salt pillar. The cavern and sinkhole are still being monitored to date.

6 Cavern 7 History and Geologic Structure

6.1 Historical Timeline (Major Events)

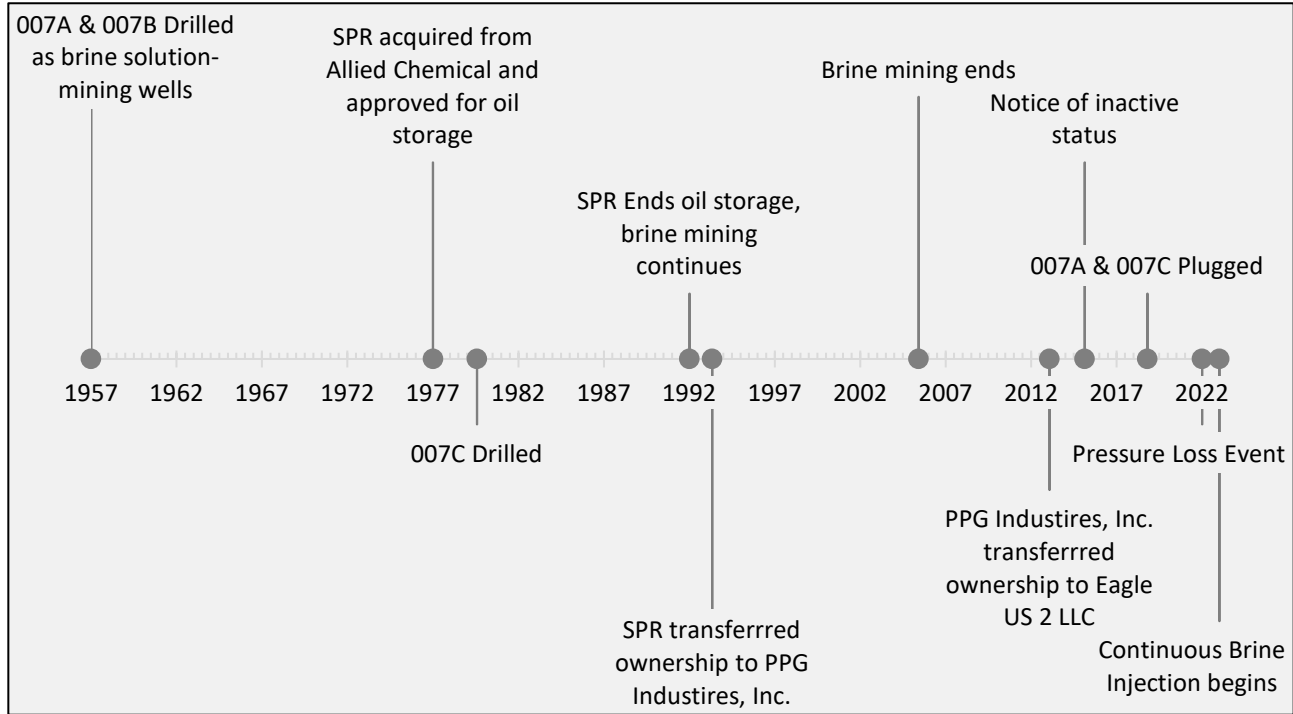


Figure 12 – Cavern No. 007 Timeline (Major Events)

6.2 Distance to Salt Dome Flank

The dome flank geometry has been estimated via geological interpretation of historical offset well data. A detailed description of the methodology used in mapping the dome surface is provided in a later section. Cavern 7 geometry and position has been modeled from a deviation survey of the 7B wellbore and sonar surveys of the Cavern 7 interior. The minimum 3D distance from Cavern 7 to the dome flank is estimated to be roughly 160 feet based on an overlay of all available digital sonar files dating from July 2011 to March 2023. Figure 13 displays the minimum distance to flank from the historical overlay of cavern 7 sonars. There are ongoing evaluation efforts to review and attempt to improve the confidence of the cavern to flank spacing, however, with the current data and understanding it is anticipated that the spacing will not deviate significantly from the current 160 foot interpretation.

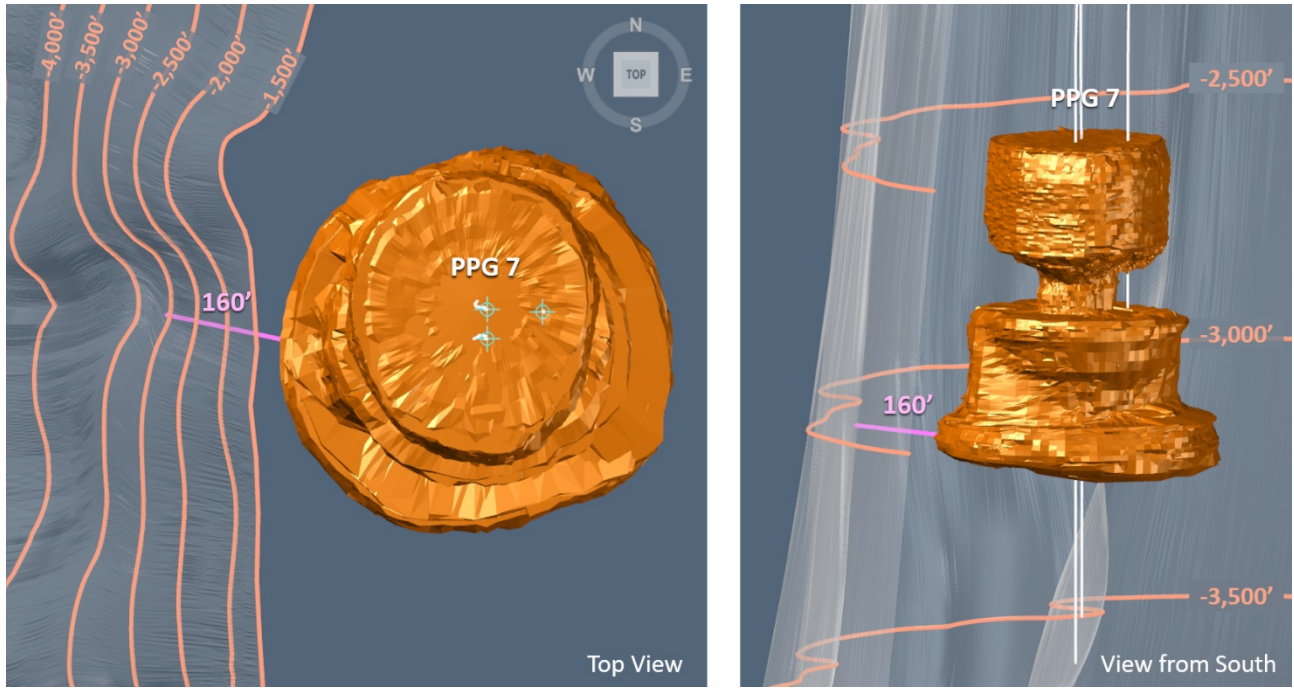


Figure 13 – Cavern 7 Minimum 3D Distance to Salt Dome Flank

6.3 Notable Workover, Inspection, and Sonar History

The following table lists all notable cavern and wellbore inspection or workover activity where sufficient records exist to list it.

Table 2 – Workover, Inspection, & Sonar History of Cavern No. 007

Date	Work Description
November 17, 1973	Sonar via 007A
October 14, 1975	Sonar via 007A
March 21, 1976	Sonar via 007B
November 29, 1977	Sonar via 007A
June 10, 1981	Sonar via 007A
February 9, 1993	Sonar via 007A
April 5, 1995	Sonar via 007B
May 21, 1997	Sonar via 007B
June 8, 1999	Sonar via 007B
October 18, 2001	Sonar via 007B
October 20, 2003	Sonar via 007B
July 14, 2011	Sonar via 007B
May 3, 2018	Sonar via 007C
May 16, 2018	Sonar via 007B
June 2018	Casing Inspection/Sonar/MIT's on 007A, 007B, & 007C
October 2018	P&A of 007A & 007C
March 2020	Temp Log
November 2020	Nitrogen Pad Install
March 11, 2022	Sonar & Density Log
April 14, 2022	Nitrogen Integrity Test
November 2, 2022	Sonar & Density Log
January 11, 2023	Sonar & Density Log
January 13, 2023	Noise/Temp/Density Log
February 1, 2023	Sonar & Density Log
March 16, 2023	Sonar & Density Log & Downhole Pressure/Temp Gauge Install

6.4 Wellbore Diagrams

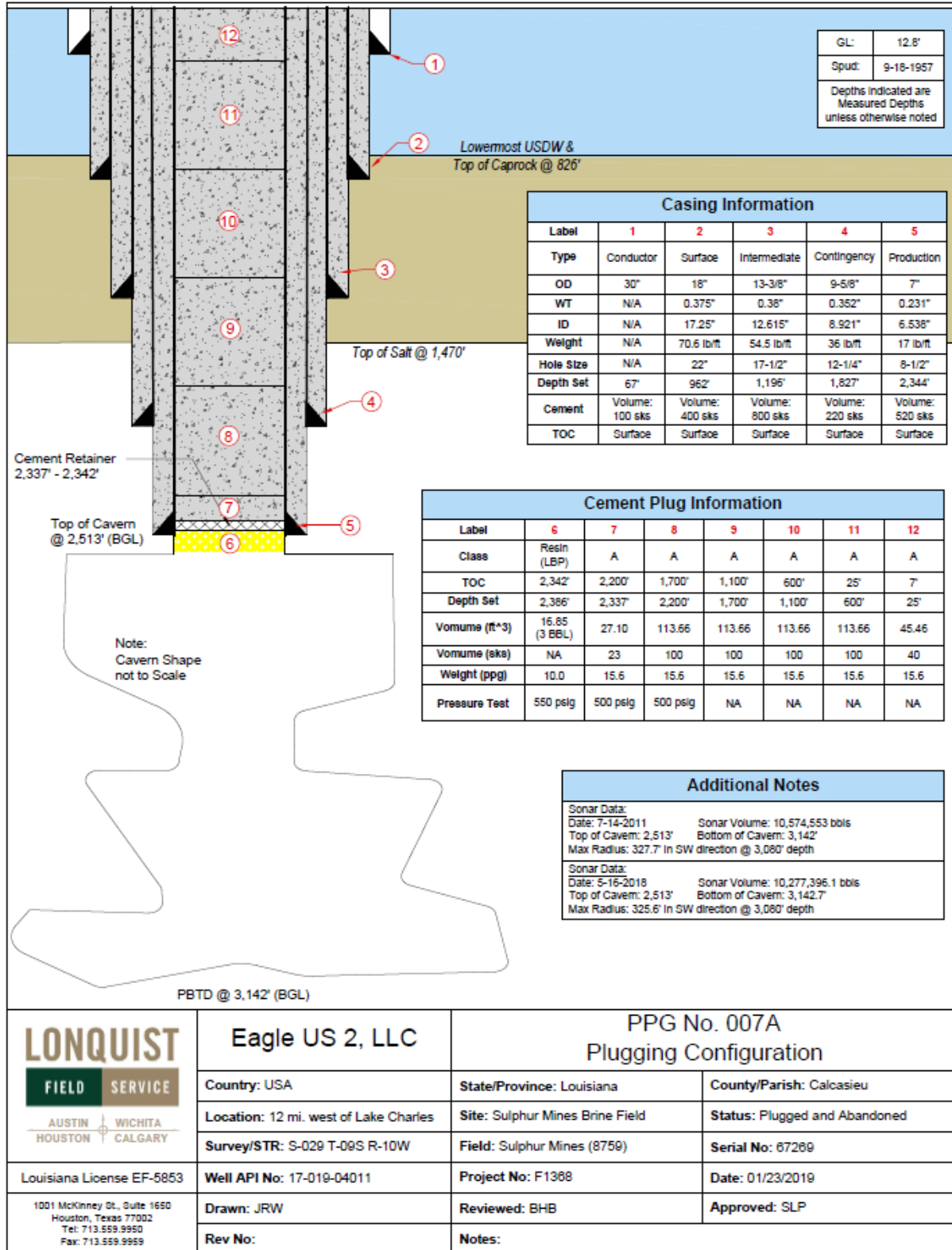


Figure 14 – As-Built Wellbore Diagram of PPG 007A

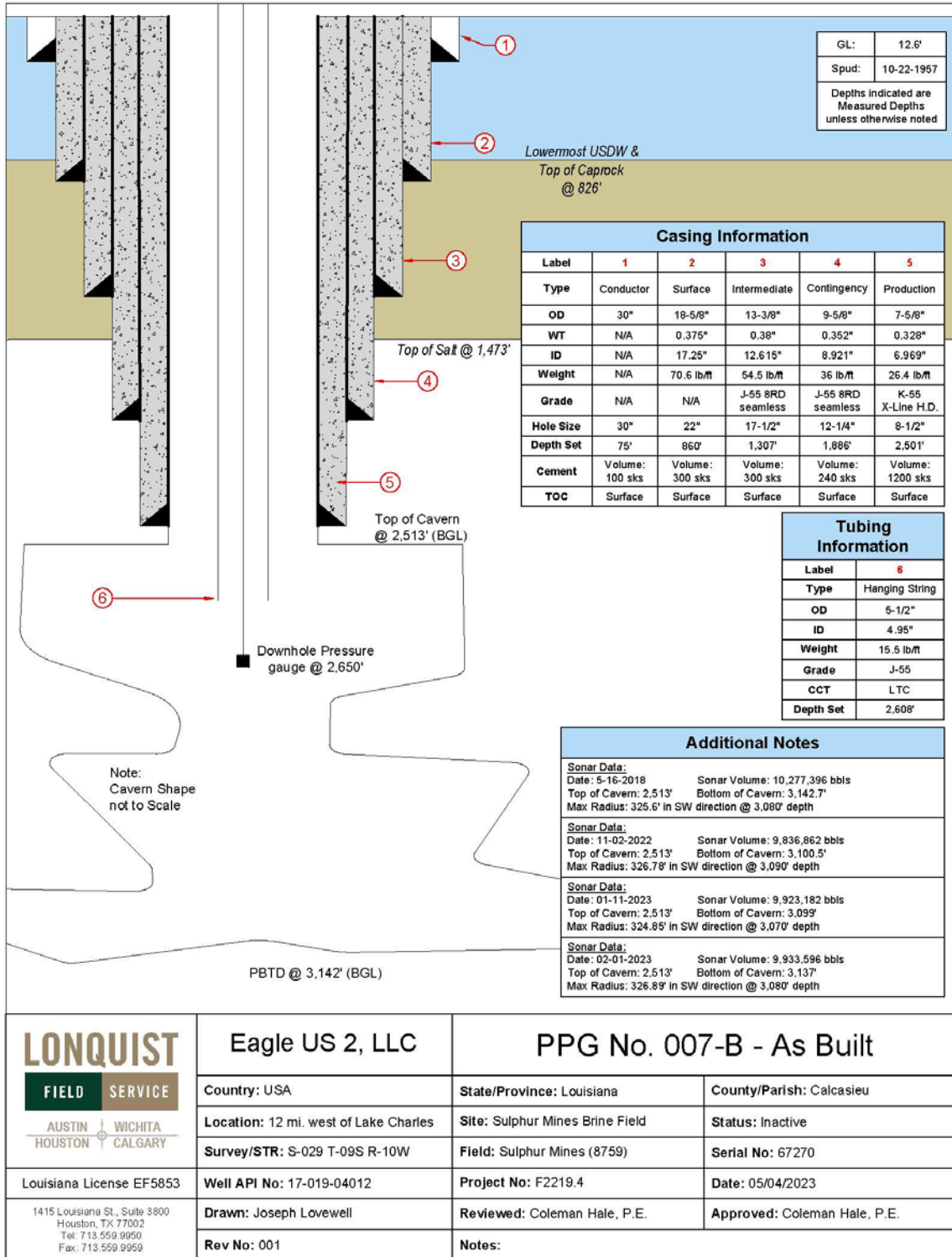


Figure 15 – As-Built Wellbore Diagram of PPG 007B

LONQUIST & CO. LLC

PETROLEUM
ENGINEERS

ENERGY
ADVISORS

AUSTIN · HOUSTON · WICHITA · DENVER · BATON ROUGE · COLLEGE STATION · CALGARY · EDMONTON

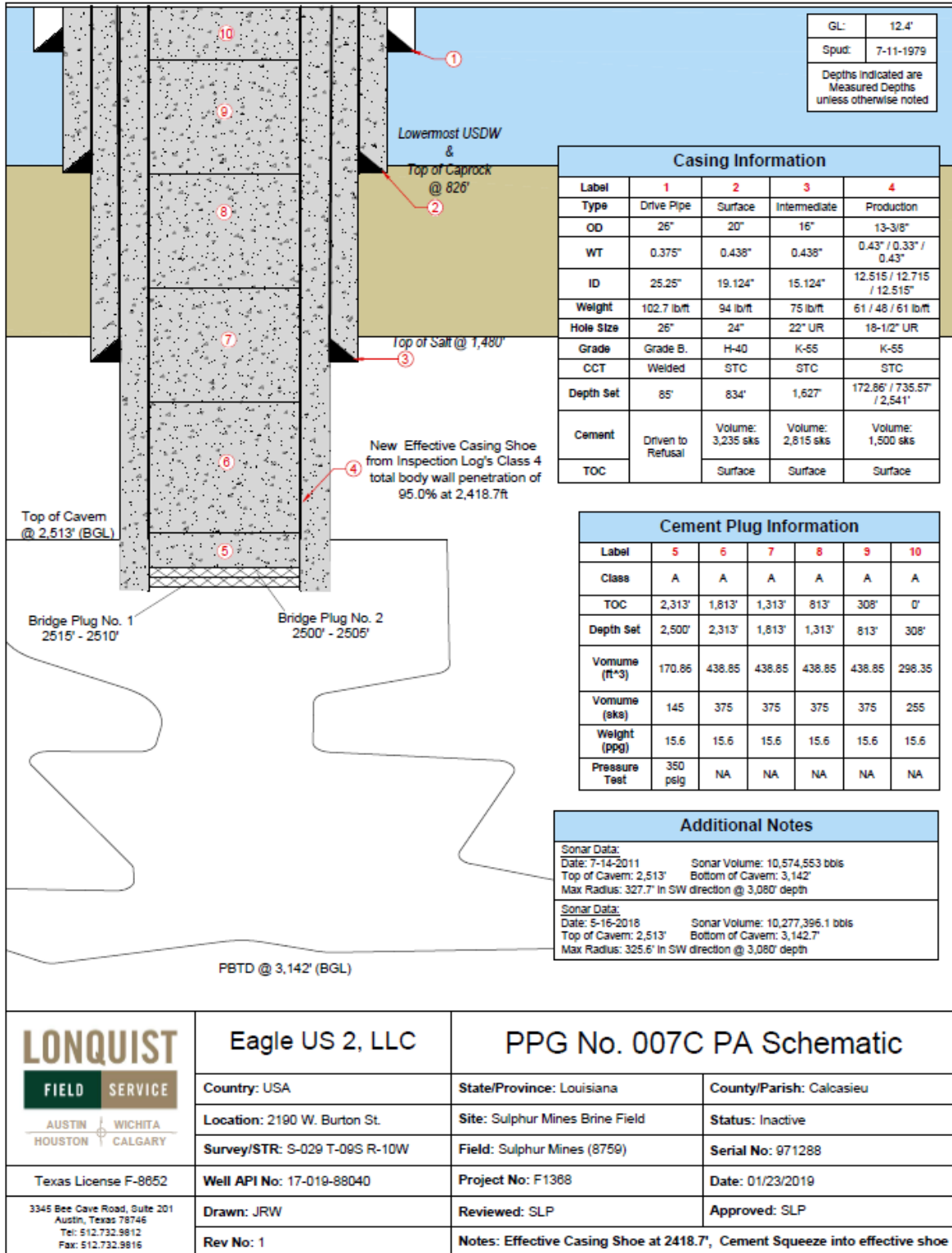


Figure 16 – As-Built Wellbore Diagram of PPG 007C

7 Cavern No. 007 Integrity Failure Pressure Analysis

7.1 Cavern No. 007 Acute Pressure Loss Event

On December 29, 2021, Cavern No. 007 exhibited an acute pressure loss event, beginning from 250.7 psi (surface saturated brine-filled tubing pressure), and dropping a total of 115.2 psi during a 24-hour period. This was followed by comparatively lower rate pressure losses over the next 12 days, for a total pressure loss of 223.3 psi by 12:00 pm on January 10, 2022, when cavern pressure measured its lowest value thus far of 27.4 psi (surface saturated brine-filled tubing pressure). Subsequently, cavern pressure began to build again. Figure 17 displays the hourly pressure history for Cavern No. 007 from December 25, 2021, to January 20, 2022, and Figure 18 displays the cumulative pressure change of 223.3 psi for the period of Cavern No. 007 pressure loss. Upon further analysis, it was observed that Cavern No. 007 had deviated from a “normal” pressure trend on September 1, 2021, and which is evaluated and discussed in more detail later in this section.

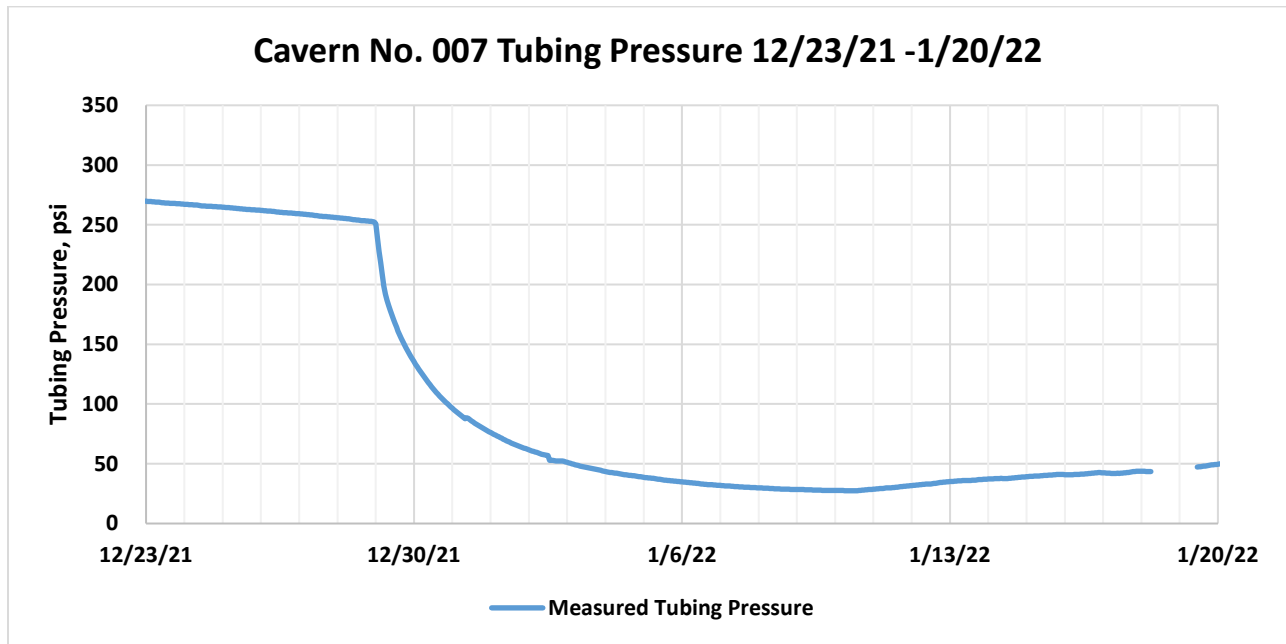


Figure 17 – Cavern 7 Recorded Pressure During Acute Pressure Loss Event

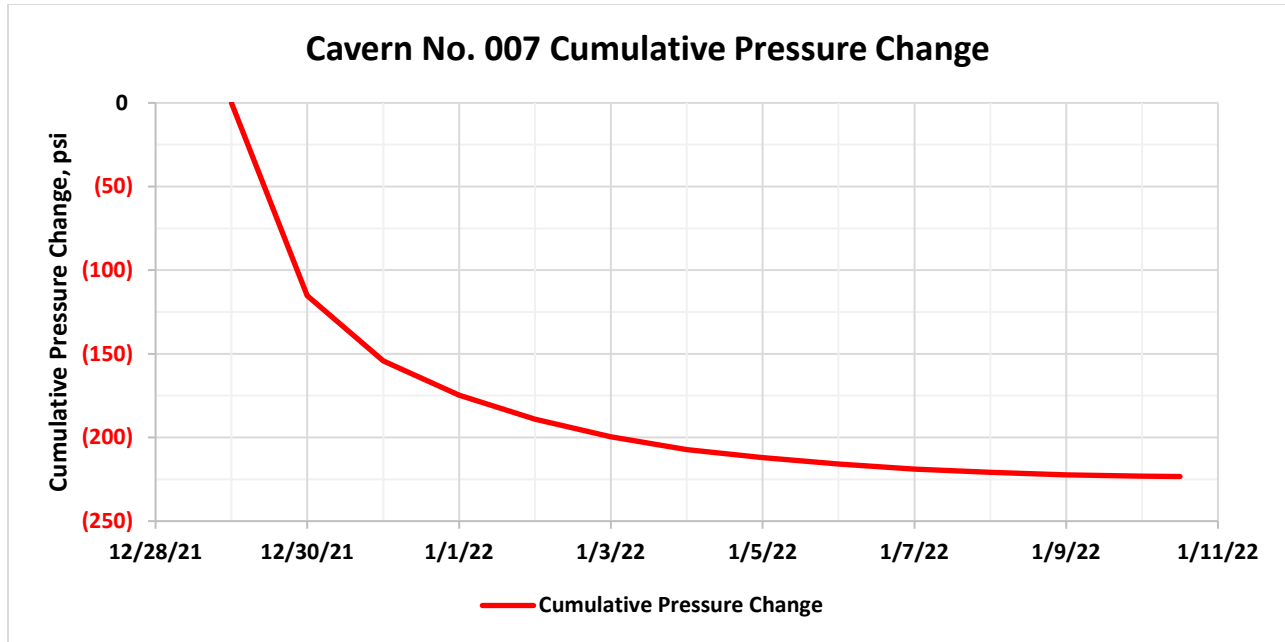


Figure 18 – Cavern 7 Cumulative Pressure Loss Recorded During Acute Pressure Loss Event

7.2 Cavern No. 007 Pressure History

Cavern No. 007 pressure history from November 15, 2020, to March 23, 2023, is presented as Figure 19. Multiple items have thus far been identified which likely influenced the measured surface pressure during this period. The primary factors include: build in cavern pressure from salt creep, modification of tubing, casing and cavern fluids, fluid withdrawal and/or injection operations, and leakage of cavern fluids. Other items which may have influenced the measured surface pressure are still being investigated. Discrete periods of this history were studied independently based upon the predominant activities of the cavern during each time period. Sections of this history provided information to facilitate determination of cavern build rate due to salt creep and a cavern compressibility value, which were then used in a mass balance calculation methodology to determine estimated cavern leak rates.

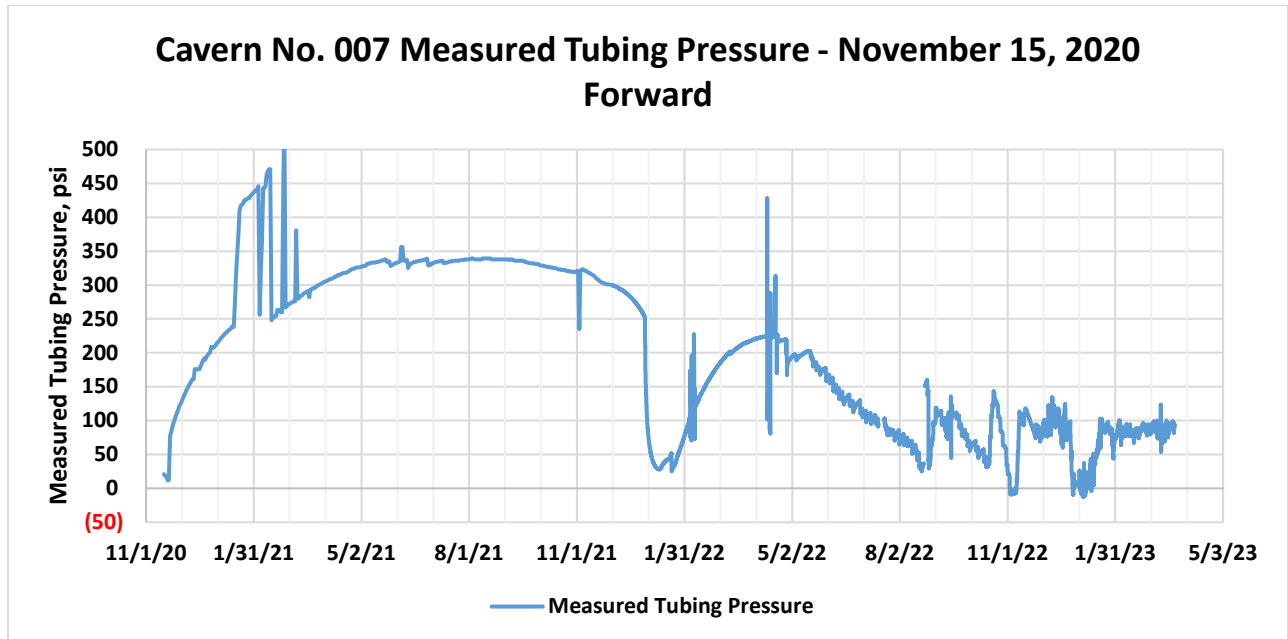


Figure 19 – Cavern 7 Pressure History, November 15, 2020, Forward

7.2.1 Cavern Compressibility Determination

Measured oil volumes and their related pressure drops for withdrawals during the period from May 18, 2022, to August 21, 2022, were used to calculate a compressibility value for the cavern. Figure 20 displays a plot of change in pressure vs. volume withdrawn. The linear fit of this data yields a compressibility value of 0.027488 psi/bbl. This value is subsequently used to convert values in measured cavern pressure (psi) to equivalent volumetric values (barrels), and vice versa.

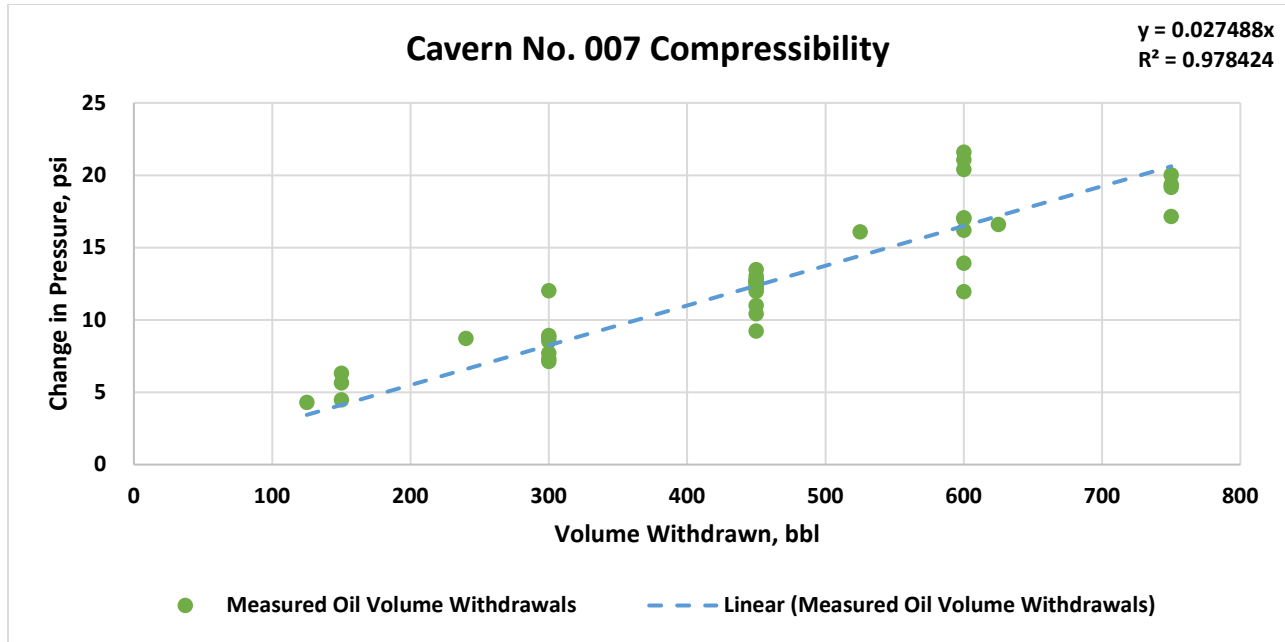


Figure 20 – Cavern 7 Compressibility Determination Trendline

7.2.2 Cavern Build Rate Determination

Multiple sections of cavern pressure history were examined to determine cavern pressure build rate (due to salt creep), which is known to be a function of cavern pressure. Curve fitting methodology over three historical periods, November 21, 2020, to January 14, 2021, February 17, 2021, to May 19, 2021, and January 20, 2023, to April 5, 2023, resulted in the following polynomial equation to estimate cavern build rate as a function of time and cavern pressure, where M_{cp} is measured cavern pressure and T_{hr} is time in hours.

Equation 1 – Cavern Build Rate Estimation

$$Cavern\ Build = (A * M_{cp}^5 - B * M_{cp}^4 + C * M_{cp}^3 - D * M_{cp}^2 + E * M_{cp}) * T_{hr}$$

Where:

Table 3 – Value of Coefficients in Cavern Build Rate Estimation Equation

Coefficient	Value
A	0.000000000047568
B	0.000000052973565
C	0.000021557250933
D	0.003879224537587
E	0.272770022624402

Cavern pressure build rate is highest (high salt creep rate) at lower cavern pressures and the cavern pressure build rate nears zero as it approaches a unique maximum pressure, a point in which the cavern and surrounding salt are in pressure equilibrium. Due to limited data in the surface tubing pressure range below 50 psi, it was decided that cavern build rate is to be a constant of 0.260 psi/hr for surface tubing pressures lower than 50 psi based on build rate trends developed approaching 50 psi.

Figure 21 presents the build rate calculation layered atop recorded historical surface tubing pressures, initiated at various start times at or near the beginning of mostly uninterrupted cavern build-ups. These curves display a progression of pressure build, beginning from the initiation point, providing no other influences on the pressure. Note the deviation that occurs September 1, 2021, and March 7, 2022. These indicate the points in time when the build rate fails to match or exceed the measured pressure.

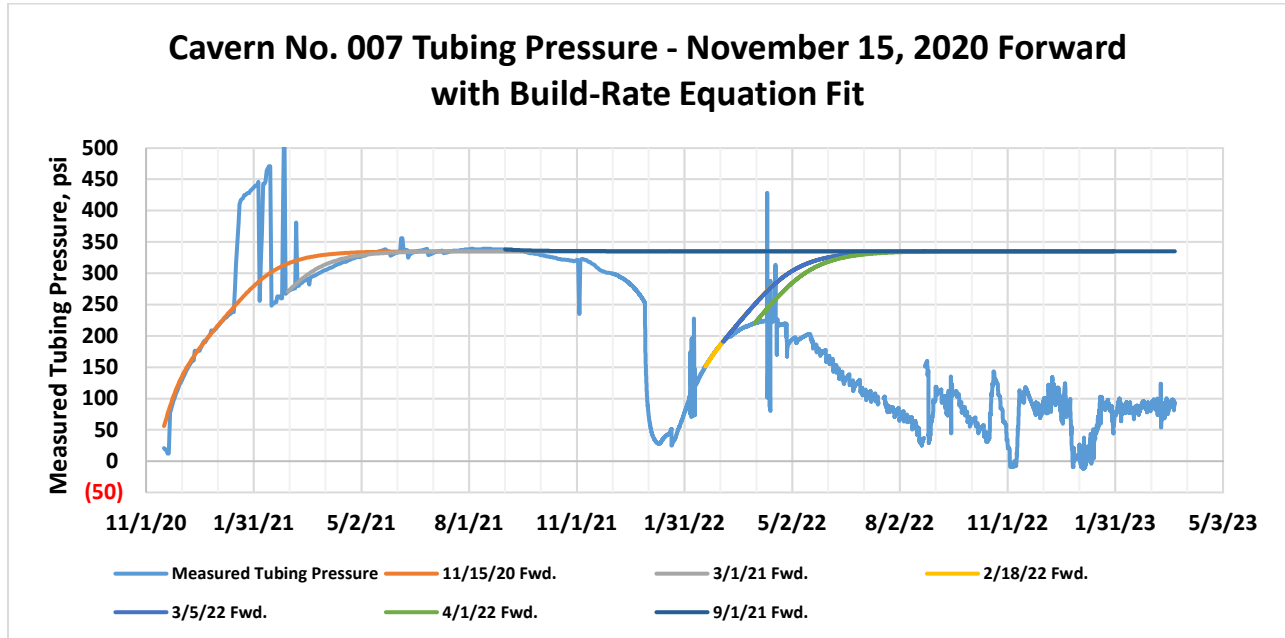


Figure 21 – Cavern 7 Build Rate Calculation Against Measured Historical Pressures

7.2.3 Oil Withdrawals

The accumulation of oil in the PPG No. 7B wellbore is most likely due to migration of residual crude oil that was stored during the DOE SPR ownership and operations. The residual oil was trapped in geometric features of Cavern 7 (e.g. within the undulation of the large flat roof or the roof of the lower “shelf”), and can be “released” due to the following: 1) Released over time due to density drift and slight changes in the cavern shape due to salt creep; 2) Released due to a salt fall event (either at the primary roof or of a geometric shelf within the cavern); 3) Released due to displacement by a lighter fluid (like natural gas or nitrogen).

In reference to cause number 3 above, the oil was initially observed after bleeding down a nitrogen cap in early April 2021. The nitrogen cap was originally put in place in November 2020. Historically, Cavern No. 7 (among other caverns at Sulphur Mines) “produces” some natural gas which due to a lighter density than brine migrates up-hole, into the cavern wellbore entry annulus, and observed accumulating in the wellhead at surface. The “production” of natural gas is a natural phenomenon for many domal salt caverns. The migration and accumulation of natural gas in the wellbore casing causes the surface annulus pressure to increase over time due to the accumulation of a lighter

hydrostatic column height as compared to a brine column. The observed annulus pressure increase does not necessarily mean the cavern pressure is increasing, as that can be better identified by observing the surface tubing pressure (remaining brine filled). However, in order to negate the surface annulus pressure increase trend, the operator decided to install a nitrogen cap within the annulus of the wellbore, and establish the gas/brine interface at or within the large cavern roof diameter. The natural gas may still be migrating up-hole within the cavern but it would then accumulate/mix with the gas volume that has filled (nitrogen and natural gas) and would continue to fill the roof. Thereby not producing a notable change in hydrostatic column height (gas/brine interface essentially doesn't move) due to the large size of the roof and the relatively slow natural gas "production" rate. With the accumulation of gas within the cavern roof, any trapped oil would be displaced from the geometric roof traps and would stratify below the gas cap. When the gas cap is withdrawn from the well, the geometric roof traps then remain full of gas, rather than oil. The un-trapped oil then can migrate and accumulate in the wellbore entry and can be withdrawn from the well.

In reference to cause number 2 above, there was a salt fall event of the lower shelf in Cavern No. 7 at some time between May 2018 and March 2022 (the dates when sonar surveys are available to identify it). It is not clear when exactly the salt fall would have occurred, however, provided the above discussion about the nitrogen cap installation it most likely occurred between November 2020 and March 2022. Long term historical sonar survey analysis (back to 1981) shows that the lower shelf has been experiencing periodic salt falls, so the recent observance of a continuation of the salt falls of the lower shelf is not abnormal. It is possible that residual trapped oil from the historical DOE SPR operations within the roof of the lower shelf could have been released due to the recent salt fall.

Eagle took a prudent approach by deciding to withdrawal any oil accumulation in the wellbore, to reduce potential environmental contamination in the event that a more severe cavern integrity failure were to occur. Therefore, the pressure analysis performed on Cavern No. 7 also incorporates the oil withdrawals.

7.3 Fluid Loss Calculations

7.3.1 Estimated Fluid Loss

Loss calculations are based on a pressure balance with the difference in end of period measured pressure (M_f), less beginning of period measured pressure (M_i), is equal to cavern creep pressure build (B), less withdrawals (W), plus injection (I), minus leakage (L).

Pressure balance:

Equation 2 – Pressure Balance Equation

$$M_f - M_i = B - W + I - L$$

Rearranged, becomes:

Equation 3 – Fluid Loss Equation

$$L = (M_i - M_f) + B - W + I - L$$

An example fluid loss volume calculation is as follows:

Equation 4 – Example Fluid Loss Equation

$$L = (M_i - M_f) + B - W + I$$

$$L = 75 + 600 - 450 + 1750 = -1975 \text{ bbl}$$

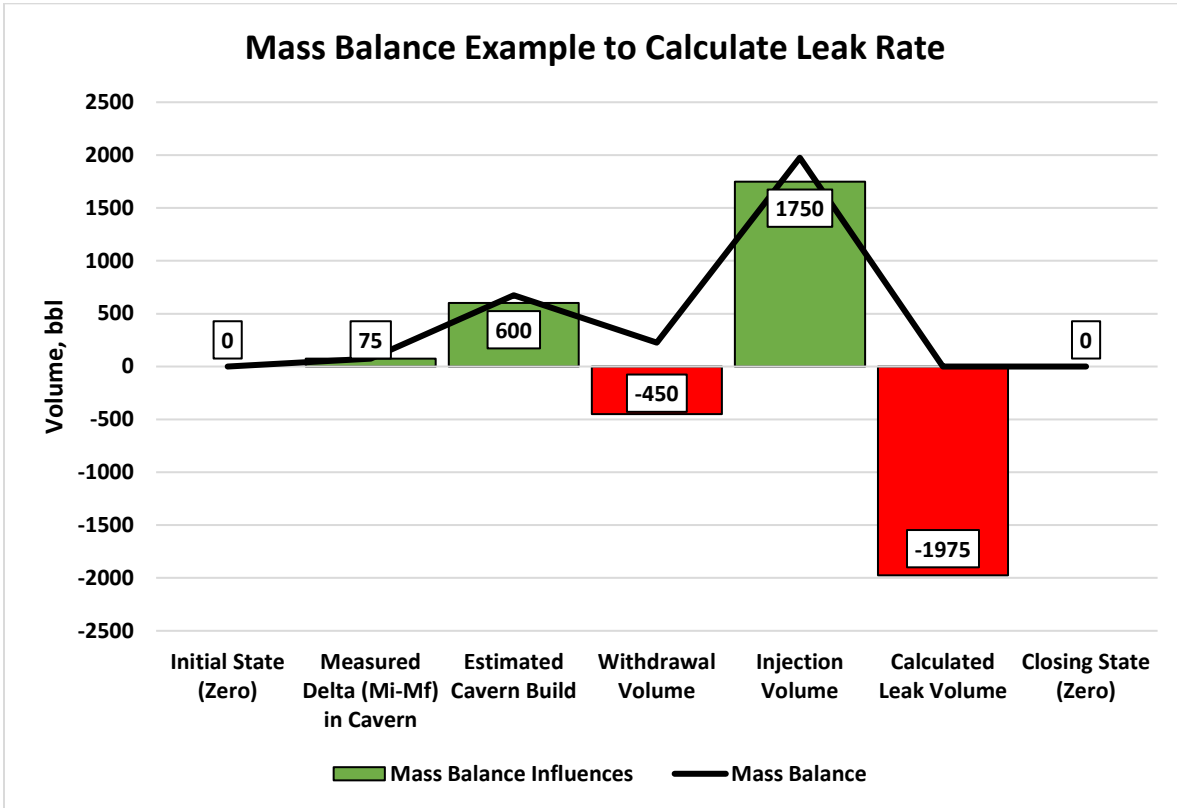


Figure 22 – Example Leak Volume Calculation

All pressure loss calculations were performed in units of psi with the compressibility value of 0.027488 psi/bbl utilized to convert psi to barrels and vice versa as necessary.

7.3.1.1 September 1, 2021 – May 18, 2022

Comparison of the measured cavern pressure to the build curves initialized at both November 15, 2020, and March 1, 2021, (Figure 23) show a departure from the pressure projection on September 1, 2021. Cavern pressure declined from 338 psi to 250.7 psi (total delta of 87.3 psi) prior to the December 29, 2021, loss event. Calculated build rate of 85.4 psi for this period, using Equation 1, added to the measured pressure loss of 87.3 psi equals total pressure loss of 172.7 psi. Conversion of this pressure loss using compressibility of 0.027488 psi/bbl yields a volume loss of 6,281 barrels from September 1, 2021, through December 28, 2021.

The December 29, 2021, pressure loss event, described in Section 7.1, accounts for 223.3 psi drop to reach minimum cavern pressure of 27.4 at 12:00 pm on January 10, 2022. Calculated build rate

of 72.6 psi for this period, added to the pressure loss of 223.3 psi equals total pressure loss of 295.9 psi. Conversion of this pressure loss using 0.027488 psi/bbl yields a volume loss of 10,766 barrels during the pressure loss event of December 29, 2021, through January 10, 2022.

Cavern pressure then began to build from 27.4 psi at 12:00 pm on January 10, 2022, to 47.7 psi at 3:00 pm on January 20, 2022, with a build rate slightly lower than that of the expected build rate. An intentional pressure bleed on the annulus of wellbore 007B then took the tubing pressure down to 25.1 psi, and the cavern began to build again. The calculated build rate of 63.1 psi for this period, minus the measured pressure gain of 20.3 psi equals total pressure loss of 42.8 psi. Conversion of this pressure loss using 0.027488 psi/bbl yields a volume loss of 1,555 barrels from January 10, 2022, to the intentional bleed on January 20, 2022.

The build rate proceeded to follow the build curves initiated from both February 18, 2022, and March 5, 2022, until departure at 194.0 psi, on March 7, 2022, (Figure 23) for a pressure gain of 169.0 psi. In this period, the total calculated build rate is 192.9 psi, however the cavern appears to track on the estimated build-rate curve for a majority of the timeframe. As a result of that trend, in conjunction with the previously stated accuracy of the build-rate equation below 50 psi, it can be assumed that the 192.9 psi minus the measured pressure gain of 169.0 psi, equaling a total pressure loss of 23.9 psi, can be attributed to the lower pressure period of this build. Conversion of this pressure loss using compressibility of 0.027488 psi/bbl yields a volume loss of 870 barrels from January 20, 2022, through March 7, 2022, with most of this volume estimated to be between January 20, 2022, and February 18, 2022.

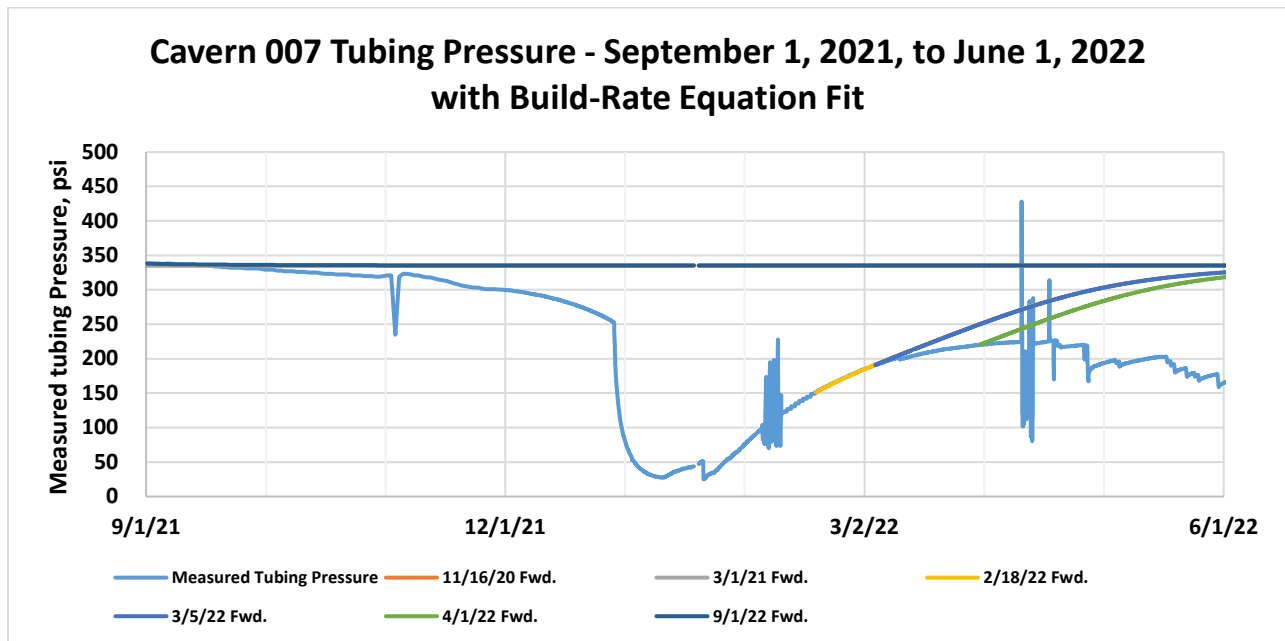


Figure 23 – Cavern 7 Historical Pressure from September 1, 2021, to June 1, 2022

Cavern pressure continued to increase at rates less than those expected from the developed build-rate curve. A maximum pressure of 224.5 psi was recorded on April 11, 2022, at 10:00 am. Subsequent pressure changes from April 11, 2022, until May 18, 2022, are result of the April 2022 brine bleed off in Cavern 6.

Calculated build rate loss of 168.4 psi minus the pressure gain of 8.9 psi results in net loss of 159.5 psi from March 7, 2022, to May 18, 2022. Conversion of this pressure loss using compressibility of 0.027488 psi/bbl. yields a volume loss of 5,802 barrels.

The following table is a summary of this period:

Table 4 – Cavern 7 Fluid Loss Calculations from September 1, 2021, to May 18, 2022

Period Begin	Period End	M _i Measured Initial Pressure psi	M _f Measured Final Pressure psi	M _i -M _f Delta P psi	B Build psi	M _i -M _f +B Leak psi	Leak bbl
09/21/2021	12/29/2021	338.0	250.7	87.3	85.4	172.7	6,281.1
12/29/2021	01/10/2022	250.7	27.4	223.3	72.6	295.9	10,766.0
01/10/2022	01/20/2022	27.4	47.7	(20.3)	63.1	42.8	1,555.2
1/20/2022	1/20/22	47.7	25.1	Intentional Cavern Pressure Bleed			
01/20/2022	03/07/2022	25.1	194.0	(169.0)	192.9	23.9	869.5
03/07/2022	05/18/2022	194.0	202.9	(8.9)	168.4	159.5	5,802.3
Total				112.4	582.4	694.8	25,274.1

Figure 24 presents calculated leak rates over time with data switching from a daily to hourly frequency on December 1, 2021. This figure shows the leak rate starting from near zero at beginning of the period and increasing from a value of approximately 2 bbl/hr on November 1, 2021, to approximately 9 bbl/hr prior to the pressure loss event. A maximum leak rate of 431 bbl/hr occurred from 12:00 am to 1:00 am on December 29, 2021, declining to 8 bbl/hr on January 10, 2022, when pressure begins building. In late January, the leak rate is nominal as the measured pressure conforms to the developed build curve until departure from it again on March 7, 2022, as the leak rate begins to increase.

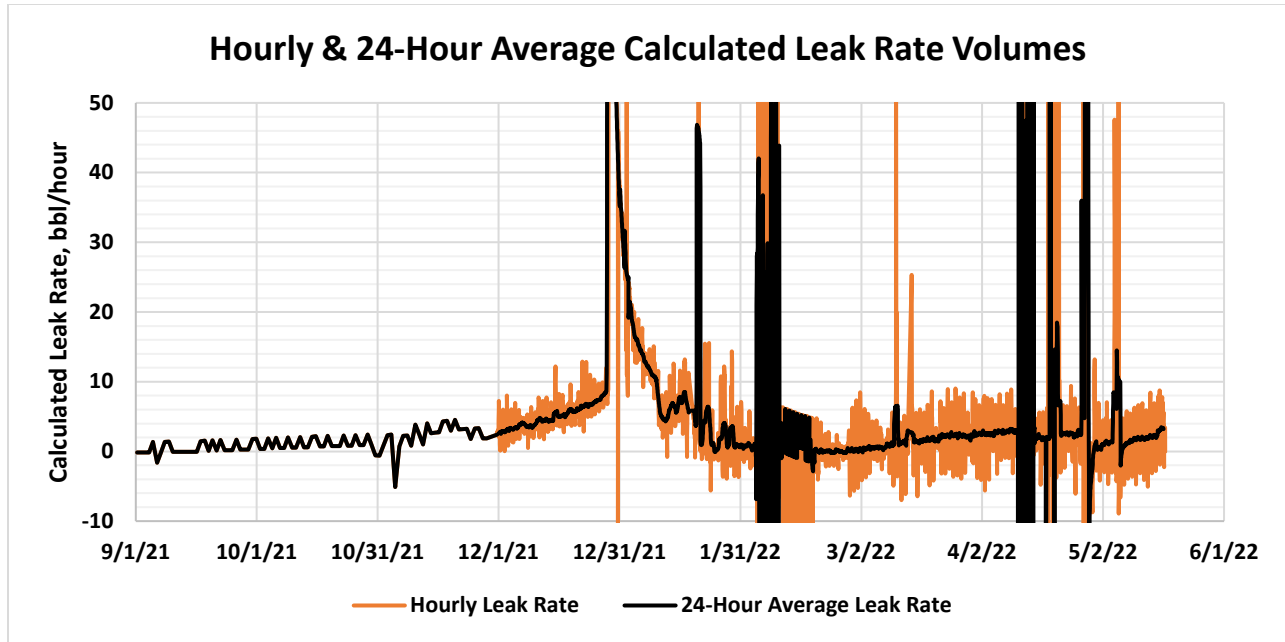


Figure 24 – Cavern 7 Estimated Leak Rate from September 1, 2021, to May 18, 2022

7.3.1.2 May 18, 2022 – August 22, 2022

This period is defined by periodic oil withdrawals that began on May 18, 2022. Cavern pressure and withdrawal volumes for this period, shown in Figure 25, display declines associated with the oil withdrawals followed by increases due to cavern build. During this period, pressures are influenced by oil withdrawals, cavern creep pressure build, and cavern leak. Cavern build is unable to recover pressure losses resulting from withdrawals and cavern leak. Pressure declines for this entire period, from an initial pressure of 202.9 psi to a final of 37.1 psi for a total of 165.8 psi loss. The calculated build rate for this period is 447.7 psi.

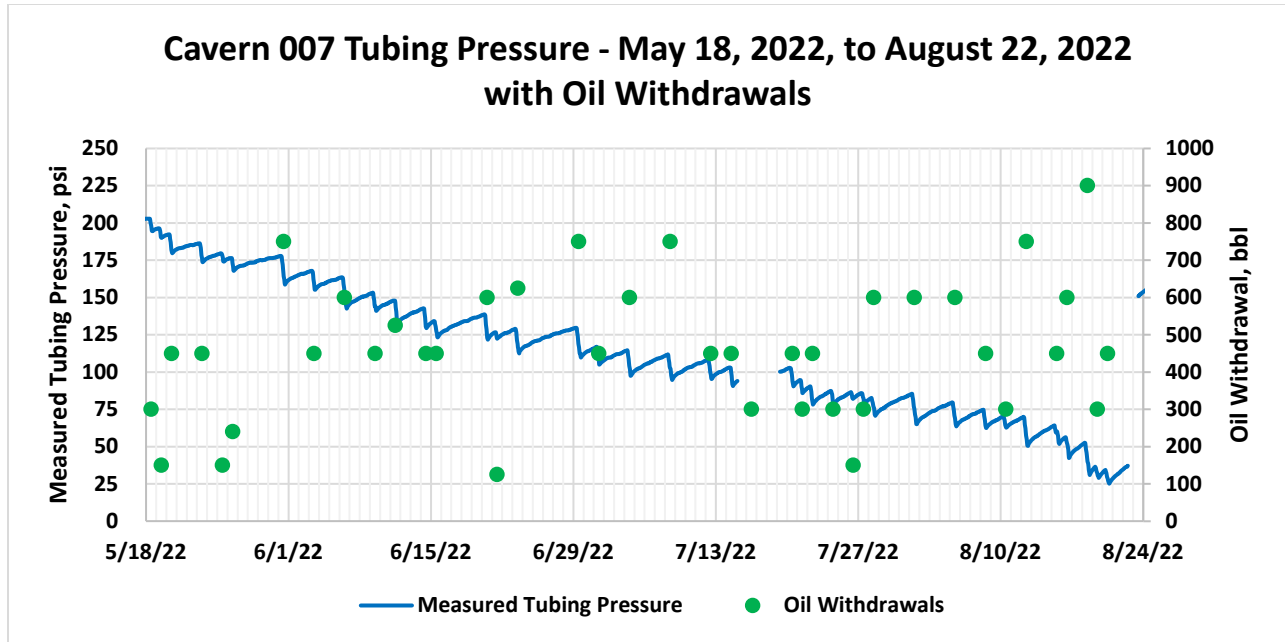


Figure 25 – Cavern 7 Historical Pressure and Oil Withdrawals from May 18, 2022, to August 22, 2022

The oil withdrawals range in size from 125 to 900 barrels at a time. Total oil volume withdrawn during this period is 18,465 barrels, and conversion of this volume to pressure using 0.027488 psi/bbl yields pressure loss of 507.6 psi.

Using Equation 3, it is possible to estimate the cavern leak during this period:

$$L = 202.9 \text{ psi} - 37.1 \text{ psi} + 447.7 \text{ psi} - 507.6 \text{ psi}$$

$$L = 105.9 \text{ psi}$$

Converting 105.9 psi to barrels at 0.027488 psi/bbl yields a volume loss of 3,852 barrels from May 18, 2022, through August 22, 2022.

Figure 26 presents calculated leak rates over time. Leak rates are nominal during this period with rates on a 7-day average basis ranging from 0.5 bbl/hr to nearly 5 bbl/hr.

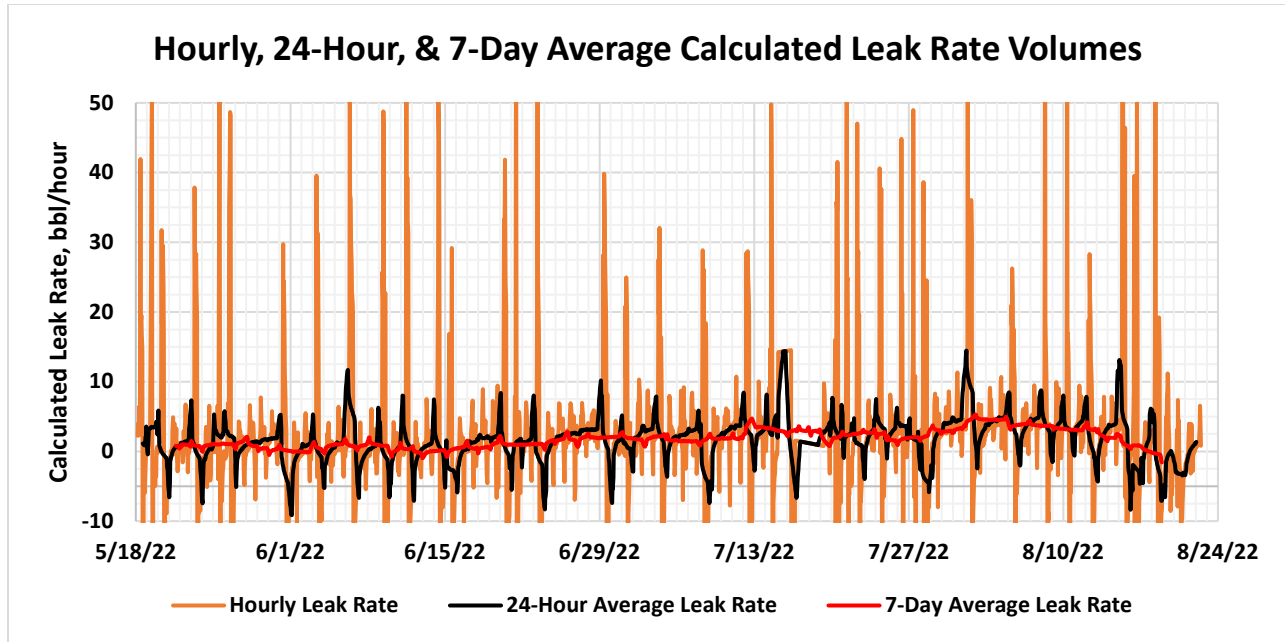


Figure 26 – Cavern 7 Estimated Leak Rate from May 18, 2022, to August 22, 2022

7.3.1.3 August 23, 2022 – March 23, 2023

Cavern pressure and oil withdrawals for the period from August 23, 2022, through March 23, 2023, are displayed in Figure 27. Pressures continue to be influenced by cavern creep pressure build, oil withdrawals, and cavern leak. In addition to these items, saturated brine injection into the cavern commenced with the objective to support cavern pressure above a brine gradient (generally, to maintain a surface tubing pressure between 50 and 100 psi). Initially brine injection began with non-metered periodic volumes, replaced by continuous (24-hour) metered brine injection on January 5, 2023.

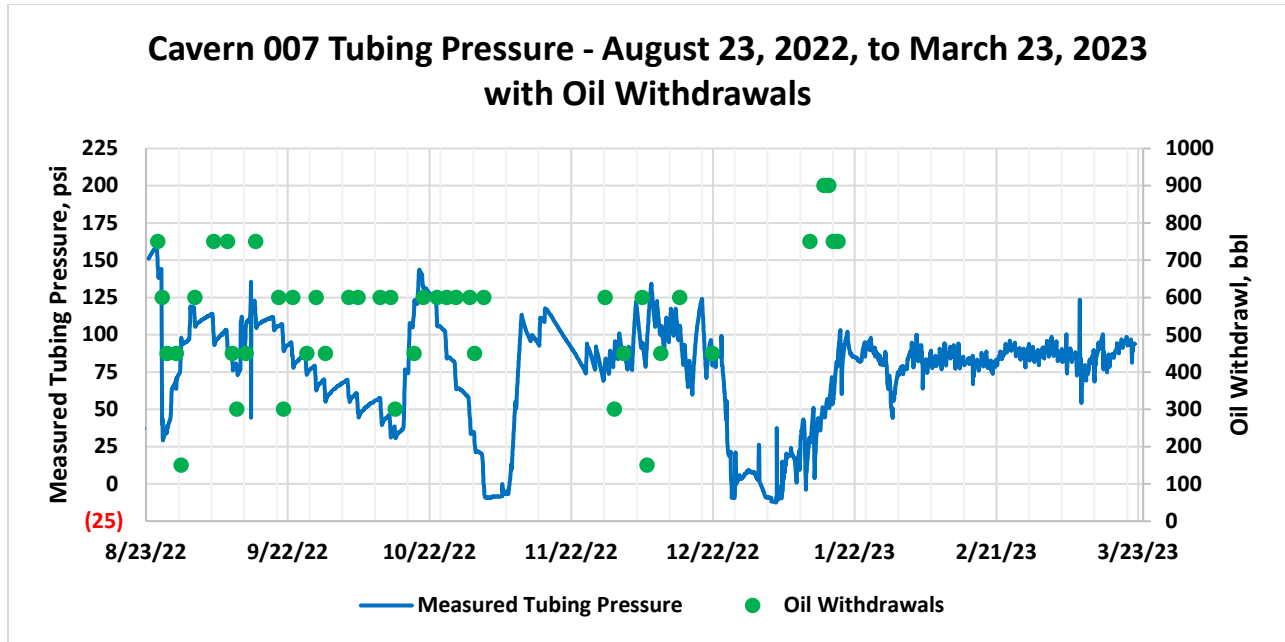


Figure 27 – Cavern 7 Historical Pressure and Oil Withdrawals from August 23, 2022, to March 23, 2023

7.3.1.3.1 Non-Metered Brine Injection (August 23, 2022 – January 5, 2023)

Periodic, non-metered volume injected from August 23, 2022, to January 5, 2023, is 80,571 barrels. Figure 28 presents measured cavern pressure, measured pressure plus withdrawals, and periodic injection volumes for the non-metered injection period. The plot of measured pressure plus withdrawals removes the estimated pressure impact of oil withdrawals, showing cavern build, cavern leak, and injection as the only items influencing cavern pressure.

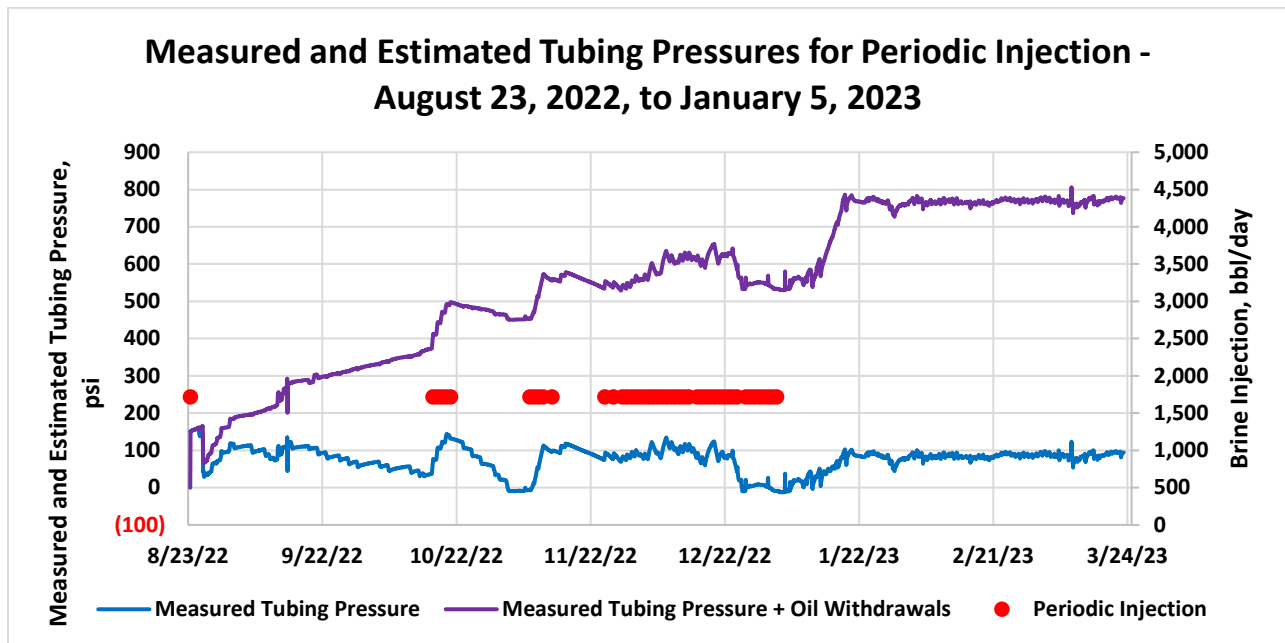


Figure 28 – Cavern 7 Historical and Estimated Pressures with Periodic Injection from August 23, 2022, to January 5, 2023

Three separate injection intervals were identified, followed by daily injection for 8 hours per day. Daily injection commenced November 25, 2022, and continued, except for 4 separate days, through January 3, 2023, when periodic brine injection ended. Non-metered injection volumes correspond well with pressure increases and are presented in Table 5 along with withdrawal amounts and the ratio of injection to withdrawal.

In total for this period, brine injection volumes exceeded the oil volume withdrawn. Comparison of injection volumes to withdrawals (Table 5, Figure 27 and Figure 28) indicate that the brine injection volume of 80,571 barrels was over four times the 19,736 barrels of oil withdrawn.

The following table is a summary of this period:

Table 5 – Cavern 7 Non-Metered Injection and Withdrawal Volumes from August 23, 2022, to January 5, 2023

Injection Frequency	Period Begin	Period End	Injection Volume bbl	Oil Withdrawal volume bbl	Injection / Withdrawal Ratio
Periodic	08/23/2022	08/23/2022	1,714	-	-
Periodic	10/17/2022	10/21/2022	8,571	13,286	0.65
Periodic	11/08/2022	11/13/2022	8,571	3,450	2.48
Daily	11/25/2022	01/03/2023	61,714	3,000	20.57
None	01/04/2023	01/05/2023	-	-	-
Total			80,570	19,736	4.08

Figure 28 shows that measured plus withdrawal pressure (purple line) increases until after the injection period ending October 21, 2022. Pressures decline after this time, increasing only during November 8, 2022, to November 13, 2022, brine injection period, then continuing to decline afterwards. Periodic brine injections did not maintain cavern pressure sufficiently as desired until daily injections commenced.

Figure 29 presents cavern pressure, periodic injection volumes, and continuous injection during the transition period from periodic to continuous injection. Daily injection of approximately 1,714 bbl/day, beginning November 25, 2022, was able to increase cavern pressure and maintain 93 psi average pressure relatively well until 11:00 am, December 24, 2022. At this time, cavern pressure began to decline rapidly from 85.9 psi to a low of -9.4 psi (total delta of 95.3 psi) on December 27, 2022. This event is similar in nature and extent to the first large-scale pressure loss event of December 29, 2021. Pressure remained below 25 psi until January 10, 2023.

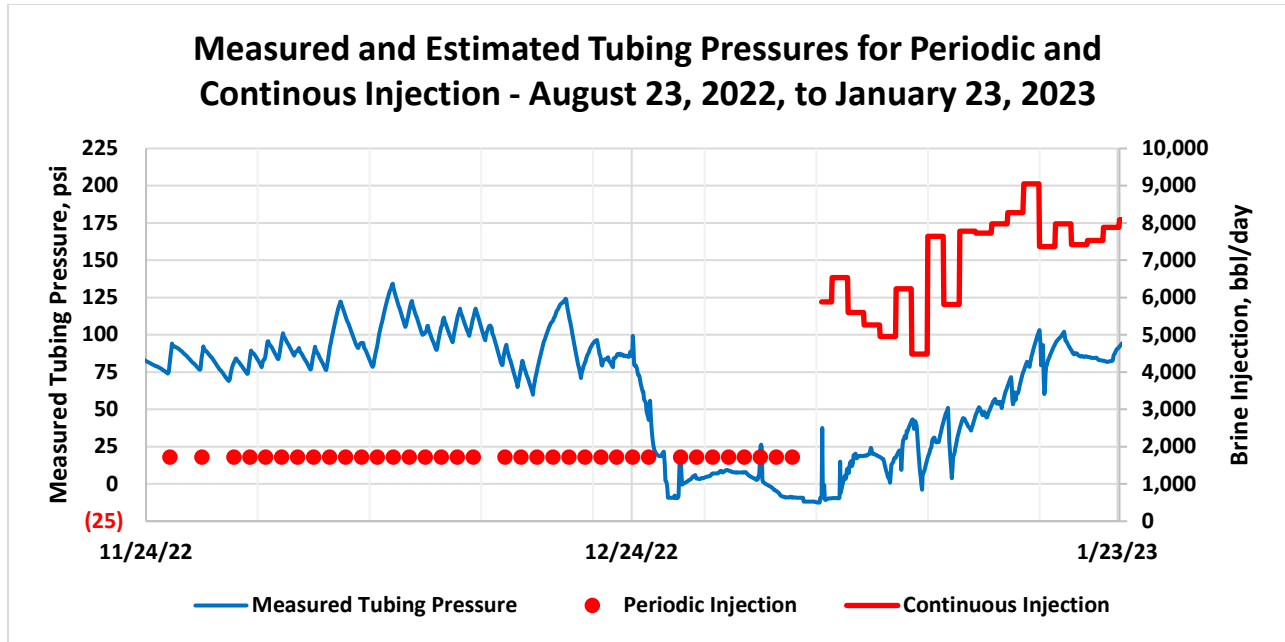


Figure 29 – Cavern 7 Historical and Estimated Pressures and Periodic Injection from August 23, 2022, to January 5, 2023

7.3.1.3.2 Metered Brine Injection (January 6, 2023 – March 23, 2023)

Following this second large-scale pressure drop in the cavern, continuous metered injection began January 5, 2023. Brine injection rates, increasing over time, were able to increase measured cavern pressure and maintain pressure between 80 to 100 psi (surface saturated brine-filled tubing) beginning January 19, 2023, through March 23, 2023. Figure 28, with metered volumes added, is presented as Figure 30.

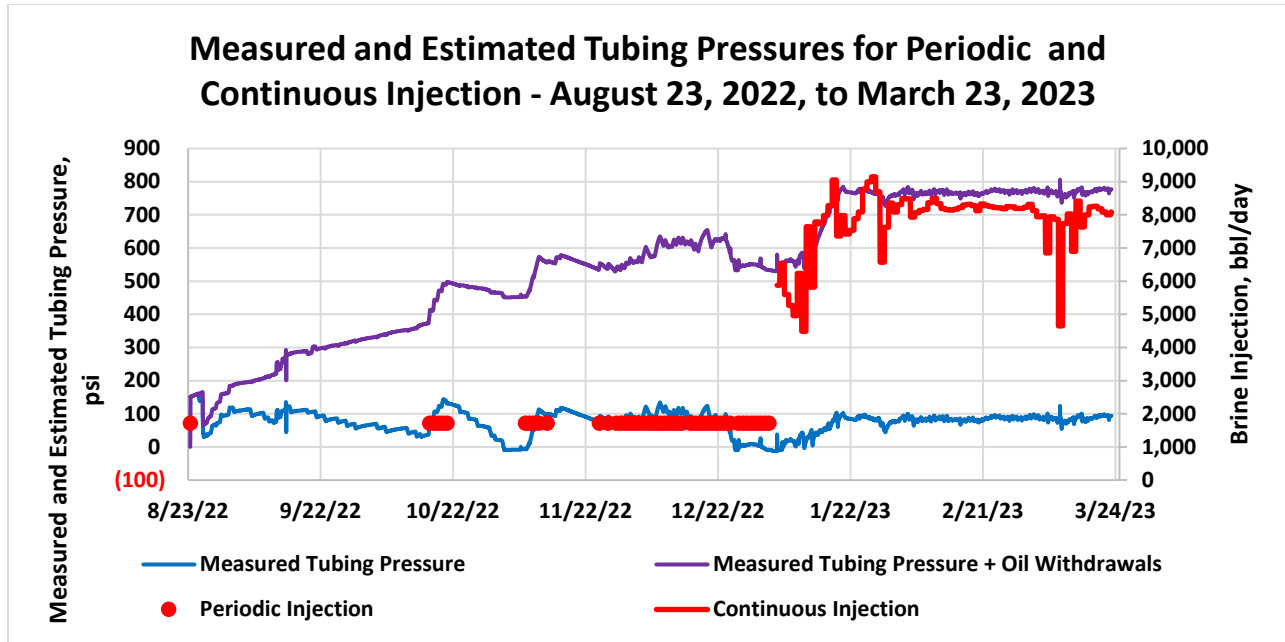


Figure 30 – Cavern 7 Historical and Estimated Pressures with Periodic and Continuous Injection from January 5, 2023, to March 23, 2023

Injection rates began January 5, 2023, at 5,880 bbl/day, increasing to 9,050 bbl/day by January 18, 2023. These rates are notably larger than the approximated 1,714 bbl/day injection rate during the periodic injection period. Cavern pressure responded by increasing from a low of -9.4 psi to 102 psi. The average injection rate and pressure for this period was approximately 6,678 bbl/day and 33 psi.

From January 19, 2023, through January 31, 2023, injection rates varied, ranging from 6,570 bbl/day to 9,150 bbl/day, averaging to 8,035 bbl/day. For this period, cavern pressure remained relatively consistent, with an average pressure of 83 psi.

Injection rates appeared to stabilize beginning February 1, 2023, averaging 8,049 bbl/day through March 23, 2023. For this period, cavern pressure remained consistent, with an average pressure of 86 psi.

Metered injection volumes, ratios of the approximated 1,714 bbl/day rate, pressures, and oil withdrawal volumes are presented in Table 6.

Table 6 – Cavern 7 Metered Injection and Withdrawal Volumes from January 5, 2023, to March 23, 2023

Injection Frequency	Period Begin	Period End	Days	Injection Volume bbl	Injection Volume bbl / day	Continuous to Periodic Ratio	Average Tubing Pressure Psi	Oil Withdrawal Volume bbl
Continuous	01/05/2023	01/18/2023	13.7	91,269	6,678	3.9	32.6	5,100
Continuous	01/19/2023	01/31/2023	12.9	103,350	8,035	4.7	82.7	-
Continuous	02/01/2023	03/23/2023	50.2	404,146	8,049	4.7	85.7	-
Total / Average bbl/day			76.7	598,765	7,803			5,100

From August 23, 2022, cavern pressure declined from 151.1 psi to 85.9 psi (total delta of 65.2 psi) leading up to a rapid pressure loss event on December 24, 2022. Measured pressure loss of 65.2 psi, plus 679.8 psi for cavern build, minus 542.5 psi caused by withdrawals, plus injection pressure gain of 1,761.2 psi equals a net pressure loss of 1,963.7 psi. Conversion of this pressure loss using compressibility of 0.027488 psi/bbl yields a volume loss of 71,439 barrels between August 23, 2022, and December 24, 2022.

Beginning 11:00 am, December 24, 2022, cavern pressure rapidly declined from 85.9 psi to -9.4 psi (total delta of 95.3 psi) at 4:00 pm, December 27, 2022 (due to cold weather causing surface line salt precipitation blockage issues). Measured pressure loss of 95.3 psi, plus 16.8 psi of cavern build, less 0.0 psi caused by withdrawals (no withdrawal volume during this time), plus injection pressure gain of 76.6 psi equals net pressure loss of 188.7 psi. Conversion of this pressure loss using compressibility of 0.027488 psi/bbl yields a volume loss of 6,866 barrels in the pressure loss event from 11:00 am, December 24, 2022, to 4:00 pm, December 27, 2022.

Cavern pressure remained low until January 5, 2023, increasing with the start of continuous injection. Pressure increased from December 27, 2022, low of -9.4 psi to 93.9 psi (total delta of 103.3 psi) by 5:00 pm, March 23, 2023. Calculated build of 509.8 psi, less the 103.3 psi gain in measured pressure, minus 140.2 psi caused by withdrawals, plus brine injection pressure gain of 16,835.8 psi equals net pressure loss of 17,102.1 psi. Conversion of this pressure loss using compressibility of 0.027488 psi/bbl yields a volume loss of 622,167 barrels between December 27, 2022, and March 23, 2022.

The following table is a summary of this period:

Table 7 – Cavern 7 Fluid Loss Calculations from August 23, 2022, to March 23, 2023

Period Begin	Period End	M _i Measured Initial Pressure psi	M _f Measured Final Pressure psi	M _i -M _f Delta P psi	B Build psi	W Withdrawal psi	I Injection psi	M _i -M _f +B- W+I Leak psi	Leak bbl
08/23/2022	12/24/2022	151.1	85.9	65.2	679.8	542.5	1,761.2	1,963.7	71,438.9
12/24/2022	12/27/2022	85.9	(9.4)	95.3	16.8	0.0	76.6	188.7	6,865.5
12/27/2022	03/23/2023	(9.4)	93.9	(103.3)	509.8	140.2	16,835.8	17,102.1	622,166.7
Total				57.2	1,206.4	682.7	18,673.6	19,254.5	700,471.1

Figure 31 presents calculated leak and injection rates since injection commenced. Following a single day of injection on August 23, 2022, the average leak rate through October 16, 2022, averaged 3.6 bbl/hr. Pressures increases (Figure 28 or Figure 30) for this time because 3.6 bbl/hr is less than cavern build value of 8.5 bbl/hr.

In general, leak rates are higher during injection periods, but the two characteristics cannot necessarily be correlated as dependent on one another. The average leak rate from October 17,

2022, through October 21, 2022, was 41.2 bbl/hr with pressure increase from 36.4 psi to 131.4 psi. For the injection period November 8, 2023, through November 13, 2022, average leak rate was 41.4 bbl/hr with pressure increase from -6.7 psi to 99.3 psi.

Leak rates increased following October 21, 2022, injection period. Average rate from October 22, 2022, through November 24, 2022, excluding injection from November 8, 2022, through November 13, 2022, was 12.0 bbl/hr. Pressures decrease (Figure 28 or Figure 30) following injection for this time because 12.0 bbl/hr is greater than cavern build value of 8.4 bbl/hr.

Leak rates increased during daily injection from November 25, 2022, until a rapid pressure decline which began December 24, 2022. Rates increased from 40 bbl/hr to 90 bbl/hr, averaging 67.5 bbl/hr. Pressure was relatively stable with an average of 93.0 psi.

Leak rate averaged 105.6 bbl/hr from December 24, 2022, to December 27, 2022, pressure loss event. Pressure declined from 85.9 psi to -9.4 psi for a total of 94.3 psi. Following this, the leak rate averaged 77.1 bbl/hr until continuous injection began on January 5, 2023. Pressures remained negative until after continuous injection began.

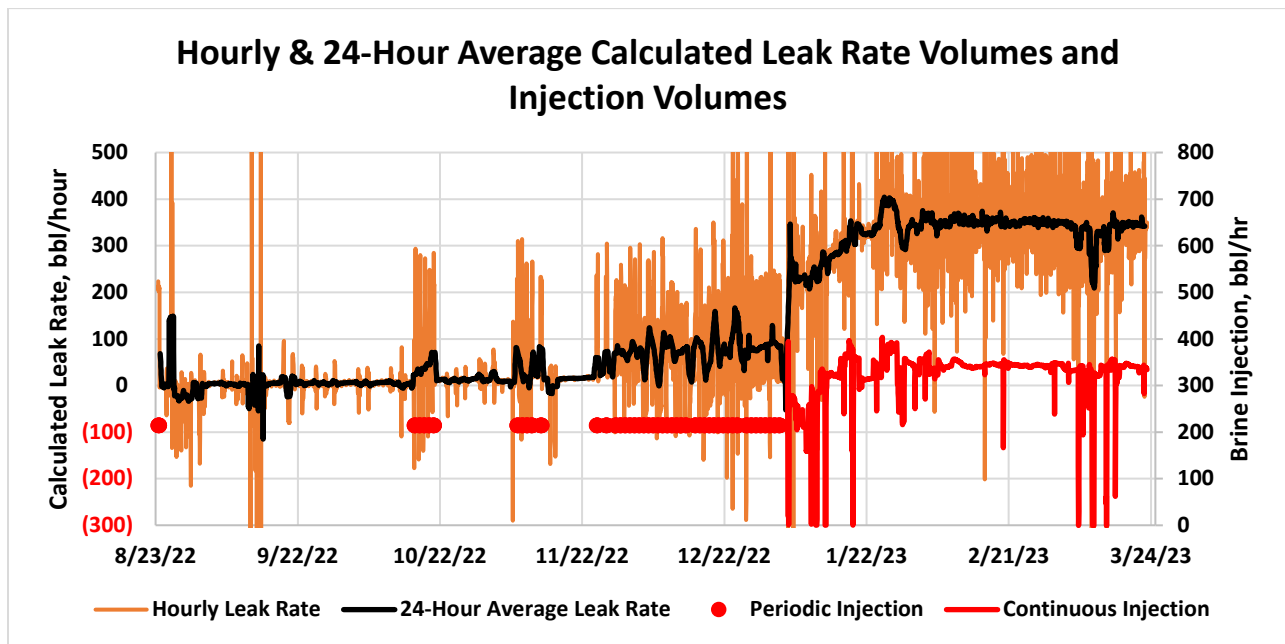


Figure 31 – Cavern 7 Estimated Leak Rate from August 23, 2022, to March 23, 2023

Since continuous injection began January 5, 2023, leak rates have paralleled injection rates and pressures respond correspondingly similar (Figure 31). From January 5, 2023, through January 18, 2023, leak rates increased from 210 bbl/hr to 320 bbl/hr with a 259.8 bbl/hr average. Pressure increased from -9.4 psi to 102.1 psi (total delta of 111.5 psi).

Leak rates varied from January 19, 2023, through January 31, 2023, ranging from 295 bbl/hr to 360 bbl/hr, with an average of 346.4 bbl/hr. More stable leak rates began February 20, 2023, and continue through March 23, 2023, with an average of 343.7 bbl/hr. Average pressure from January 19, 2023, through March 23, 2023, is 85.1 psi.

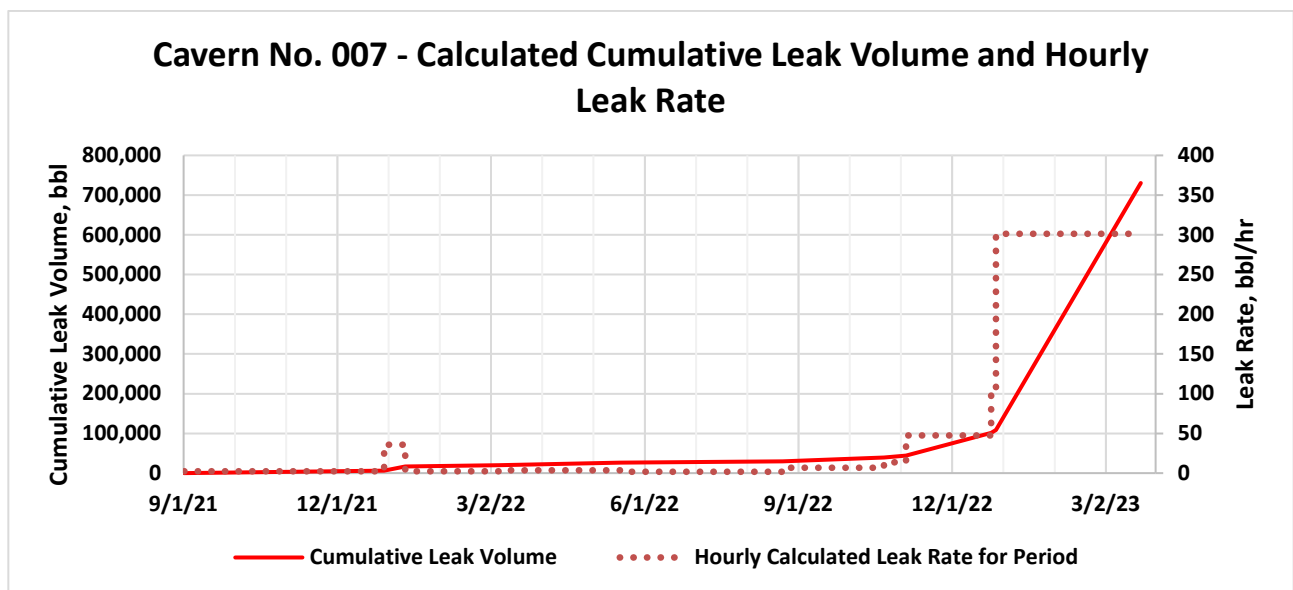
Leak rates of 340+ bbl/hr, since the rapid pressure decline of December 24, 2022, are significantly higher than 67.5 bbl/hr rate prior to that date.

7.4 Summary of Cavern 7 Pressure Loss Event and Estimated Fluid Loss

Total volumes, for the period from September 1, 2021, through March 23, 2023, were leak volume of 729,597 barrels (20,055.2 psi), withdrawal volume of 43,301 barrels (1,190.3 psi) and injection volume of 679,335 barrels (18,673.5 psi). Table 8 details volumes for the discrete periods examined. Figure 32 displays cumulative leak volume over time and average leak rate for each period between cumulative volumes. Both curves increase significantly with initiation of continuous injection.

Table 8 – Fluid Loss Calculations from September 1, 2021, to March 23, 2023

Period Begin	Period End	M _i Measured Initial Pressure psi	M _f Measured Final Pressure psi	M _i -M _f Delta P psi	B Build psi	W Withdrawal psi	I Injection psi	M _i -M _f +B- W+I Leak psi	Leak bbl	
09/01/2021	01/20/2022	338.0	47.7	290.3	221.1	-	-	511.3	18,602.4	
01/20/2022	01/20/2022	47.7	25.1	Intentional Cavern Pressure Bleed						-
01/20/2022	05/18/2022	25.1	202.9	(177.8)	361.2	-	-	183.4	6,671.8	
05/18/2022	08/22/2022	202.9	37.1	165.8	447.7	507.6	-	105.9	3,851.9	
08/22/2022	08/23/2022	37.1	151.1	Assumed Brine Injection (Unmetered)						-
08/23/2022	03/23/2023	151.1	93.9	57.3	1,206.4	682.7	18,673.6	19,254.5	700,471.1	
Total				335.5	2,236.4	1,190.3	18,673.6	20,055.2	729,597.2	



Loss calculations provided in this report begin with departure from flat portion of pressure history on September 1, 2021, through March 23, 2023. No consideration of the possibility of cavern leakage prior to this is included. It is possible that leakage may have begun prior to this date as described by the following scenarios.

Leakage at less than build rate, still allowing the pressure to increase, may have occurred from November 15, 2020, to May 22, 2021. If this occurred, observed pressure increases would be less than the cavern build since total pressure changes were diminished by leak rates.

Leakage equivalent to build rate, allowing for no change in pressure, may have occurred from May 22, 2021, to September 1, 2021. Pressure remained essentially flat with a 336.0 psi average until departure from projected build curve on September 1, 2021.

8 Cavern 6 History & Geologic Structure

8.1 Historical Timeline (Major Events)

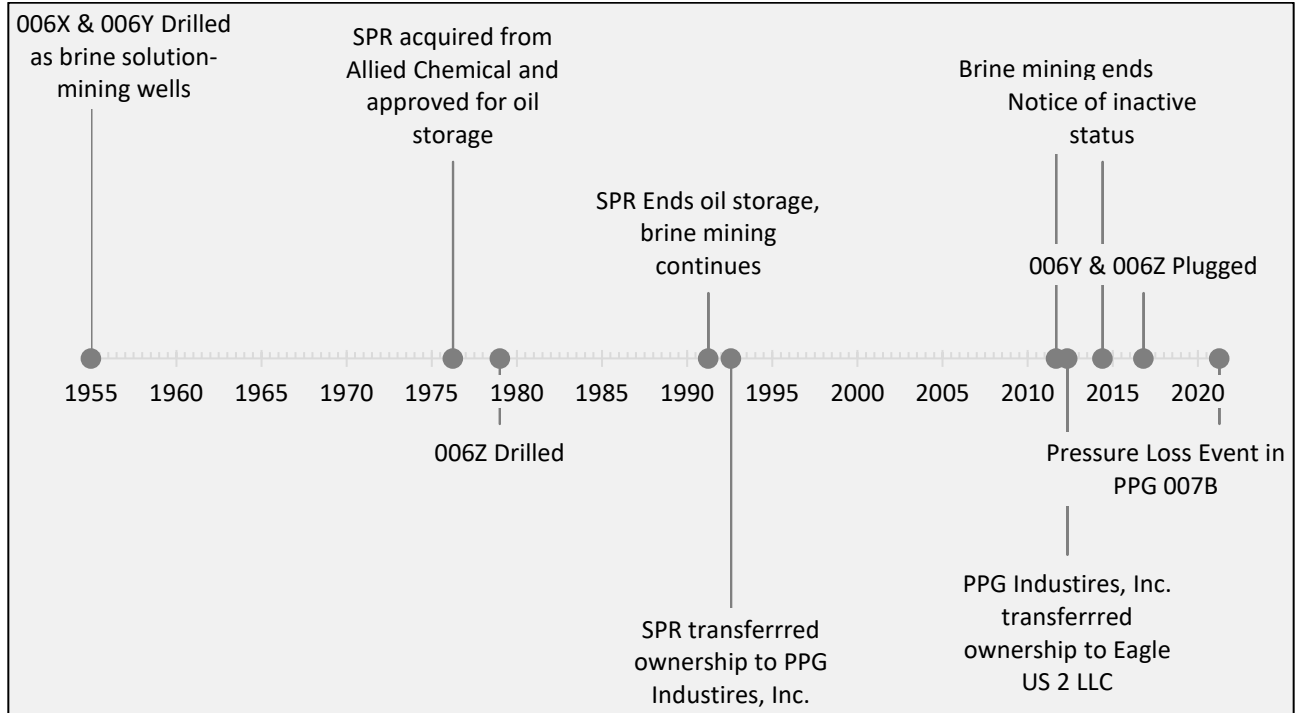


Figure 33 – Cavern 6 Timeline (Major Events)

8.2 Distance to Salt Dome Flank

The dome flank geometry has been estimated via geological interpretation of historical offset well data. A detailed description of the methodology used in mapping the dome surface is provided in a later section. Cavern 6 geometry and position has been modeled from a deviation survey of the 6X wellbore and sonar surveys of the Cavern 6 interior. The minimum 3D distance from Cavern 6 to the dome flank is estimated to be roughly 301 feet based on an overlay of all available digital sonar files dating from July 2011 to March 2023. Figure 34 displays the minimum distance to flank from the historical overlay of cavern 7 sonars. There are ongoing evaluation efforts to review and attempt to improve the confidence of the cavern to flank spacing, however, with the current data and understanding it is anticipated that the spacing will not deviate significantly from the current 160 foot interpretation.

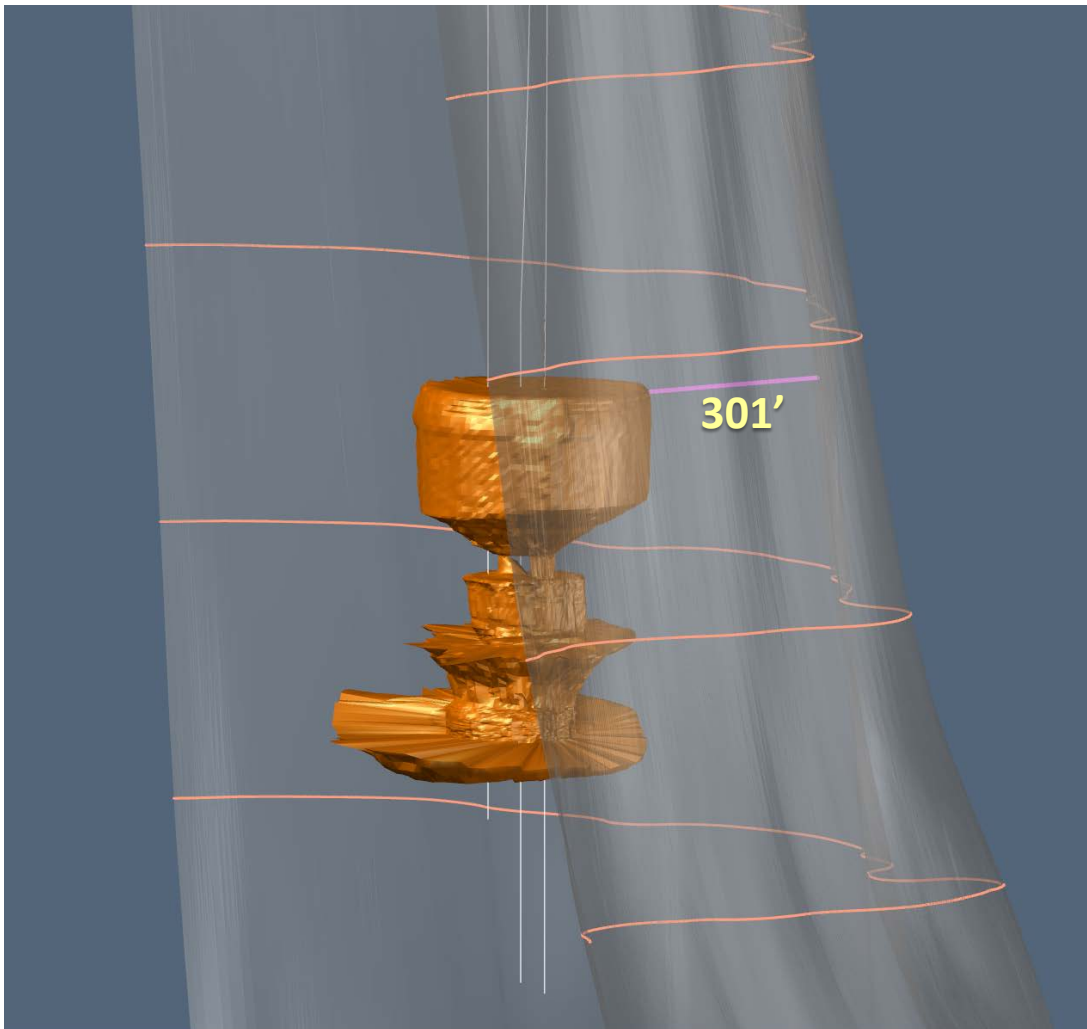


Figure 34 – Cavern 6 Minimum 3D Distance to Salt Dome Flank

8.3 Cavern 6 Distance to Cavern 7

Cavern 6 is located northeast of Cavern 7 with a minimum spacing distance of 29.4 feet based upon most recent sonar surveys, wellbore directional surveys, and three-dimensional geo-spatial analysis. Figure 35 and Figure 36 display relative position and minimum distance between caverns.

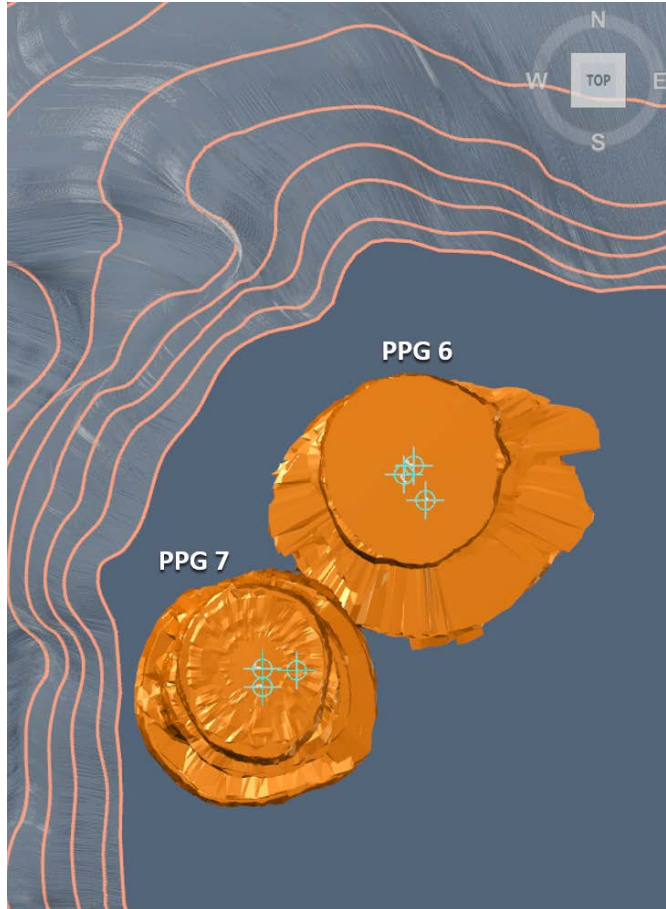


Figure 35 – Plan view of Cavern 6 and Cavern 7

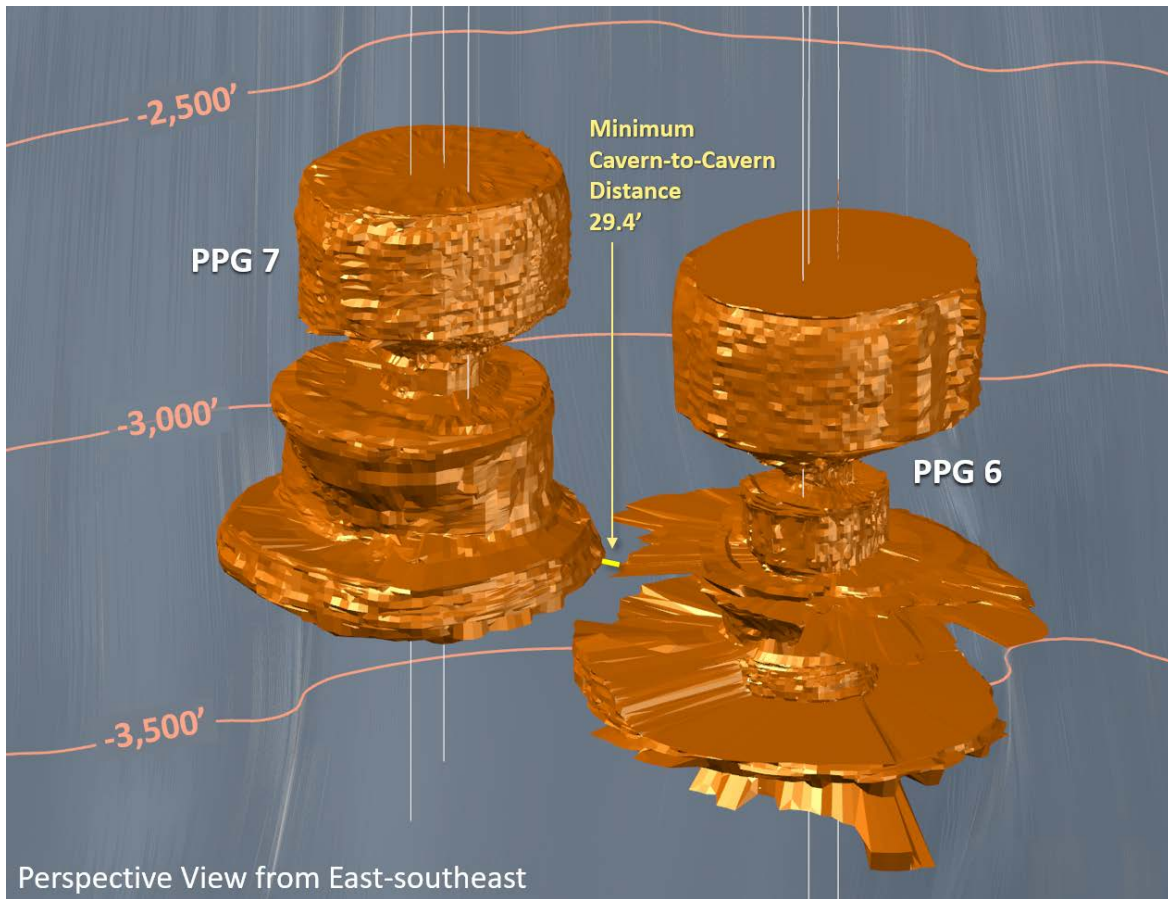


Figure 36 – Perspective view of Cavern 6 and Cavern 7 showing minimum web thickness

Cavern 6 is deeper than Cavern 7, with approximately 120 feet difference in their top of cavern vertical elevations. Relative depths of the caverns are shown in Figure 37.

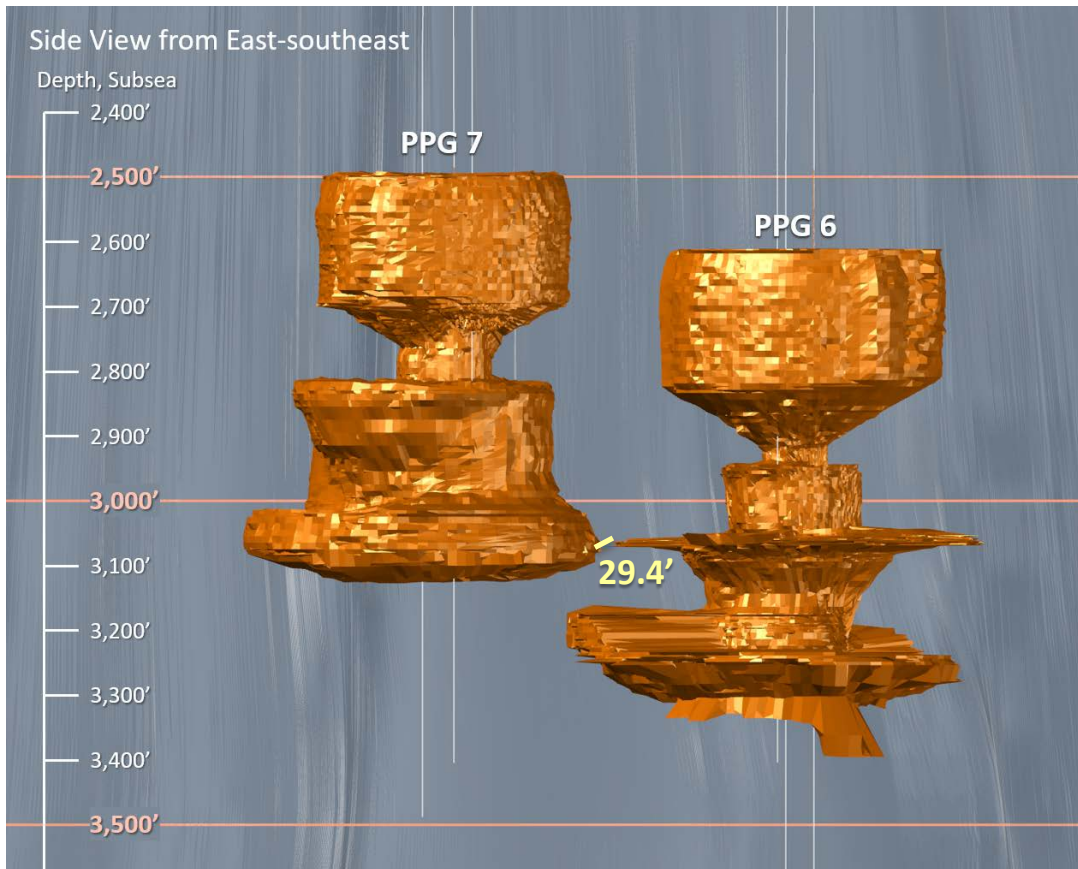


Figure 37 – Side view of Cavern 6 and Cavern 7

8.4 Notable Workover, Inspection, and Sonar History

The following table lists all notable cavern and wellbore inspection or workover activity where sufficient records exist to list it.

Table 9 – Workover, Inspection, & Sonar History of Cavern No. 006

Date	Work Description
December 29, 2977	Sonar via 006X
February 19,1993	Sonar via 006X
April 7, 1995	Sonar via 006X
May 22, 1997	Sonar via 006X
June 10, 1999	Sonar via 006X
October 19, 2001	Sonar via 006X
October 30, 2003	Sonar via 006X
November 10, 2005	Sonar via 006X
January 30, 2008	Sonar via 006X
July 11, 2011	Sonar via 006X
July -October 2016	Casing Inspection/Sonar/MIT's on 006X, 006Y, & 006Z
July 2017	P&A of 006Y & 006Z
March 2020	Temp Log
December 13, 2021	Sonar & Nitrogen Integrity Test
March 12, 2023	Sonar

8.5 Wellbore Diagrams

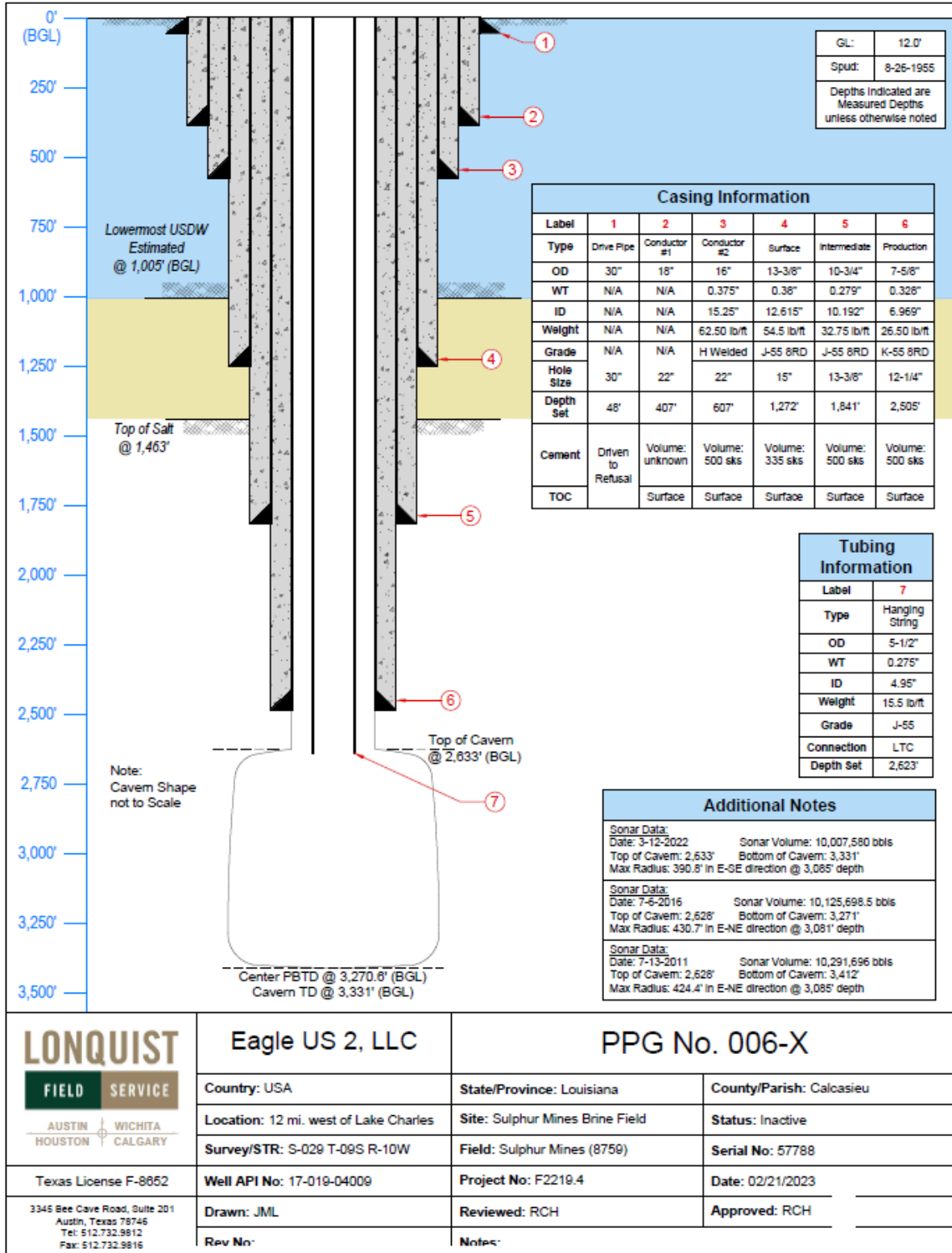


Figure 38 – As-Built Wellbore Diagram of PPG 006X

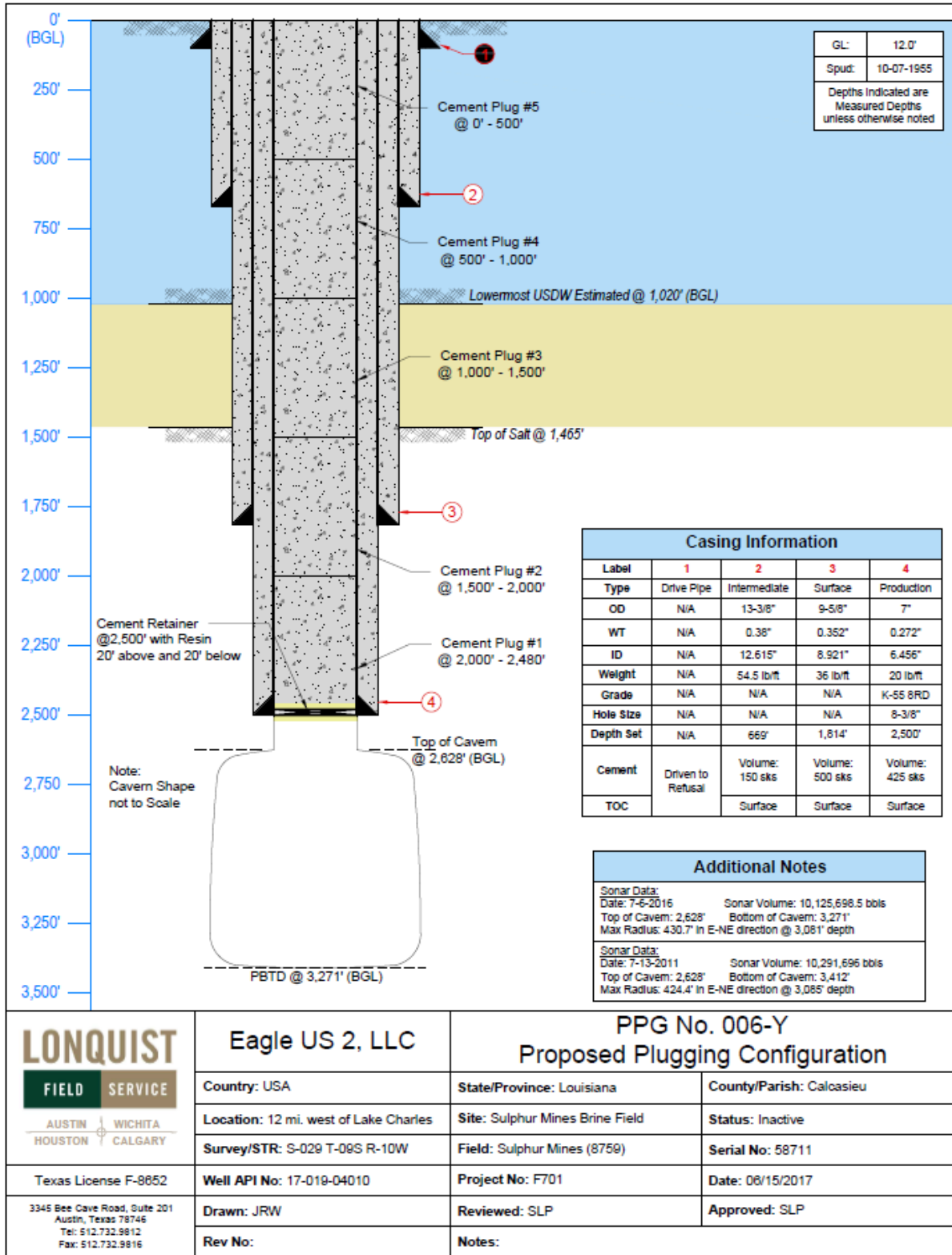


Figure 39 – As-Built Wellbore Diagram of PPG 006Y

LONQUIST & CO. LLC

PETROLEUM
ENGINEERS

ENERGY
ADVISORS

AUSTIN · HOUSTON · WICHITA · DENVER · BATON ROUGE · COLLEGE STATION · CALGARY · EDMONTON

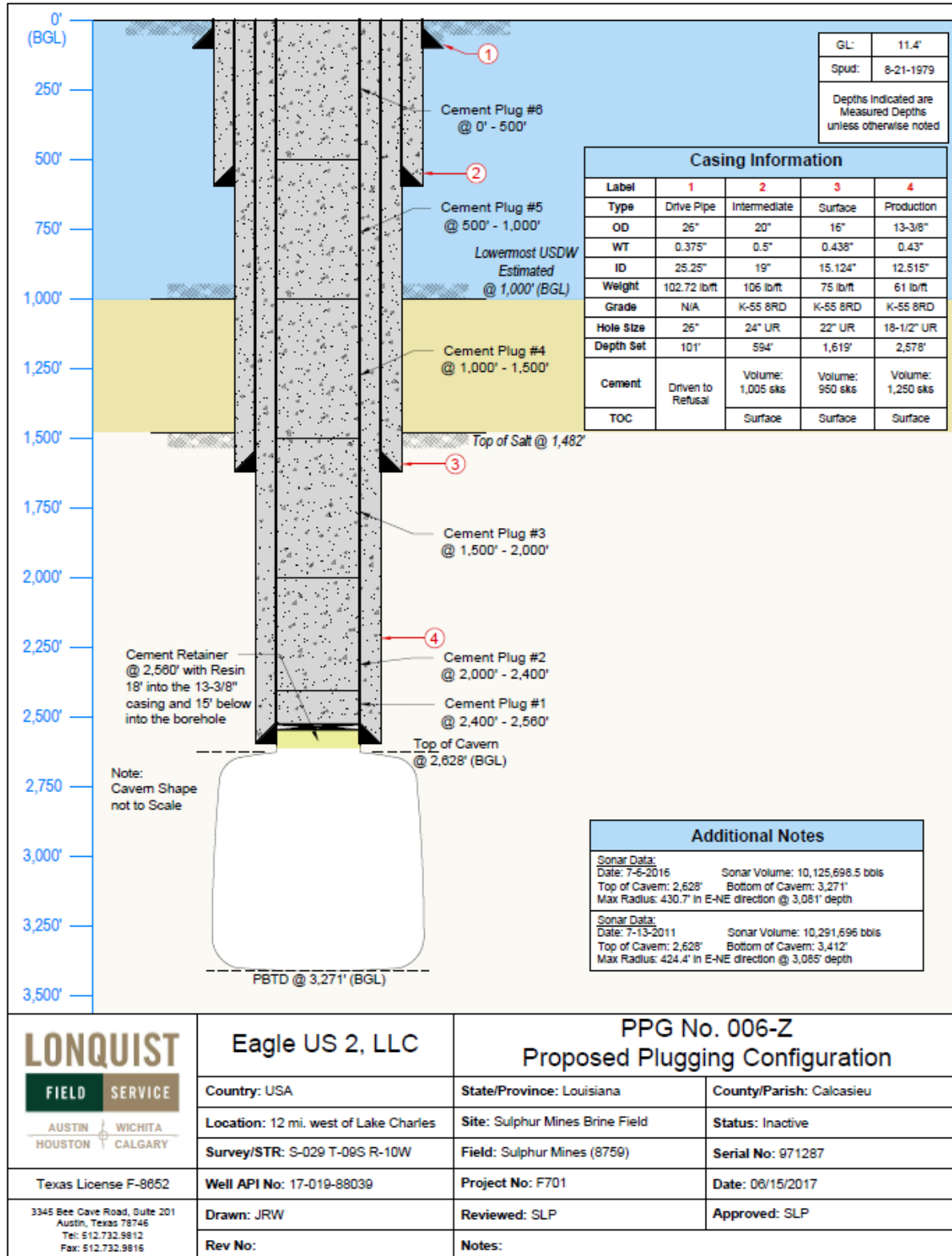


Figure 40 – As-Built Wellbore Diagram of PPG 006Z

9 Cavern 6 Integrity Failure Pressure Analysis

9.1 Pressure History

Cavern 6 pressure history, from November 15, 2020, to March 23, 2023, is presented in Figure 41. Cavern No. 7 pressure history is included for comparison and reference. Throughout this period multiple instances may be noted when Cavern 7 behavior or activity appears to influence Cavern 6.

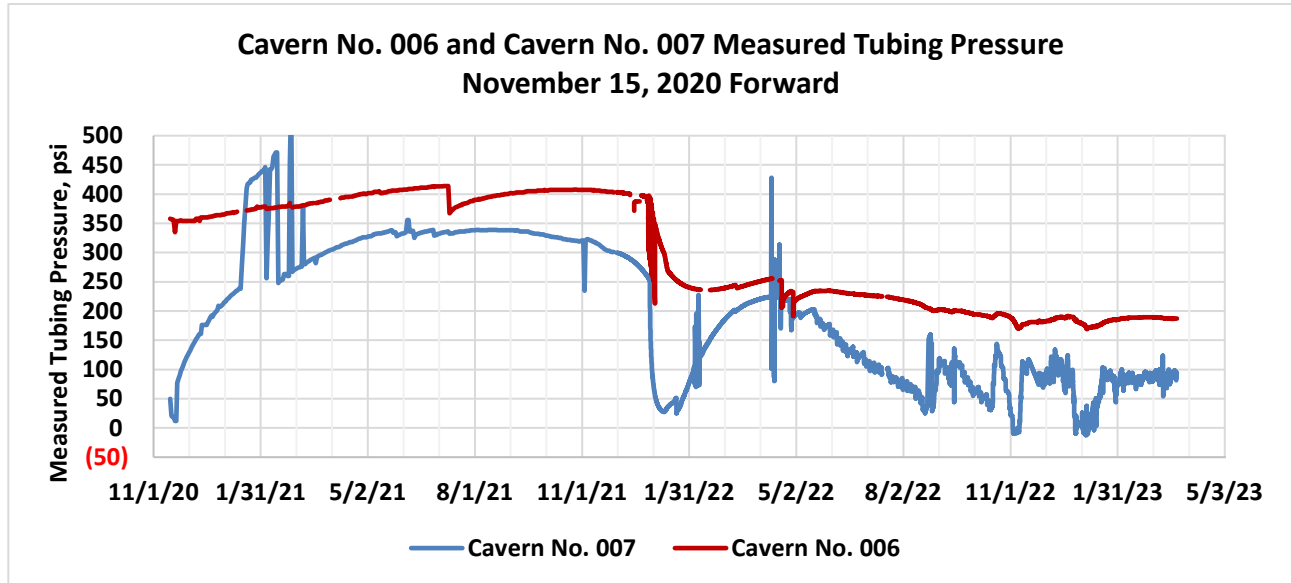


Figure 41 – Measured Tubing Pressure History for Cavern 6 & Cavern 7

On September 1, 2021, which coincides with the timing of the beginning of the pressure decline in Cavern 7, the rate of pressure increase for Cavern 6 begins to decrease. The surface tubing (brine filled) pressure reached 408 psi on October 27, 2021, declining to 397.6 psi by the December 29, 2021, pressure loss event.

Both caverns experienced rapid pressure decline following the December 29, 2021, pressure loss event. By January 10, 2022, Cavern 6 pressure declined 100.2 psi compared to Cavern 7 pressure decline of 223.3 psi. Pressure decrease for Cavern 6, not as rapid as Cavern 7, totaled 161.3 psi by February 10, 2022.

Pressures for both caverns increased from their minimums until declining as a result of April 2022 brine removal from Cavern 6. Increases in pressure resumed for both caverns, continuing until Cavern 7 oil withdrawals began May 18, 2022. During the period of Cavern 7 oil withdrawals, prior to the beginning of periodic brine injections on August 23, 2022, Cavern 6 pressure declined 29.0 psi while Cavern 7 pressure declined by 165.8 psi.

Since the beginning of oil withdrawals on Cavern 7, Cavern 6 pressure has not shown any increase without the benefit from some manner of injection into Cavern 7. Cavern 6 pressures increased

coincidentally with periodic injection into Cavern 7 on August 23, October 17 to October 21, and November 8 to November 13 (all in the year 2022). Daily brine injection into Cavern 7, beginning November 25, 2022, coincides with Cavern 6 pressure increase until December 24, 2022, when a rapid decline in Cavern 7 pressure occurred. In response to a 96.8 psi pressure drop for Cavern 7 by January 5, 2023, Cavern 6 pressure declined 20.9 psi over the same period. Cavern 6 pressure began increasing shortly after initiation of continuous brine injection into Cavern 7 on January 5, 2023.

When evaluating the aggregate pressure loss from October 27, 2021, through March 23, 2023, Cavern 6 pressure decreased 221.1 psi, while Cavern 7 pressure decreased by 227.1 psi.

9.2 Fluid Loss Calculation

Cavern 6 pressure data was available for determination of the salt creep closure build rate for pressures above 350 psi. No pressure data exists for Cavern 6 below 350 psi. Equation 1, developed from Cavern 7 data, was used for pressures below 350 psi. For pressures above 350 psi, a minimum build rate of .01140 psi/hr was used which was derived using Cavern 6 data from November 30, 2020, through July 10, 2021.

Compressibility value of 0.027488 psi/bbl, calculated from Cavern 7 data, is used to convert measured cavern pressure (psi) to equivalent volumetric values (barrels), and vice versa. Cavern 6 and Cavern 7 have a similar sonar volume of approximately 10,000,000 barrels and which commonly produces a similar cavern compressibility value based on supportive operational data. In this case, Cavern 7 had what was viewed to be the more favorable supportive operational data to calculate a cavern compressibility value whereas Cavern 6 did not have that operational data. This was the reasoning for using the same cavern compressibility value for both caverns.

From September 1, 2020, through March 23, 2023, Cavern 6 pressure declines from an initial pressure of 402 psi to a final pressure of 186.9 psi for a total of 215.1 psi loss. The calculated build due to salt creep closure for this period was 1,529.0 psi.

Using Equation 3, it is possible to estimate leakage volume from Cavern 6 from September 1, 2021, through March 23, 2023.

$$L = 402.0 \text{ psi} - 186.9 \text{ psi} + 1529.0 \text{ psi}$$

$$L = 1744.1 \text{ psi}$$

Converting 1,744.1 psi to barrels at 0.027488 psi/bbl yields a volume loss of 63,449 barrels for Cavern 6. When considering the total leakage volume from Cavern 7, this value would be in addition to the leak volume calculated for Cavern 7 of 729,597 barrels. It is highly likely that all volume leakage from Cavern 6 is migrating directly into Cavern 7, and most likely at the point of minimum web thickness between the two caverns.

Figure 42 presents calculated leak rates over time for Cavern 6. Leak rates for Cavern 6 were below 1 bbl/hr prior to December 29, 2021, pressure loss. Declining from peak rates after the event, leak rates declined until reaching less than 3 bbl/hr from March 2022 until mid-May 2022. After mid-May 2022, leak rates increased overall until reaching a range of 5 bbl/hr to 7 bbl/hr beginning August 2022. The variance in leak rates over this period is most likely due to Cavern 6 responding to pressure changes in Cavern 7.

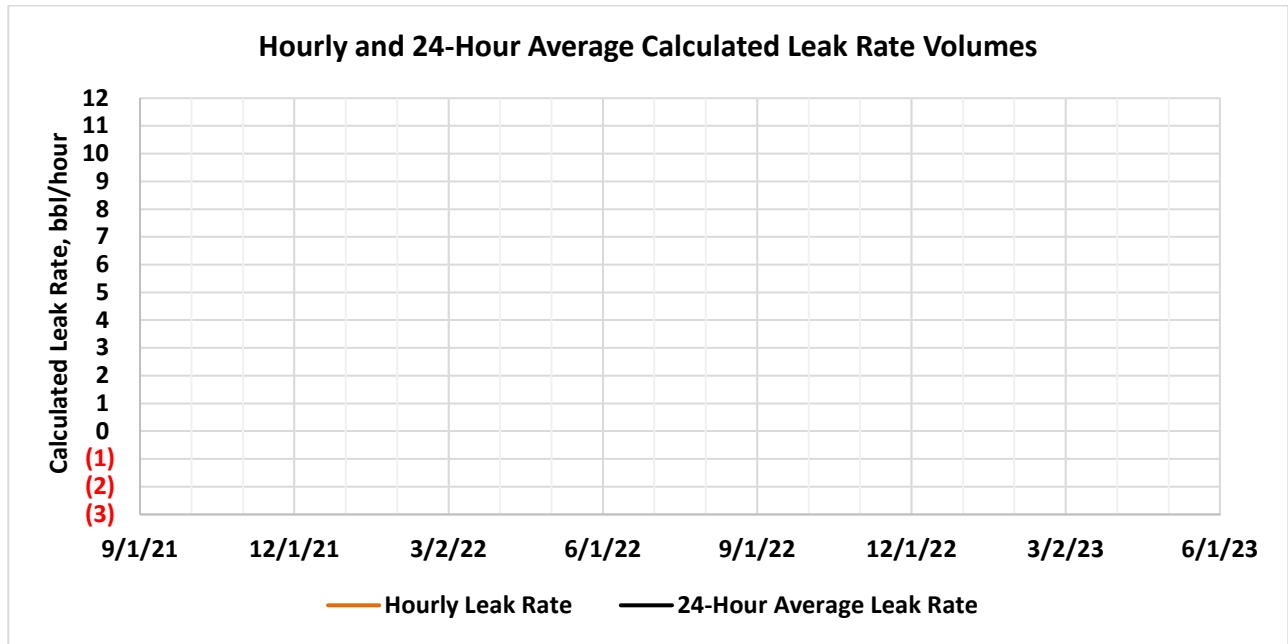


Figure 42 – Cavern 6 Estimated Leak Rate from September 1, 2021 to March 23, 2023

10 Post-Failure Evaluation & Monitoring

10.1 Monitoring

10.1.1 Surface Observations/Monitoring

Prior to the events on Cavern 7, pressures were monitored and documented twice daily by Eagle technicians. Field observations of the wellsite and wellhead were conducted at least once a day. As of January 2023, the decision was made to increase observations and monitoring of Cavern 7 and Cavern 6. Observations on dayshift include a Eagle technician who monitors pressures throughout a 12-hour shift and personnel who perform field wide observations twice daily. A nightshift observer was added in which this person monitors pressures on Cavern 7 and Cavern 6 and observes the field every hour throughout the night. The observer's role is to monitor pressures on Cavern 6 and 7, observe the entire dome looking for any surface expressions, identify any existing surface expressions for change in intensity, and perform air monitoring at all surface expression locations (bubble sites).

10.1.2 Wellhead & Downhole Pressure Monitoring

Prior to the December 2021 acute pressure loss event, casing and tubing surface pressures were recorded via digital instrumentation at a frequency of one minute average which was stored on a computer hard drive. Additionally, manual pressure readings were taken once per day and stored via computer spreadsheet.

Subsequent to the December 2021 acute pressure loss event, casing and tubing surface pressures are recorded via digital gauges. Once per week, or more frequently, if necessary, the data is analyzed to assess field-wide pressure trends.

A downhole pressure-temperature gauge was installed in Well No. 7B of Cavern 7 on February 13, 2023, at a depth of 2,650'. This gauge records cavern pressure and temperature at a frequency of one reading every nine seconds. Once per week, or more frequently, if necessary, the data is analyzed to assess trends and align with well operations.

10.1.3 Surface Seismic Monitoring Stations / Downhole Seismic Geophones

A three-phase passive seismic monitoring plan has been developed for monitoring seismic activity at Sulphur Mines Salt Dome, using a 1) temporary surface seismic array (in operation from January 30, 2023, to about April 3, 2023), 2) a semi-permanent telemetered surface seismic array (operational April 5, 2023 and currently in operation) and 3) a dual-array borehole seismic array in two existing cavern wellbores (proposed). These phases are described in detail below.

10.1.3.1 Phase 1: Temporary Surface Seismic Array

Seven "temporary" seismic boxes were installed at the end of January 2023 to quickly initiate passive seismic recording of seismic data on the dome. The location of the seismic stations has varied; the current locations (as of March 6, 2023) are shown in Figure 43.

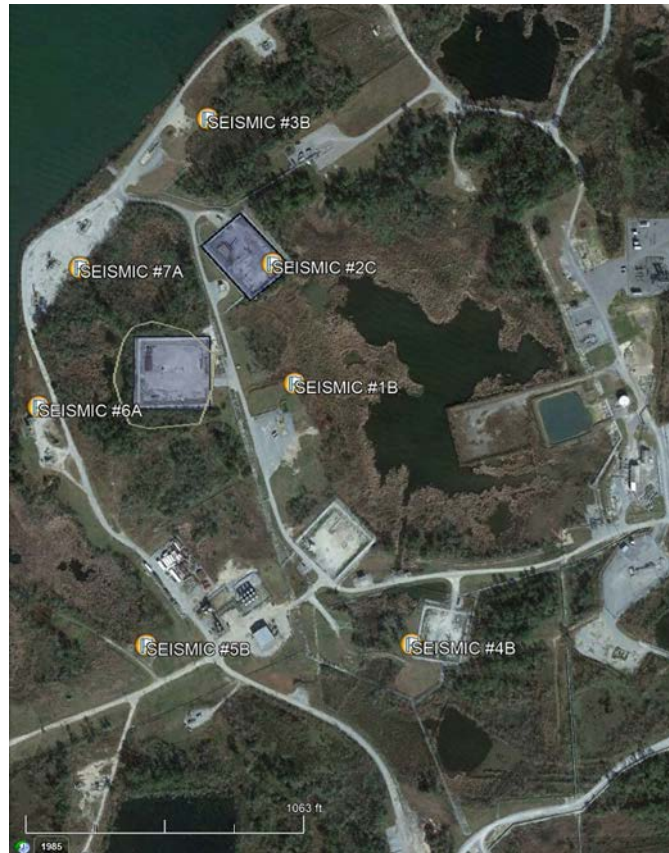


Figure 43 – Temporary Seismic Recording Station Locations at Sulphur Mines Salt Dome. Station Locations as Of Feb 27, 2023 As Provided By Eagle.

Each temporary seismic station records on a removable disk (SD Data card). The removable data cards were exchanged and shipped for data processing every two to three days.

The temporary seismic array was functional beginning mid-February 2023, with some intermittent monitoring in early February. The magnitude detection threshold of the surface array based on the background noise levels was magnitude 1.0. One seismic event was detected on the Sulphur Mines Dome Phase 1 seismic array on March 18 at 4:06:06 PM, however, there was not enough information to compute an accurate event location, but it can be confirmed the event was not in proximity to Cavern 7. The magnitude was likely in the 0 to 1 range. The evaluation of this event prompted the relocation of certain stations for implementation in Phase 2.

10.1.3.2 Phase 2: Semi-Permanent Surface Seismic Array

The semi-permanent seismic stations have replaced the Phase 1 stations. The network stations directly transmit a live, continuous data stream via cell phone telemetry to the analytical company for seismic data processing. The analytical company processed the data weekly, including event detection and locations.

The Phase 2 array was installed in early April 2023, and the seismic sensor for each station was buried about six inches below ground level. The electrical equipment for recording and transmitting the data is placed in a sealed box and mounted on a pole. The station is solar powered via a solar panel mounted above the equipment box. The data is sampled at 125 samples per second with a GPS-synced timing system and continuously telemetered to the analytical company to perform weekly data processing.

Notification to the LDNR will be made within 24 hours if a seismic event is detected and identified. If seismic activity becomes more common, a discussion will be held with the LDNR on an appropriate seismicity level for 24-hour reporting. Currently, a bi-weekly seismic monitoring report is provided to the LDNR. The semi-permanent surface array currently has a magnitude threshold of about -0.5 to 3.5. Figure 44 shows an example of a semi-permanent, pole-mounted JDS surface seismic station installation. It is expected that this semi-permanent surface seismic array will operate until the proposed borehole array (Phase 3) is operational. The Phase 2 array will eventually be decommissioned after verifying the Phase 3 borehole array is performing as desired.



Figure 44 – Example of a JDS Pole-Mounted Seismic Station

10.1.3.3 Phase 3: Borehole Seismic Network

Experience in seismic monitoring at the Napoleonville salt dome in response to the 2012 failure of Oxy Geismar 3 cavern has demonstrated that placing geophone sensors into the salt dome 1) greatly lower the background noise levels, 2) allows the recording of seismic vibrations at closer distances, and 3) the seismic signals are not transmitted through the cap rock and near surface swampy surface sediments which attenuate the signal. Borehole arrays have shown to greatly improve the magnitude detection threshold. At Napoleonville, the magnitude detection threshold of the borehole seismic array is about magnitude < -2 for events within 3,000' of the array (Shemeta, 2023).

Borehole arrays are superior for collecting small-magnitude microseismic activity and should indicate areas of low-level subsurface fracturing that might indicate potential areas of concern.

Two retrievable arrays are proposed to constitute a borehole seismic network at Sulphur Mines dome, using existing available cavern wellbores PPG 6X (Serial No 57788) and PPG 20 (Serial No. 973364). These wellbores are proposed because 1) they are either inactive or near end of solution mining life, 2) they have a preferred wellbore casing configuration, 3) the feasibility modeling indicated favorable results (discussed in more detail below). The two wellbores are proposed to be instrumented with a custom-built, six-level analog 15 Hz geophones array. Each array will include a pressure and temperature (PT) gauge: at the time of this plan, it is proposed for the 6X PT gauge to be below the geophones (~2,500' depth) and PPG 20 array to have a PT gauge suspended into the salt cavern body (~3,600'). Six geophone levels are the maximum number of sensors available for Avalon's retrievable seismic array.

The sensor placement in each well was chosen to 1) place the geophones in a single layer of cemented casing to improve signal coupling to the salt and 2) extend the length of the array as much as possible to improve the resolution of interpreting the event locations. The geophones in the PPG 6X wellbore will be placed approximately 120' apart, within the 7-5/8" cemented production casing from approximately 1,900' to 2,500'. The sensors proposed for the wellbore of PPG 20 will be within the 13-3/8" cemented production casing, spaced at approximately 280' apart and span from approximately 1,875' to 3,300' (Figure 45).

Wellbore inspection work including casing inspection logs, a cement bond log, a background noise wellbore survey, and a sonar survey will be performed in each wellbore. To further support feasibility of the Phase 3 plans, these inspection workovers will be performed prior to ordering the long lead time borehole seismic equipment. Build time for the custom seismic arrays varies but is estimated to be completed in roughly 20 to 40 weeks upon initiation of the materials/design order, and installation of the materials into the wellbores would be completed within two to three weeks of material delivery. Once the Phase 3 system is operating, the Phase 2 surface array seismic reporting will be replaced by the borehole seismic monitoring.

10.1.3.3.1 Borehole Modeling

A seismic monitoring company, performed a feasibility study for borehole monitoring using the geometries described above for PPG 6X and PPG 20. The feasibility study was designed to model the location of seismic events in the vicinity of Cavern 7 (the salt and sediments above and below the cavern to a depth about 4,500'). The location uncertainty modeling results are shown in Figure 46 and Figure 47.

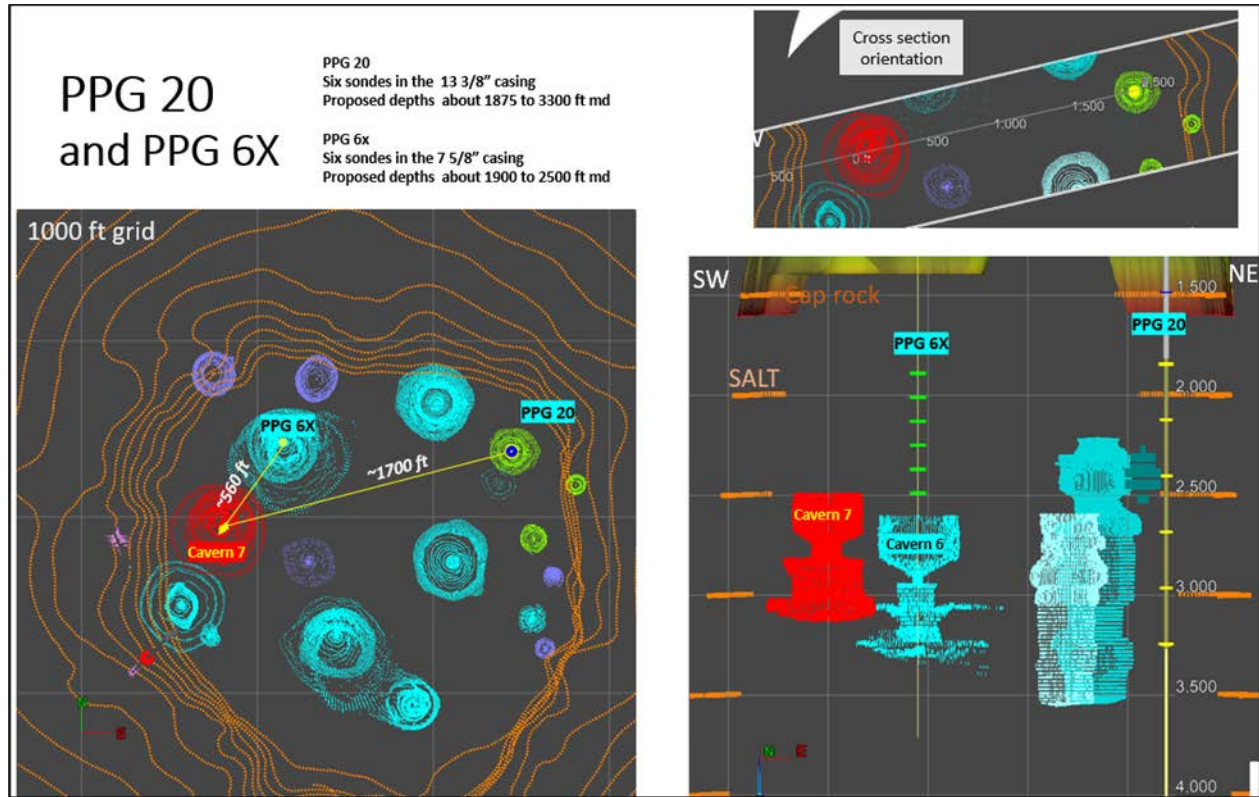


Figure 45 – Proposed Geophone Locations

Map (left) and SW-NE cross section (lower right, upper right inset shows orientation of cross section) of the Sulphur Mines Salt Dome showing the location of various caverns. Cavern 7 is shown in red. Potential monitoring wells are PPG 6X and PPG 20 (labeled in figures). The proposed geophone locations are shown in the cross section marked along the wellbores. Salt boundary is shown by orange dots.

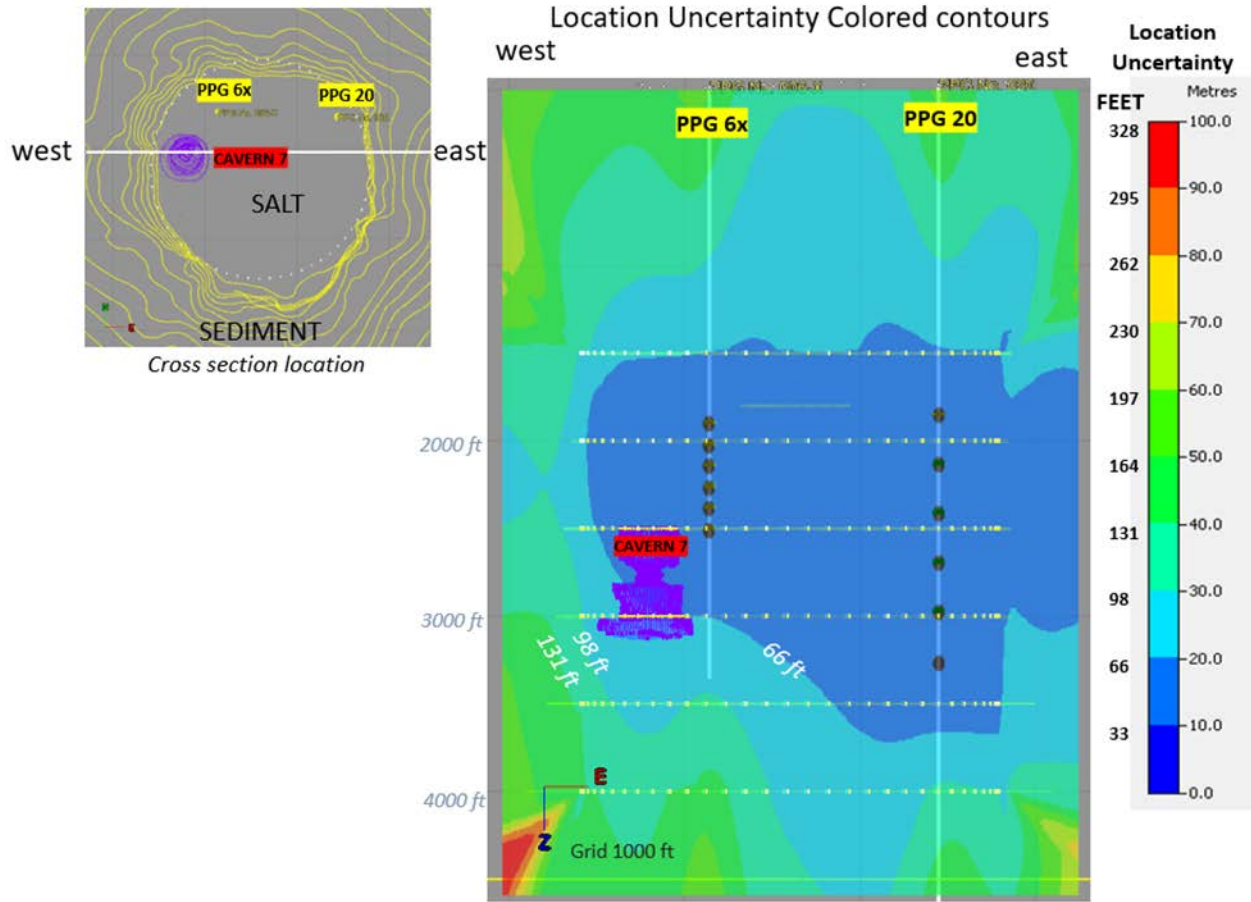


Figure 46 – Proposed Geophone Location East-West Cross-Section Uncertainty Modeling
 (Right) An east-west cross section showing the uncertainty modeling results using wells PPG 6X and PPG 20. Depth is labeled. The upper left plot shows the location of the east-west cross section, bisecting Cavern 7. The location of PPG 6X and PPG 20 wellbores and geophones are projected onto the cross section (black dots). The scale for the colored plots is shown in the far right, labeled in both feet and metres. The location of Cavern 7 is shown by purple dots, as labeled. The white dots show the modeled salt location.

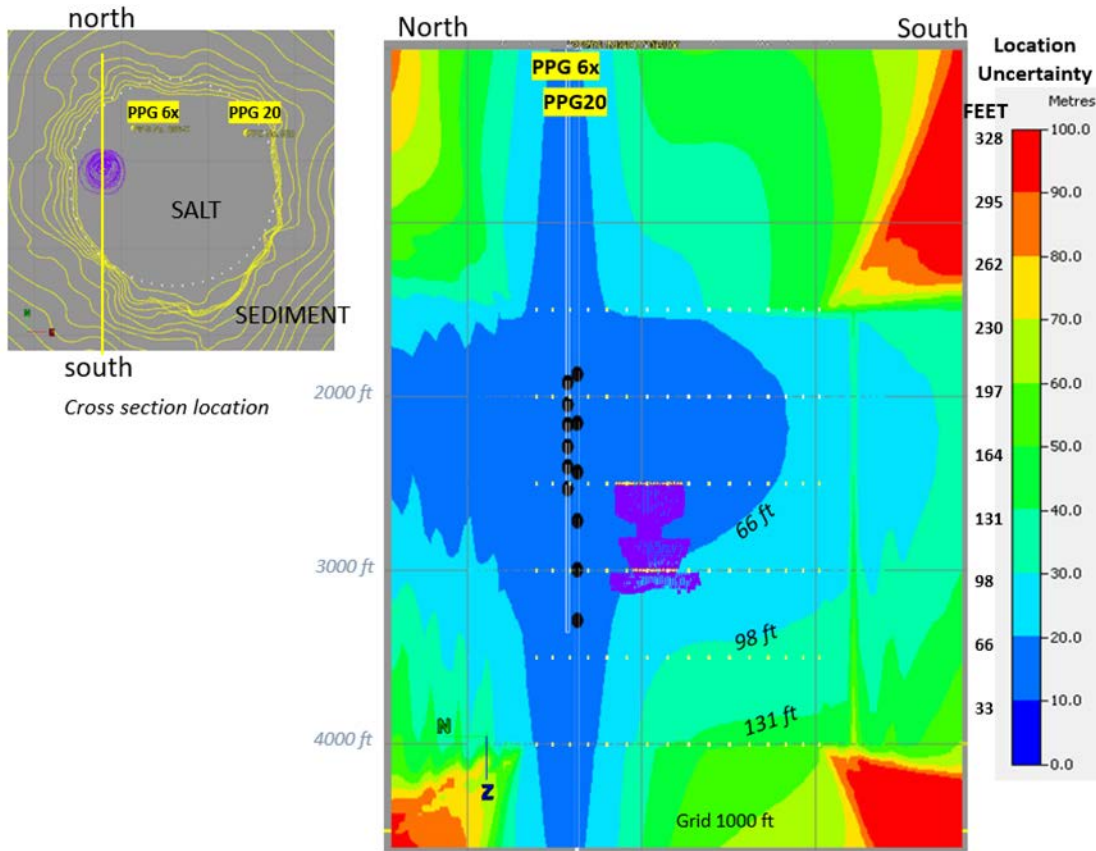


Figure 47 – Proposed Geophone Location North-South Cross-Section Uncertainty Modeling

(Right) A north-south cross section showing the uncertainty modeling results using wells PPG 6X and PPG 20. Grid on cross section is 1000 feet. The upper left plot shows the location of the east-west cross section, bisecting Cavern 7. The location of PPG 6X and PPG 20 wellbores and geophones are projected onto the cross section (black dots). The scale for the colored plots is shown in the far right, labeled in both feet and metres. The location of Cavern 7 is shown by purple dots. The white dots show the modeled salt boundary.

The magnitude sensitivity modeling results using geophones in PPG 6X and PPG 20 are shown in Figure 48 and Figure 49. The model results show a magnitude sensitivity of at least -2.25 for the entire region around Cavern 7, with slightly higher magnitude sensitivity on the east side and above Cavern 7. For reference, the median magnitude from borehole monitoring at Napoleonville salt dome is about magnitude -1.

The modeling results for both location accuracy and magnitude sensitivity suggest placing six-level removeable geophone arrays in both PPG 6X and PPG 20 will be suitable for borehole seismic monitoring resulting in event locations with both good location accuracy (< ±100 ft) and magnitude sensitivity (> -2.25).

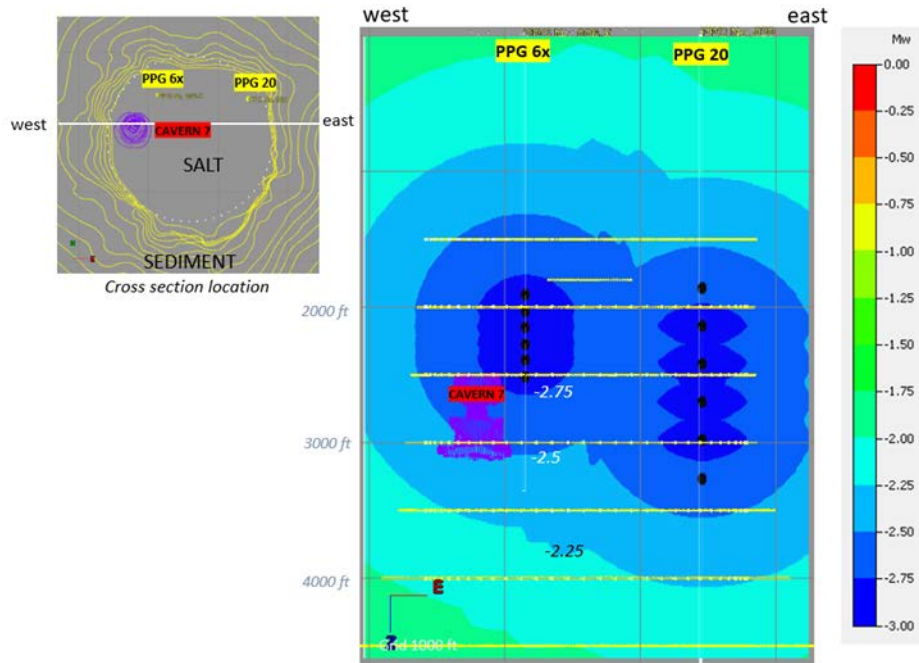


Figure 48 – Proposed Geophone Location East-West Cross-Section Magnitude Sensitivity Modeling
 (Right) An east-west cross section showing the magnitude sensitivity modeling results using wells PPG 6X and PPG 20. Grid on cross section is 1000 feet. The upper left plot shows the location of the east-west cross section, bisecting Cavern 7. The location of PPG 6X and PPG 20 wellbores and geophones are projected onto the cross section (black dots). The scale for the colored plots is shown on the far right. The location of Cavern 7 is shown by purple dots and label. The white dots show the modeled cylindrical salt boundary, the yellow dots the interpreted salt geometry.

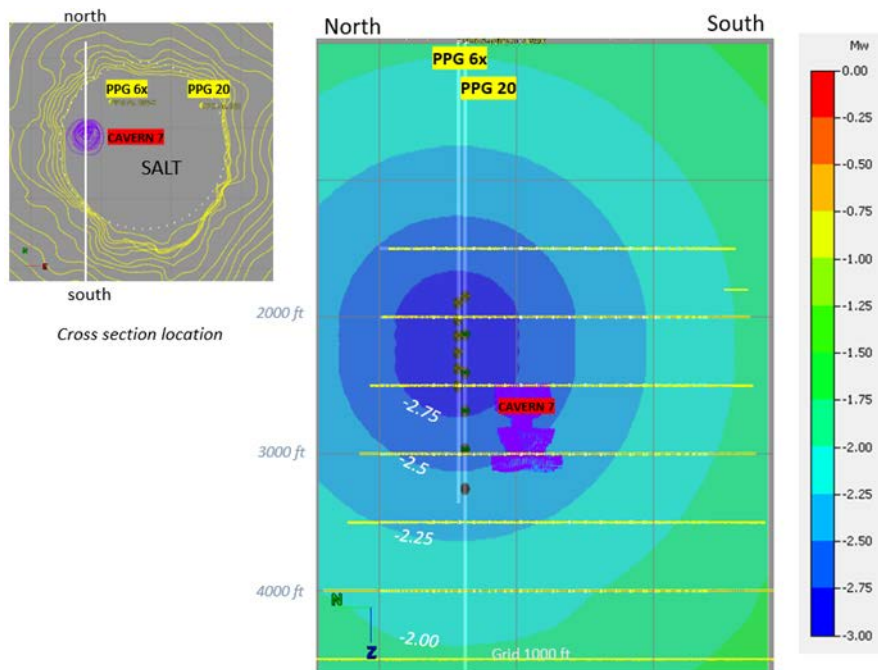


Figure 49 – Proposed Geophone Location North-South Cross-Section Magnitude Sensitivity Modeling
 (Right) A north-south cross section showing the magnitude sensitivity modeling results using wells PPG 6X and PPG 20. Grid on cross section is 1000 feet. The upper left plot shows the location of the north-south cross section, bisecting Cavern 7. The location of PPG 6X and PPG 20 wellbores and geophones are projected onto the cross section (black dots). The scale for the colored plots is shown

on the far right. The location of Cavern 7 is shown by purple dots and label. The white dots show the modeled cylindrical salt boundary, the yellow dots the interpreted salt geometry.

If the inspection workovers find the wells to be suitable for the Phase 3 array design, then the array design will be finalized and built. Provided the above-mentioned prerequisite is understood and completed in a timely fashion, the placement of the materials order likely could not be made until early June 2023.

For Phase 3, the microseismic activity reporting for the borehole arrays will be weekly and a preliminary seismic alert system will be developed in order to inform LDNR of any significant changes of microseismic activity. Depending on the seismic activity level and other monitoring data, we will continue to discuss reporting, alerts with LDNR to assure the results are reported in a timely manner.

Depending on the seismic activity at Sulphur Mines dome, the semi-permanent surface array (Phase 2) will likely be removed once the borehole array (Phase 3) is confirmed to be functional.

10.1.4 InSAR Enhanced Monitoring

10.1.4.1 Methodology

An investigation of the technologies and methods available for frequent monitoring of ground displacement was performed. Interferometric Synthetic Aperture Radar (InSAR) was identified as the most well established and rapidly deployable method to continually evaluate small, normally undetectable, ground movement over a large area. InSAR is a high-accuracy, remote sensing technology that effectively provides an updated level survey of a target area with each successive pass of an orbiting satellite. Spatial density of the measurement points varies, but in areas of non-vegetated ground cover, a great number of datapoints can be continually gathered. This is the primary feature that sets the technology apart from other surveying methods.

A global leader in InSAR ground displacement monitoring, has been contracted to collect, process, and deliver ground displacement data with each orbital pass from a collection of satellites. Utilizing an advanced, proprietary form of InSAR data processing that tracks ground movement by analyzing a stack of radar images collected over time. This technology, termed SqueeSAR, provides a collection of spatially distributed measurement points that each contain a time-series of ground deformation measurements reported to a 0.1 mm (0.004 inch) scale.

10.1.4.2 Data Properties

Imagery collected via satellites over successive orbital passes is used to identify and define measurement points on the ground. Objects or ground features providing a stable reflection of radar energy such as buildings, roads, and infrastructure produce the highest quality measurement points. Measurement points can be generated in some areas with vegetation, but data quality is affected by changing ground characteristics over time, leading to data gaps in areas with dense vegetation or wetlands. In the absence of stable reflectors, additional datapoints can sometimes be generated

in areas with lower but homogenous signal return by averaging groups of readings into a single measurement point.

InSAR uses phase and amplitude in the radar signal images to measure the distance between the satellite sensor and the measurement points on the ground. The data generated from the InSAR technique results in a time-series of displacement values at each measurement point. These displacement values are reported in relation to the original distance measured for each point in the dataset.

When a measurement point on the ground moves, whether that be vertically or laterally, the phase value detected by the sensor on the satellite is impacted due to a change in the distance between the sensor and ground target. Displacement values generated in this way are referred to as 1-D Line-of-sight (“LOS”) measurements, referring to the line-of-sight of the satellite to the ground target. Data collected in this manner is understood to convey a movement distance that is not purely vertical. This distinction only affects the assignment of a precise direction to the movement identified. As the primary component of the observed displacement is often vertical, InSAR analyses based on 1-D data are regularly used to identify and monitor the consistency of movement trends related to ground subsidence.

Analysis of an InSAR dataset allows for the identification of displacement velocity in inches per year and acceleration in inches per year². Measurement precision is affected by the satellite sensor resolution and the timeframe of the dataset. Average accuracy ranges for individual measurements can vary between ± 0.20 inches for a low-resolution satellite and ± 0.03 inches for a high-resolution satellite. With time, velocity trends can be measured with high accuracy yielding standard deviations in the range of ± 0.01 inches/year.

10.1.4.3 Data Frequency

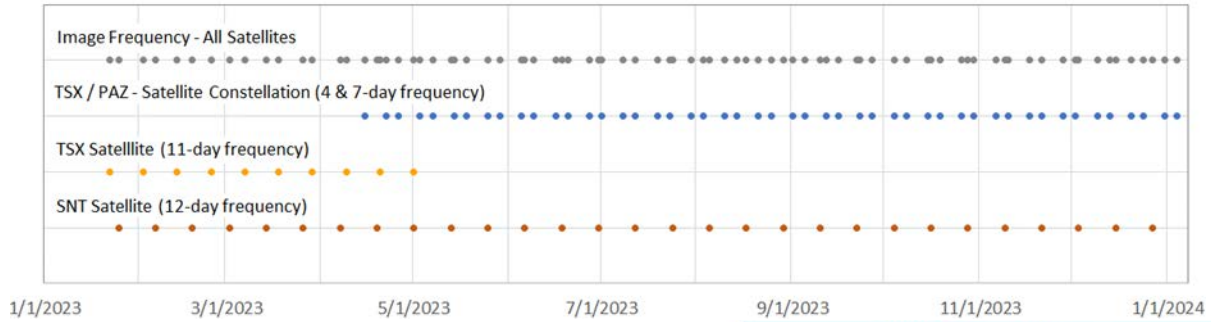
The two InSAR datasets that will be used to facilitate continuous monitoring of the Sulphur Mines Salt Dome are 1-D readings acquired from InSAR satellites on both ascending and descending orbits. An ascending orbit denotes the satellite's longitudinal course from south to north as it passes over the site, while a descending orbit denotes the satellite is moving from north to south.

The first dataset is captured from a Sentinel 1 (“SNT”) low-resolution satellite on an ascending orbit. The dataset timeframe covers October 4, 2016, to present and new images are captured with each pass on a 12-day revisit frequency. The second dataset is gathered via a TerraSAR-X (“TSX”) high-resolution satellite on a descending orbit with an 11-day revisit frequency. The dataset timeframe covers June 16, 2022, to present. As of the date of this report, four (4) SNT datasets and five (5) TSX datasets have been received and evaluated for trend consistency over the western part of the dome as part of this continuous monitoring effort.

Beginning in late-March 2023 the source for the second dataset will transition to a pair of high-resolution satellites that share the same orbit. These are a second TSX satellite and the PAZ satellite,

both with an 11-day revisit frequency. Their orbits are offset with the PAZ satellite passing over the site 4 days after the TSX satellite. This pair is referred to as the TSX/PAZ satellite constellation. The reason for the transition to the TSX/PAZ constellation in April is the increased data frequency that will result from a 4 and 7-day revisit period. Data capture for the TSX/PAZ constellation began in late January 2023 and a sufficient image stack for processing is estimated to be available by late-March 2023. Figure 50 below provides additional information on the image timeline, satellite data parameters, and a diagram of the orbital paths in relation to the Sulphur Mines Salt Dome.

Image Frequency



	TSX/PAZ Constellation			
	Sentinel-1	TerraSAR-X	TerraSAR-X	PAZ
Mode / Resolution	16 x 65 ft	Spotlight (3 x 3 ft)	Spotlight (3 x 3 ft)	Spotlight (3 x 3 ft)
Track	T136	T29	T67	T120
Band (wavelength)	C-Band (2.32 in)	X-Band (1.22 in)	X-Band (1.22 in)	X-Band (1.22 in)
Nominal frequency	12- day	11- day	11- day	11- day
Orbit (LOS angle)	Ascending 43°	Descending 17°	Descending 37°	Descending 37°
Date range	04 Oct 2016 – 20 Jan 2024	16 Jun 2022 – 01 May 2023	24 Jan 2023 – 11 Jan 2024	28 Jan 2023 – 15 Jan 2024
Number of images	199	30	34	33

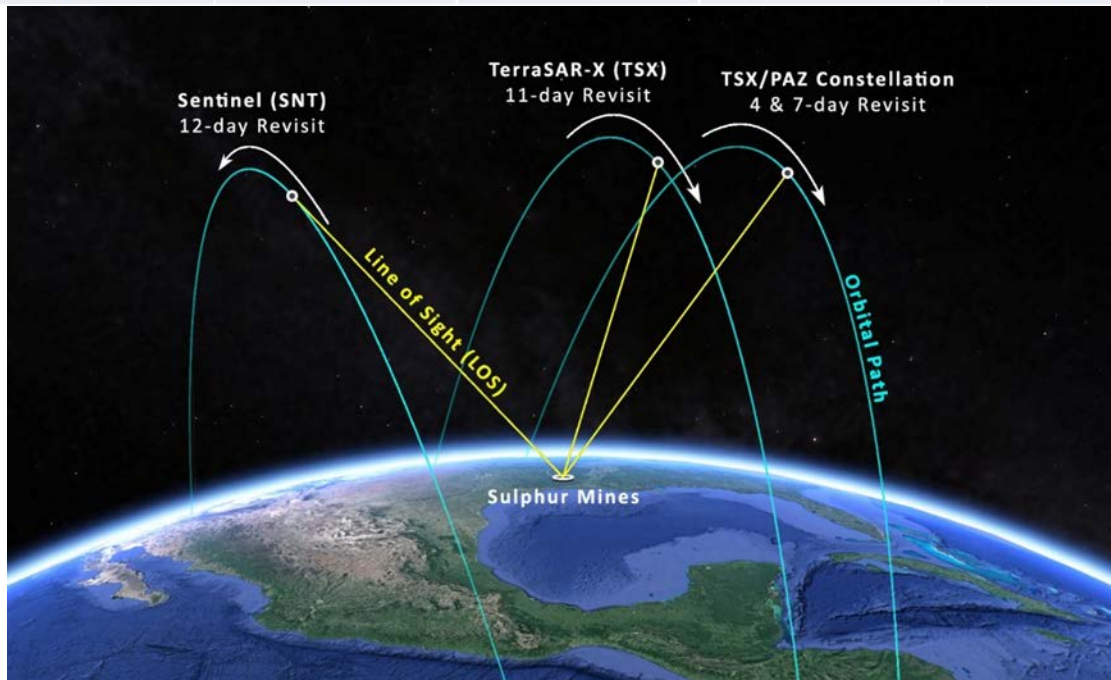


Figure 50 – InSAR Image Collection Frequency, Satellite Data Parameters and Orbit Visualization

10.1.4.4 Subsidence Monitoring Areas of Interest (AOIs)

Each of the InSAR datasets cover a 14-square mile area that extends roughly 1.85 miles out from the center of the Sulphur Mines Salt Dome. Figure 51 below depicts the measurement point locations and data extent for the most recent SNT and TSX datasets in relation to the dome structure contours.

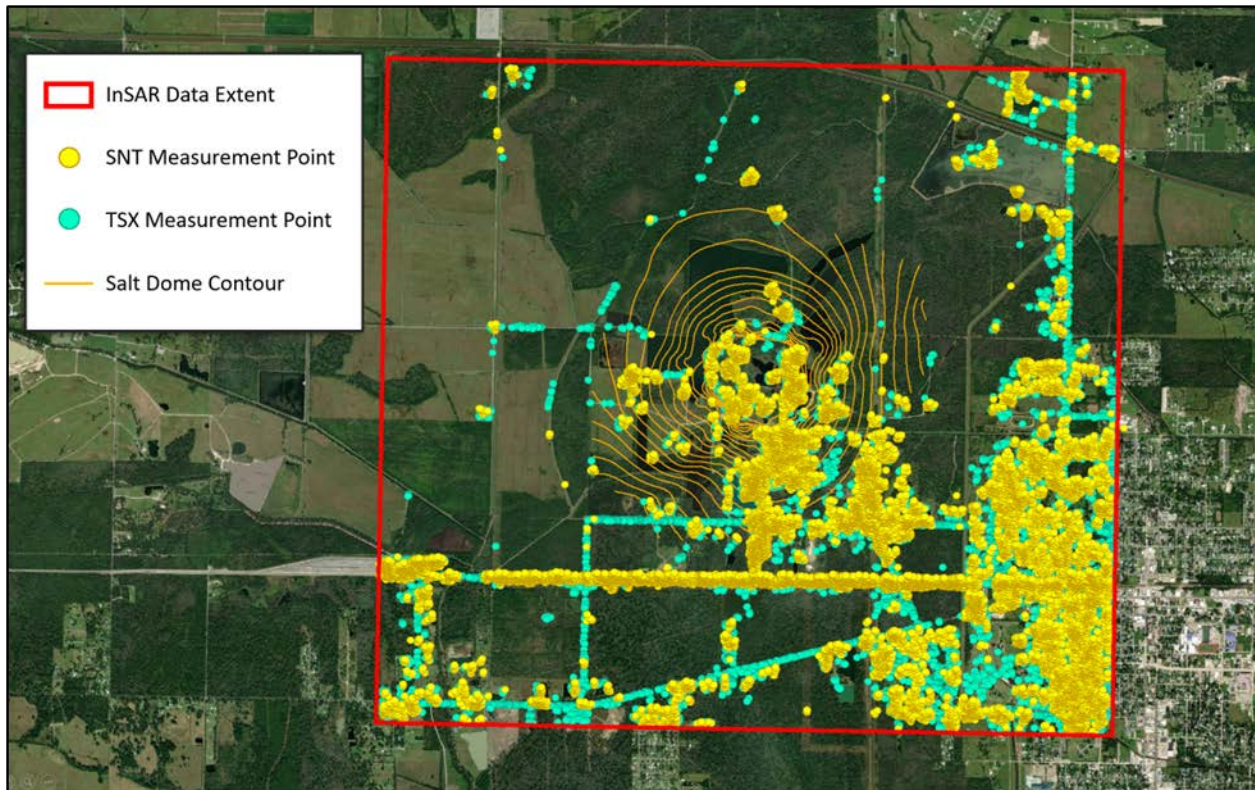


Figure 51 – SNT and TSX InSAR Measurement Points

The displacement values associated with each measurement point can be used to generate contour maps of displacement velocity and acceleration, indicating the spatial distribution of subsidence magnitudes. Velocity and acceleration rates are determined via trend analysis of the displacement time-series for each individual measurement point. In total, 1,051 measurement points lie within the analysis extent planned for this continuous monitoring effort. In order to visually convey and evaluate trend consistency in each displacement time-series, it is necessary to group measurement points and generate time-series charts of the averaged displacement values for each group. Averaging of the displacement data within point groups also allows for the reduction of scatter (noise) associated with measurement accuracy in the time-series charts of individual measurement points.

To accomplish this, nine (9) Areas of Interest (“AOIs”) have been defined as proposed point groups for calculation and display of average displacement rates and trend behavior. These AOIs are listed below in Figure 52 along with their associated areas and measurement point counts, as identified in

the most recent SNT and TSX datasets. The map in Figure 52 depicts the AOI boundaries in relation to the InSAR data, dome contours, and cavern extents.

Name	Area (Acres)	SNT Count	TSX Count	Total MP Count
AOI 1 (LGS 1)	3.86	13	38	51
AOI 2	2.49	15	9	24
AOI 3	2.94	29	22	51
AOI 4	4.28	62	65	127
AOI 5 (PPG 21)	3.59	25	66	91
AOI 6 (PPG 6)	6.35	134	119	253
AOI 7 (PPG 7)	7.20	140	170	310
AOI 8 (PPG 22)	4.43	21	43	64
AOI 9 (PPG A1)	5.09	39	41	80

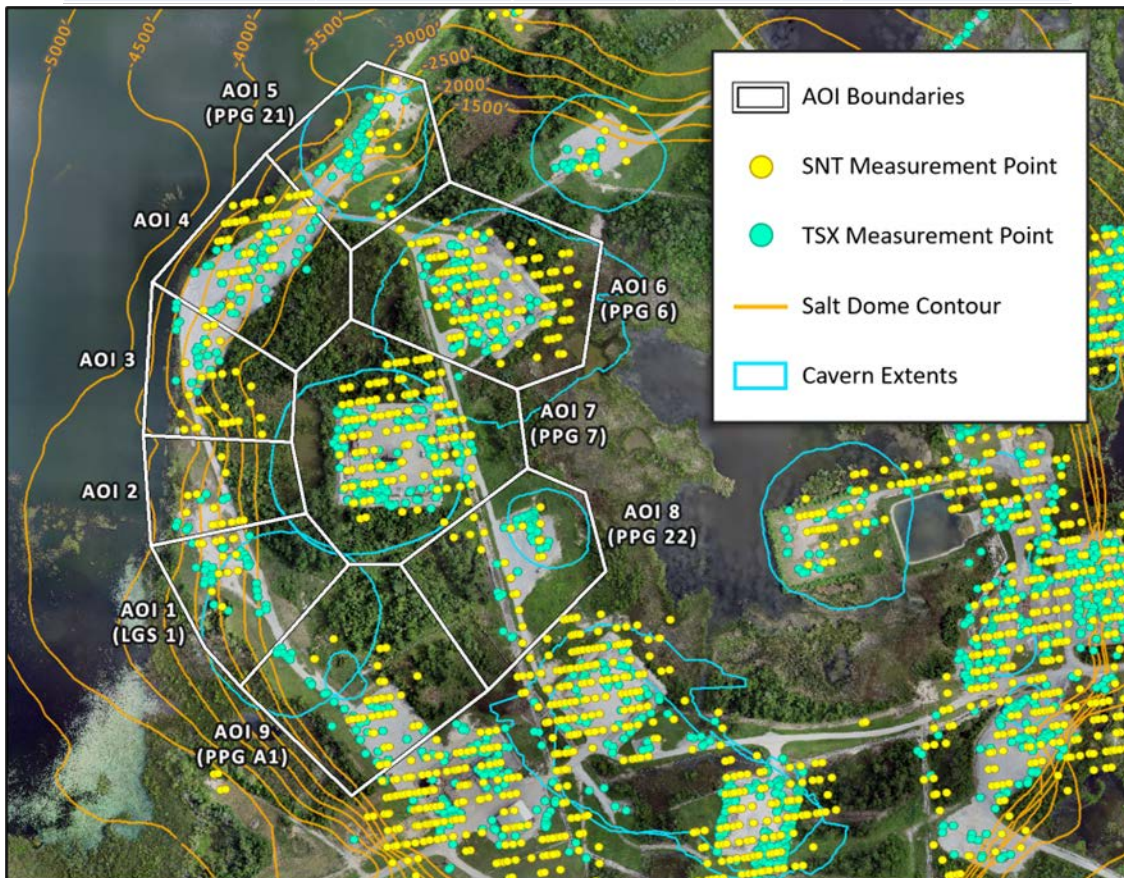


Figure 52 – InSAR Areas of Interest (AOIs)

10.1.4.5 Continuous Monitoring and Evaluation Plan

New data gathered with each pass of the InSAR satellites is processed and delivered by TREA within 48 hours of image capture. Once received, a same-day, preliminary review of the data will be

performed and confirm that no material deviations from the established linear subsidence trends have been observed.

Following the preliminary review, the data will be processed and evaluated, and a standardized report issued within 24-48 hours. To date there has been no material deviation from the established subsidence trends in the areas investigated.

Grouping and averaging of the measurement points defined in the nine (9) AOI regions will be used to depict subsidence trends on a time-series plot for each AOI. Both recent and long-term trends will be depicted, and the associated velocity and acceleration values generated by each trend line will be indicated on the plots for comparison.

In addition, both recent and long-term velocity and acceleration rates will be calculated for each individual measurement point and used to produce contour maps over the western side of the dome. An additional pair of maps depicting the difference (subtraction) of the recent and long-term velocity and acceleration will be generated to highlight the intensity and location of trend variation if present. This approach will provide a clearer distinction between locations that may be experiencing slight changes in subsidence behavior in relation to historically consistent motion.

If notable observations are made during these efforts, additional investigation of key regions will be performed and reported, and these regions will remain an area of focus in subsequent datasets. Additional deliverables may be utilized as necessary to convey specific observations such as time-series plots of smaller point groups and their associated trends or cross sections of certain dome regions depicting profiles of displacement magnitude over time.

10.1.5 Periodic Sonar Surveys

The Cavern No. 007 sonar survey history outlined in *Section 6.3* shows that a survey was completed roughly every two years between 1993 and 2003, and approximately every seven to eight years from 2003 through 2018. Per state regulatory requirements, the next sonar survey on an inactive salt cavern would have needed to be performed in 2023.

Similarly for Cavern No. 006, a survey was completed roughly every two years between 1993 and 2003, plus an additional 2-year sonar occurring in 2005. The next sonar was done approximately six years later, in 2011, and then two were completed at the state regulatory required five-year increments in 2016 and 2021. Per state regulatory requirements, the next sonar survey on an inactive salt cavern would have needed to be performed in 2026.

Since the acute pressure loss event in December 2021, several periodic sonar surveys of Cavern No. 007 have been performed in order to monitor for changes in cavern geometry. As of the date of this report, five sonar surveys have been completed on Cavern No. 007, on the following dates:

- March 11th, 2022
- November 2nd, 2022
- January 11th, 2023
- February 1st, 2023
- March 16th, 2023

Starting March 16th, 2023, a schedule for periodic sonar surveys of Cavern No. 007 approximately every eight weeks was created to routinely monitor for changes in cavern geometry. Comparisons in cavern geometry are done in CAD software with every new sonar survey. There have been no significant changes in cavern shape when comparing to historical sonars, however, a relatively minor change in cavern geometry was identified in Cavern 7 based upon an evaluation of the May 2018 sonar survey with sonars performed after the December 2021 acute pressure loss event. There have been no observed geometry changes in Cavern No. 007 from all sonars conducted subsequent to the December 2021 acute pressure loss event. Due to the timing of the sonar surveys it cannot be definitely proven if the geometric changes observed between the 2018 and 2022 data sets are connected to the integrity failure. Additionally, the cavern geometry changes identified between the 2018 and 2022 sonars coincide with similar geometric changes that have occurred over many decades and appear to relate to the collapse of an internal geometric feature of the cavern (a “shelf”). The collapse of a shelf over time is generally a common occurrence for caverns, and that alone is very unlikely to lead to an integrity failure. Also, the cavern geometry changes identified between the 2018 and 2022 sonars showed no apparent reduction to the previously established cavern-to-flank spacing.

Since the acute pressure loss event in December 2021, one sonar survey of Cavern No. 006 has been completed on March 12, 2022. No notable or anomalous changes in cavern shape were found when comparing to historical sonars.

10.1.6 Sampling of Groundwater, Surface Water, Oil & Gas, Bubbles

10.1.6.1 Groundwater

Eagle currently utilizes four industrial water wells southwest of the salt dome, with a fifth well installed but not currently operational (Figure 53). Samples were collected from the four active Eagle water wells on January 26, 2023; data from that sampling event are summarized in Table 10. The results from this initial sampling event will serve as a baseline dataset for subsequent monitoring. For reference, the results of a brine sample collected from Brine Well 6X on January 25, 2023, are also included in Table 10. The installation of additional groundwater monitoring wells in the vicinity of Caverns 6 and 7 has been proposed. Plans for the monitoring well installation are currently being developed.

Groundwater sampling will occur at regular intervals and is currently on a monthly schedule. The sampling schedule may be modified based on results, regulatory compliance, or other recommendations. Samples are currently being analyzed by a Louisiana accredited environmental laboratory for the following parameters:

- Metals (As, Ba, Cd, Ca, Cr, Fe, Pb, Mg, Mn, Hg, K, Se, Ag, Na, Ni, Sr, V, Zn),
- Chloride, Bromide,
- Bicarbonate, Carbonate
- Sulfate, Sulfide, Hydrogen Sulfide,
- Total Dissolved Solids (TDS),
- pH
- Benzene, Toluene, Ethylbenzene, and Xylenes (BTEX), and
- Total Petroleum Hydrocarbon (TPH) fractions

Samples will also be collected for dissolved gases and submitted to a reputable lab for isotopic evaluation. The data collected will include compositional analysis of each water sample's headspace gas as well as isotopic evaluations of the gas and/or water.



Figure 53 – Known Active Water Well Locations

Table 10 – Groundwater Data Summary

TABLE 1
Groundwater Data Summary
Sulphur Dome
Calcasieu Parish, Louisiana

Sample ID	019-580	019-582	019-995	019-1055	6X Brine
	1/26/23	1/26/23	1/26/23	1/26/23	
Sample Date					1/25/23
Sample Interval (ft)	469'	609'	485'	520'	Brine
Sampler	ERM	ERM	ERM	ERM	ERM
Constituent	Groundwater				Brine
Zone	Groundwater				Brine
Total Metals (mg/L)					
Arsenic	0.000477 J	0.000812 J	0.000762 J	0.000419 J	0.0300 J
Barium	0.23	0.239	0.214	0.265	0.220
Cadmium	<0.0002	<0.0002	<0.0002	<0.0002	<0.01
Calcium	26.8	25.5	26.4	28.7	722
Chromium	<0.0004	<0.0004	<0.0004	<0.0004	0.243
Iron	5.12	4.03	0.821	3.81	25.7
Lead	0.00144 J	<0.0006	<0.0006	<0.0006	<0.03
Magnesium	8.03	7.81	8.02	8.66	8.16 J
Manganese	0.412	0.417	0.388	0.42	0.953
Mercury	<0.00003	<0.00003	<0.00003	<0.00003	<0.00003
Potassium	2.93	2.94	3.00	3.10	14.4
Selenium	<0.0011	<0.0011	<0.0011	0.00114 J	<0.0550
Silver	<0.0002	<0.0002	<0.0002	<0.0002	<0.01
Sodium	31.9	28.0	29.9	34.4	100,000
Strontium	0.246	0.240	0.241	0.262	2.66
Zinc	0.0147	0.0107	0.00426	0.00993	0.481
Anions/Water Quality Parameters					
Bicarbonate Alkalinity (mg/L CaCO3)	200	180	258	250	159
Bromide	0.0992 J	0.0860 J	0.0931 J	0.0982 J	<3
Carbonate Alkalinity (mg/L CaCO3)	<5	<5	<5	<5	<5
Chloride	35.7	23.4	28.7	38.3	213,000
Sulfate	2.91	4.11	3.63	3.51	1,380
Total Dissolved Solids (TDS)	236	212	226	244	239,000
Sulfides					
Hydrogen Sulfide	<0.5	<0.5	<0.5	<0.5	<0.5
Sulfide	<1	<1	<1	<1	<1
Volatile Organic Compounds					
Benzene	<0.0002	<0.0002	<0.0002	<0.0002	0.170
Ethylbenzene	<0.0003	<0.0003	<0.0003	<0.0003	0.0075 J
Toluene	<0.0002	<0.0002	<0.0002	<0.0002	0.110
m,p-Xylene	<0.0005	<0.0005	<0.0005	<0.0005	0.013 J
o-Xylene	<0.0003	<0.0003	<0.0003	<0.0003	0.0091 J
Xylenes, Total	<0.0003	<0.0003	<0.0003	<0.0003	0.022
TPH Fractions					
Aliphatics >C6-C8	<0.01	<0.01	<0.01	<0.01	0.0997
Aliphatics >C8-C10	<0.01	<0.01	<0.01	<0.01	<0.01
Aliphatics >C10-C12	<0.001	<0.001	<0.001	<0.001	<0.001
Aliphatics >C12-C16	<0.002	<0.002	<0.002	<0.002	<0.002
Aliphatics >C16-C35	<0.008	<0.008	<0.008	<0.008	<0.008
Aromatics >C8-C10	<0.01	<0.01	<0.01	<0.01	0.0284
Aromatics >C10-C12	<0.001	<0.001	<0.001	<0.001	<0.001
Aromatics >C12-C16	<0.004	<0.004	<0.004	<0.004	<0.004
Aromatics >C16-C21	<0.003	<0.003	<0.003	<0.003	<0.003
Aromatics >C21-C35	<0.009	<0.009	<0.009	<0.009	<0.009

NOTES:

J - Estimated Value reported below the detection limit.

< - Not Detected at the reporting limit shown.

Bolded values detected in the sample.

10.1.6.1.1 Water Well Survey

A water well survey within a one-mile radius of the salt dome will be performed beginning in May 2023. This survey is intended to identify users of groundwater nearest to the dome. The water well survey will consist of a letter survey mailed to property owners, followed by a visual inspection and face-to-face follow-up visit, as necessary. Owners of any unregistered water wells identified will be asked to register the wells with LDNR.

10.1.6.1.2 Capture Zone Analysis

The four active Eagle water wells are pumping a total of approximately 2,000 gallons per minute (gpm) from the 500-foot sand of the Chicot Aquifer (i.e., approximately 2.9 million gallons per day) for use in salt cavern solution mining to produce brine fluid. This large-scale pumping is likely inducing a hydraulic gradient causing groundwater to flow toward the wells. However, the extent of the influence of pumping in the vicinity of the salt dome and the influence of pumping occurring by other operators is unknown. A capture zone model of the USDW interval is currently being developed. Various predictive modeling scenarios will be evaluated to assist in understanding the impacts of brine to the USDW if a release at or near the caverns were to occur.

10.1.6.2 Surface Water

The surface water in the vicinity of the salt dome is generally isolated with little or no connection to other surface waters within the drainage basin (Figure 54). “Bubble sites” have been observed in and around the well pads, and within a pond centrally located above the salt dome (“the central lake”). The majority of the surface water bodies are shallow. The central lake was measured at <1 inch near the marshy banks and approximately 6 feet deep in the center.

Samples from the bubble sites have been collected and will also be collected as soon as possible if new bubble sites are identified. Three additional samples will be collected from the central pond (Figure 54) quarterly for the first year, then semi-annually for one additional year. Samples will be submitted to a Louisiana accredited environmental laboratory for analysis of the following parameters:

- Metals (As, Ba, Cd, Ca, Cr, Fe, Pb, Mg, Mn, Hg, K, Se, Ag, Na, Sr, Zn),
- Chloride, Bromide,
- Bicarbonate, Carbonate
- Sulfate, Sulfide, Hydrogen Sulfide,
- Total Dissolved Solids (TDS),
- pH
- Benzene, Toluene, Ethylbenzene, and Xylenes (BTEX), and
- Total Petroleum Hydrocarbon (TPH) fractions

At active bubbles sites, samples will also be collected for dissolved gases and sent to Isotech Laboratories Inc. (Champaign, IL), a Stratum Reservoir company, for isotopic evaluation. The data

collected will include compositional analysis of each water sample's headspace gas as well as isotopic evaluations of the gas and/or water.

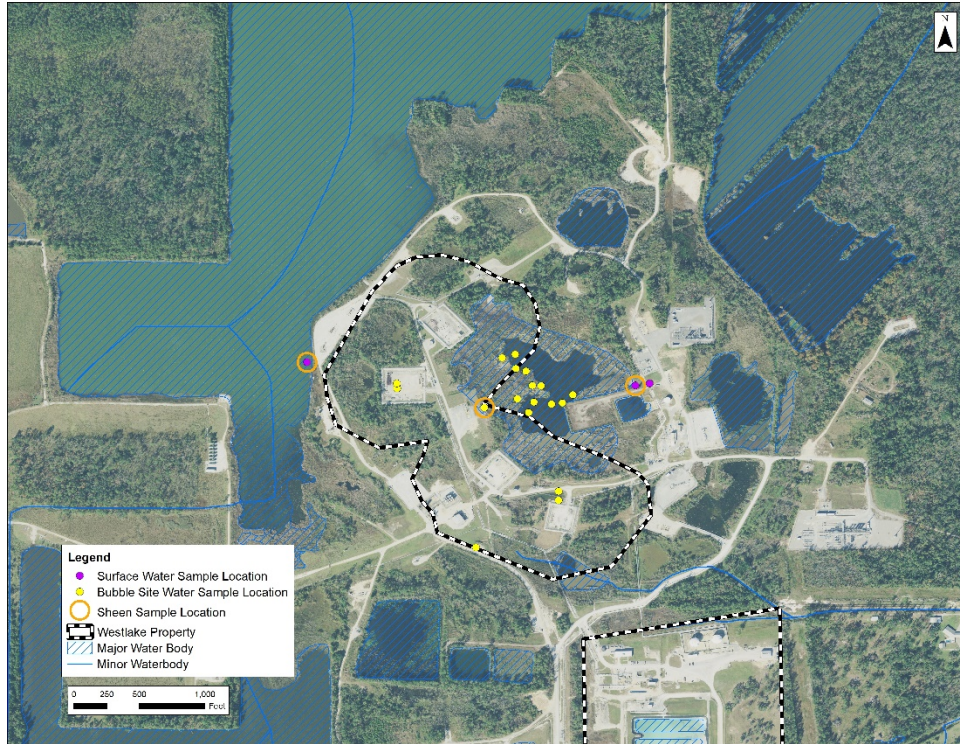


Figure 54 – Surface Water Sampling Locations

Table 11 – Surface Water Data Summary

TABLE 2
Surface Water Data Summary
Sulphur Dome
Calcasieu Parish, Louisiana

Constituent	Sample ID	Brine Well 22 BS	Brine Well 7A BS	CP BS 1	CP BS 2	CP BS 3	110159-BS	Brine Pond 4 BS	Culvert	Central Pond
	Sample Date	1/25/23	1/25/23	1/30/23	1/30/23	1/30/23	2/10/23	2/10/23	1/25/23	1/25/23
	Sample Interval (ft)	Surface	Surface	Surface	Surface	Surface	Surface	Surface	Surface	Surface
Sampler	ERM	ERM	ERM	ERM	ERM	ERM	ERM	ERM	ERM	ERM
Zone	Bubble Site (Surface Water)							Surface Water		
Total Metals (mg/L)										
Arsenic	0.00149 J	0.000767 J	0.000862 J	0.000868 J	0.000769 J	IP	IP	0.00141 J	0.00192 J	
Barium	0.300	0.232	0.160	0.367	0.155	IP	IP	0.0832	0.146	
Cadmium	<0.0002	<0.0002	<0.0002	<0.0002	<0.0002	IP	IP	<0.0002	<0.0004	
Calcium	71.2	24.5	75.3	64.2	77.7	IP	IP	58.2	149	
Chromium	0.000847 J	0.000474 J	<0.0004	<0.0004	<0.0004	IP	IP	0.00101 J	0.00458 J	
Iron	1.14	0.0406 J	0.132 J	0.0258 J	0.125 J	IP	IP	0.207	2.07	
Lead	0.00208	<0.0006	<0.0006	<0.0006	<0.0006	IP	IP	<0.0006	<0.00120	
Magnesium	19.8	1.54	15.0	12.6	15.0	IP	IP	5.44	37.8	
Manganese	0.797	0.0215	0.266	0.458	0.232	IP	IP	0.00934	0.847	
Mercury	<0.00003	<0.00003	<0.00003	<0.00003	<0.00003	IP	IP	<0.00003	<0.00003	
Potassium	2.57	1.02	2.90	2.58	2.83	IP	IP	2.86	3.22	
Selenium	<0.0011	<0.0011	<0.0011	<0.0011	<0.0011	IP	IP	<0.0011	<0.00220	
Silver	<0.0002	<0.0002	<0.0002	<0.0002	<0.0002	IP	IP	<0.0002	<0.0004	
Sodium	156	8.45	174	166	19.1	IP	IP	158	1,080	
Strontium	0.619	0.167	0.556	0.482	0.578	IP	IP	0.341	0.941	
Zinc	0.00857	0.0466	0.00452	0.00213 J	0.00748	IP	IP	0.0153	0.0258	
Anions/Water Quality Parameters										
Bicarbonate Alkalinity (mg/L CaCO3)	269	159	241	238	245	IP	IP	210	495	
Bromide	<0.03	<0.03	<0.03	<0.03	<0.03	IP	IP	<0.03	<0.0600	
Carbonate Alkalinity (mg/L CaCO3)	<5	<5	<5	<5	<5	IP	IP	<5	<5	
Chloride	317	6.45	308	296	343	IP	IP	215	2,090	
Sulfate	45.2	2.97	113	111	135	IP	IP	92.1	183	
Total Dissolved Solids (TDS)	676	320	80.0	512	892	IP	IP	498	3,600	
Sulfides										
Hydrogen Sulfide	<0.5	<0.5	<0.5	<0.5	<0.5	IP	IP	<0.5	<0.5	
Sulfide	<1	<1	<1	<1	<1	IP	IP	<1	<1	
Volatile Organic Compounds										
Benzene	0.00120	0.00034 J	<0.0002	<0.0002	<0.0002	IP	IP	<0.0002	<0.0002	
Ethylbenzene	<0.0003	0.00180	<0.0003	<0.0003	<0.0003	IP	IP	<0.0003	<0.0003	
Toluene	0.00079 J	0.00055 J	<0.0002	<0.0002	<0.0002	IP	IP	<0.0002	<0.0002	
m,p-Xylene	<0.0005	0.00020 J	<0.0005	<0.0005	<0.0005	IP	IP	<0.0005	<0.0005	
o-Xylene	<0.0003	<0.0003	<0.0003	<0.0003	<0.0003	IP	IP	<0.0003	<0.0003	
Xylenes, Total	<0.0003	0.00200	<0.0003	<0.0003	<0.0003	IP	IP	<0.0003	<0.0003	
TPH Fractions										
Aliphatics >C6-C8	<0.01	<0.01	<0.01	<0.01	<0.01	IP	IP	<0.01	<0.01	
Aliphatics >C8-C10	<0.01	<0.01	<0.01	<0.01	<0.01	IP	IP	<0.01	<0.01	
Aliphatics >C10-C12	<0.001	<0.001	<0.001	<0.001	<0.001	IP	IP	<0.001	<0.001	
Aliphatics >C12-C16	0.0746	<0.002	<0.002	<0.002	<0.002	IP	IP	<0.002	<0.002	
Aliphatics >C16-C35	0.249	<0.008	<0.008	<0.008	<0.008	IP	IP	<0.008	<0.008	
Aromatics >C8-C10	<0.01	0.0285	<0.01	<0.01	<0.01	IP	IP	<0.01	<0.01	
Aromatics >C10-C12	<0.001	<0.001	<0.001	<0.001	<0.001	IP	IP	<0.001	<0.001	
Aromatics >C12-C16	0.0417	<0.004	<0.004	<0.004	<0.004	IP	IP	<0.004	<0.004	
Aromatics >C16-C21	0.121	<0.003	<0.003	<0.003	<0.003	IP	IP	<0.003	<0.003	
Aromatics >C21-C35	<0.009	<0.009	<0.009	<0.009	<0.009	IP	IP	<0.009	<0.009	

NOTES:

J - Estimated Value reported below the detection limit.
 < - Not Detected at the reporting limit shown.
 Bolded values detected in the sample.
 IP - In Progress

10.1.6.2.1 Surface Water Profile

A profile of the surface water column at the central lake has been performed, and continued monitoring of the water column profile is currently proposed. The profiling consists of taking measurements of pH, Specific Conductivity (SC), Oxidation Reduction Potential (ORP), and temperature within the water column. Measurements are made using a handheld meter while water is pumped at the upper, middle.

10.1.6.3 Oil and Gas

10.1.6.3.1 Chemical Fingerprinting of Oil

Detailed chemical analysis of crude (and refined) oils, i.e., chemical fingerprinting, can reveal source-specific features used to determine whether two oil samples are, in fact, the same oil. Chemical fingerprinting relies on the inherent diversity of crude oils produced from different oil-producing regions and oil fields, which also can extend to individual reservoir zones within a field or individual well.

The laboratory and interpretive methods used in chemical fingerprinting of oils have developed over 40+ years and are presently well-established within the “oil spill” scientific community. Briefly, using modified U.S. EPA (SW-846) analytical methods and stringent quality control, the concentrations of more than 150 highly diagnostic chemicals in oil, including acyclic isoprenoids, polycyclic aromatic hydrocarbons, sulfur-containing polycyclic compounds, and petroleum biomarkers (triterpanes, steranes, and aromatic steroids) are measured and then used to make statistical comparisons between oil to determine their “match” category.

Chemical fingerprinting will be used in the failure analysis of Cavern 7 through the collection and analysis of oil(s) recovered from within Cavern 7, as well as any oil(s) manifesting in the area’s surface as seeps or sheens. At this time, the chemical fingerprint of oil recovered from within Cavern 7 (i.e., Well 7B) in January 2023 was established and serves as a baseline. It is planned to collect and analyze additional cavern oil samples over time for comparison to the January 2023 baseline (or, for samples from the distant future, any predecessor cavern samples) to determine any changes in cavern oil composition over time.

It is also planned to establish the chemical fingerprints any locally-produced crude oil samples from existing production wells made available for analysis so that they can be compared to cavern oils – and to one another to assess the degree of heterogeneity among different producing reservoir zones or wells. If, in the future, monitoring of cavern oil indicates local crude oil has entered the cavern it may be possible to determine its specific source (reservoir zone). By the same approach, it is also planned to chemically fingerprint any oils reaching the area’s surface for their comparison to both cavern oils and locally produced oils in order to best determine their apparent source.

Finally, because of the potentially confounding impact of inter-laboratory variations in chemical fingerprinting, it is planned to conduct all chemical fingerprinting analyses within a single laboratory wherein intra-laboratory variation(s) can be monitored and accounted for in any statistical comparisons. This will occur at a reputable lab.

10.1.6.3.2 Chemical Fingerprinting of Gas

Despite their simple chemical composition (relative to crude oil), methane and other gases in the environment can also be distinguished using chemical fingerprinting. This is accomplished through a combination of both molecular compositions (e.g., methane, ethane, propane, carbon dioxide, etc.) and their isotopic compositions. The latter relies mostly on the variations in the stable isotopes (e.g., $^{13}\text{C}/^{12}\text{C}$ and $^2\text{H}/^1\text{H}$) of gases derived from different general sources (e.g., biogenic gas versus thermogenic gas) or different specific sources (thermogenic gases from different geologic formations or production zones). These data are routinely obtained on gas samples collected from producing oil/gas wells, near-surface soil gases, or from water containing dissolved gases.

Chemical fingerprinting of gas samples may be used in the failure analysis of Cavern 7 if gas is found to accumulate within the cavern or manifests in the area’s near-surface environment, for example,

dissolved in groundwater, cavern brine, or surface water (Sections 7.1.6.1 and 7.1.6.2.) In any such instance, any recoverable gas samples from the cavern will be collected and analyzed using standard gas fingerprinting methods, again ideally within a single laboratory. As is currently planned for dissolved gases in groundwater, cavern brine, and surface water (Sections 7.1.6.1 and 7.1.6.2), this will occur at a reputable lab. These methods may include hydrocarbon and fixed gas compositional analysis, $\delta^{13}\text{C}$ of methane, ethane, propane, δD of methane, $\delta^{13}\text{C}$ of CO_2 , ^{14}C of methane, ^3H of tritium, δD and $\delta^{18}\text{O}$ of water, $\delta^{13}\text{C}$ of dissolved inorganic carbon (DIC).

Any locally-produced or vented natural gas samples or produced water samples from nearby production wells made available for analysis will be appropriately analyzed for comparison to any gases or waters collected from the cavern or surface environment, again with the objective of possibly determining the specific source(s) of gas within the cavern or surface environment.

10.1.7 Aerial Thermal Imaging

A thermal imaging of the Sulphur Dome area was captured via a pre-programmed drone with a thermal imaging payload attached.

This payload allows for the collection of radiometric thermal images. Each separate image contains temperature values for every pixel.

10.1.7.1 Data Collection

The drone is pre-programmed with the flight path to reduce human error of manual flight. Due to Federal Aviation Administration (FAA) regulations, the drone cannot fly above 400' above ground level (AGL). While conducting the flight path over the Sulphur Dome area at 399' AGL, thermal images were collected in two second intervals, equating to over 5,000 images captured.

10.1.7.2 Data Processing

The collected data was processed by an industry leading cloud-based software allowing for the processing of Radiometric Thermal maps. Each image was processed through an AI-engine which aligns images via visible pixels and then processes the map with the embedded Radiometric data. The embedded temperature values from each Radiometric image results in a consistent, broad-area thermal image with temperature values.

The benefit of using Radiometric processing is the use of absolute thermal data embedded into each image. This provides consistent thermal processing of all 5,000 plus images across the entire map area. Image-only processing ignores temperature values embedded in each pixel and instead creates a wide-area orthomosaic stitch solely relying on the thermal field-of-view at the time of capture. Image-only processing provides adequate detail when looking at a single image, or single study area, but relative temperatures are lost when comparing multiple images against one another.

10.2 Evaluation

10.2.1 Current Geologic Understanding and Further Evaluation

The Sulphur Mines Salt Dome is located in the Gulf Coast geosyncline and developed as a piercement structure (diapir) of Jurassic Louann Salt in response to subsidence associated with the Tertiary sedimentation in the geosyncline. The Gulf Coast geosyncline has been developing since the Triassic and has been filling with thick sequences of sand, silts, clays, limestones, and evaporates. In the area of the Sulphur Mines dome, the Louann Salt is estimated to be 30,000-ft below surface. Increasing sediment loading caused increasing pressures which resulted in plastic flow of the Louann Salt. Due to gravity and differential overburden densities the salt began to flow in a southerly direction forming salt anticlines trending parallel to the coast.

The stratigraphy of the Gulf Coast geosyncline is primarily comprised of unconsolidated clays and sands of the Miocene, Pliocene, and Quaternary ages from the surface to approximately 7,000 feet. Below 7,000 feet to 30,000 feet, the stratigraphy is mainly consolidated Tertiary, Cretaceous and Jurassic deposits. The Louann Salt is estimated to be 30,000 feet below surface in the area of the Sulphur Mines dome.

The deepest formation penetrated in the area of the dome is the Oligocene-aged Vicksburg formation at 9,500 feet. The Frio is located above the Vicksburg and is also of Oligocene age. The Frio is approximately 2,500 feet thick and consists of shales and massive calcareous sands. A 500 foot thick Oligocene Anahuac formation is located above the Frio. The Anahuac is dark greenish calcareous clay and shale with occasional limestone lenses.

On top of the Anahuac is the 4,210 feet thick Miocene Fleming Group, which consists of alternating fluvial deltaic and shallow marine sands. Overlying the Fleming is the Pleistocene Citronelle Group (Foley Formation). Neither the Fleming nor the Citronelle is present over the top of the Sulphur Mines Salt Dome. The Houston Group is 800 foot thick and consists of muds, sands and shales.

The Houston group contains the Chicot aquifer system, a major source of industrial and domestic fresh water in Calcasieu Parish. The surface formations of the Sulphur Mines area consist of Quaternary fluvial and marsh deposits specifically from the Pleistocene Epoch. The formations consist of fine-grained sands and silts with local clays and gravels. In the area immediately surrounding the Sulphur Mines dome the deposits are typically clays and sandy to silty clays.

The Sulphur Mines Salt Dome is a steeply sloping, circular piercement structure with an abnormally shaped caprock. The salt has been encountered as shallow as 1,460 ft BGL and as deep as approximately 7,635 ft BGL. The salt dome has a measured extent in the east-west and north-south axes of approximately 2,400 ft and 2,100 ft respectively. The flanks of the dome are steeply dipping with an approximate angle of dip at about 80 degrees typical.

Salt structure determination is currently based upon a 2014 vintage effort that relied on offset well control penetrating the Sulphur Salt Dome. These offset wells were primarily historical oil and gas

exploration wells with some being drilled as early as the 1930's. Well information for control points was obtained from DrillingInfo, IHS Energy, and the Office of Conservation SONRIS databases. Open-hole well logs, drillers' records, scout tickets, surface survey plats, and directional drilling surveys were obtained from these sources and incorporated into the map.

Historical maps were also evaluated for pertinent information. These maps included:

- Union Oil & Gas Well Locations (1930)
- Union Texas Petroleum Well Locations (1941)
- New Orleans Geological Society Top of Salt Map and Well Locations (1960)
- Union Texas Petroleum Well Locations (1977)

Information obtained from these maps included original well surface locations and directional drilling info. This information was compared with SONRIS digital data and conflicts were resolved in favor of the original operators' historical information.

In an effort to improve upon the existing 2014 vintage salt dome contour mapping, an additional integrated geologic and geophysical (G&G) evaluation is underway (at the time of this report) which will incorporate 3D seismic data licensed over the Sulphur Mines storage facility and surrounding area. The evaluation will utilize the following data and process:

- Additional review of wellbore penetration to provide geologic control.
- Extensive research regarding wellbore locations (surface / bottom hole) and directional surveys.
- Confirmation of current sonar surveys of all salt caverns within the dome.
- 3D surface seismic data – licensed from SEI.
- Local velocity surveys.
- Synthetic seismograms generated from nearby sonic logs.
- Utilization of the 2004 VSP data provided by Liberty Gas Storage, LLC, with incorporation of a reprocessing effort of that data.
- An integrated interpretation of the 3D seismic data which honors well control (formation tops).
- Initial seismic interpretation will utilize commercially available PSTM data (Pre-Stack Time Migration).
- Final interpretation of 3D seismic will be after reprocessing thru PSDM (Pre-Stack Depth Migration).

Approximately 400 wells will be included in this integrated G&G interpretation. Extensive historical research of both surface locations and bottom hole locations for wellbores have historically been conducted, and further research will be conducted when utilizing the formation top information of these well penetrations. This effort will include the most recent information from publicly available well information sources such as SONRIS, IHS, Enervus, TGS.

Sonar information that has been archived since 2007 will also be utilized. In some cases, sonar records dating back to 1973 are available and will be utilized where appropriate to reflect cavern void that has subsequently been filled by insolubles. The sonar surveys will be visualized utilizing CAD software in order to present the vertical and horizontal relationship between caverns, geologic formations (including salt dome flank) and nearby well control.

Five square miles of 3D seismic data was licensed. It is a data set comprised of two separate 3D surveys, Houston River and Sulphur surveys, that have been merged and processed together as one. The Houston River 3D was acquired in 2009 with 110' by 110' bins. And the Sulphur 3D survey was acquired in 1998 and also has 110' by 110' bins. The data is of overall good quality. The acquisition parameters utilized to acquire the data contains sufficient far offset data and shot/receiver spacing to undertake this study. Nearby velocity surveys will be incorporated into the study to establish the time to depth relationship necessary to produce integrated G&G maps. Additionally, local sonic logs will be utilized to generate synthetic seismograms to further validate the time to depth relationship. Ultimately, a comprehensive velocity model will be generated for the area covered by the licensed 3D data. This velocity model will be used for mapping purposes and for the planned reprocessing through PSDM.

Initial mapping will utilize the PSTM versions of the 3D seismic provided by SEI. The PSTM interpretation will honor the local well control and synthetic seismograms. The subsequent PSDM also will be processed to honor local well depths via a velocity model calibrated to the local well. Our expectation is that the resulting PSDM will yield the "highest" resolution for the given seismic data, and as importantly, will more accurately locate the position and dip of the salt dome flank and adjacent formations.

Final deliverables for this integrated study will be:

- Depth calibrated Top of Salt Map.
- Depth calibrated maps for at least two additional horizons adjacent to the salt face.
- Map representing best estimates for cavern distances to salt face (edge of salt) will be integrated into this study, particularly on the western flank of the dome study area.
- In addition to historical research of well information, a surface survey will be conducted to verify existing wellhead GPS locations for wells that are known to traverse the western flank of the dome or penetrate the top of salt on the western portion of the Sulphur Mines dome.

10.2.2 Vertical Seismic Profile

A single-offset vertical Seismic profile (VSP) recorded in the Sulphur Mines Fee #1016 well in 2004 will be reprocessed. The purpose of the reprocessing will be to improve mapping of the southwest flank of the salt dome between 2000' and 4500' depth (as this is the location on the salt dome where the data is focused) and to gain a better understanding of salt flank sediment velocities at that

depth. Both the position of the salt edge and the refinement of velocities will be of assistance to the reprocessing of the 3D surface seismic survey.

VSP processing technology has made significant advances in the past two decades, even for the relatively simple recording geometry that was used in the 2004 effort. Please see Figure 55 below. One-way transit arrivals were recorded in the deviated borehole for 58 levels from about 500’ down to about 5000’ depth. The source was a Vibroseis truck offset about 1250’ to the north-northeast. The data will provide salt proximity exit points on the southwest flank of the dome in the area shown in green. For reference, the surface well pad for Cavern No. 007 is located to the North/Northwest of the annotated source location below.

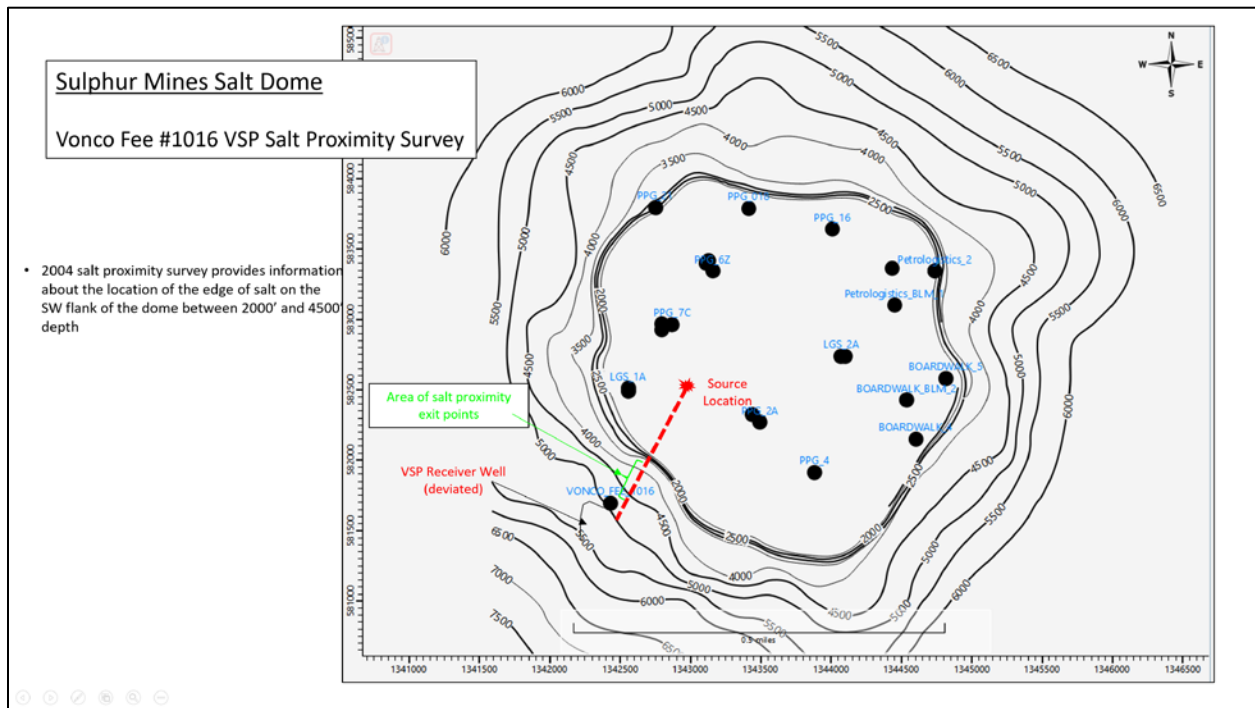


Figure 55 – Sulphur Mines Fee #1016 VSP Salt Proximity Survey

10.2.3 Magnetometer Survey

A magnetometer survey will be conducted via drone and boots-on-the-ground surveying to detect abandoned wellbores below ground level. This survey will be conducted to confirm placement of wellbores in the sub-surface, as some of them are utilized for dome flank positioning, and this data will be integrated into the 3D seismic evaluation.

10.2.4 Geomechanics Modeling

A reputable geomechanics lab and engineering company is performing a geomechanical evaluation of hypothetical low-pressure conditions in Cavern No.006 (via wellbore 6X) and Cavern No. 007 (via wellbore 7B) to determine if the caverns will become unstable, assuming various pressure

stabilization conditions. Additionally, the proposed study will evaluate the impact of low-pressure conditions in Caverns 6 and 7 on the surrounding caverns in the salt dome.

The geomechanical evaluation is being conducted in a phased approach. The situation involving a solution-mined cavern near the edge of a salt dome encompasses many different geomechanical phenomena that have complex inter-relationships. The proposed study will initially develop a three-dimensional (3D) numerical model using the currently available information and historically employed modeling techniques to provide a baseline for the geomechanical response of the caverns under hypothetical low-pressure conditions. The baseline modeling effort will inform the development of any additional modeling scenarios that may provide further insight into potential risks associated with low-pressure conditions in the caverns, such as the deformation and strength characteristics of the non-salt formations next to the salt dome, the presence of a depleted reservoir next to the salt dome, the presence of a caprock sheath along the flank of the salt dome, or the effects of a theoretical coalesce of Cavern 6 and 7. These additional scenarios, among other, will be considered and scoped based on the findings of the initial modeling effort.

10.2.4.1 Background

The fluid pressure in a solution-mined cavern helps support the geologic loads that act on the rock surrounding and overlying the cavern. As the cavern pressure decreases, the loads that must be supported by the surrounding rock increase. If the loads exceed the rock strength, the rock will fail and lose strength. Unlike brittle rock types that fail suddenly, rock salt around a solution-mined cavern will typically begin to fail through micro-fracturing along the grain boundaries, which is a process referred to as dilation (or damage). If dilatant states of stress are maintained, the micro-fractures will increase and coalesce, which, in turn, reduces the strength of the salt. Salt damage is a progressive process that can lead to the salt spalling from the roof and walls of the cavern and may lead to salt-web failure or roof collapse. It is desirable to design and operate salt caverns in a manner that precludes the onset of salt dilation to maintain cavern stability.

The cavern and salt-web stability between caverns and between the caverns and the edge-of-salt (i.e., dome flank) is a function of web thickness, web height, and cavern fluid pressures. If the web thickness is small and the cavern pressure is too low, the shear stresses in the salt surrounding the caverns can exceed the strength of the salt. The stability of the caverns and the salt webs will be evaluated by post-analyzing the model-predicted stress states to determine factor-of-safety values with respect to salt dilation using dilation criterion. The dilation criterion parameter values previously developed for the Sulphur Mines salt dome will be used in this study.

10.2.4.2 Methodology

A 3D numerical analysis will be conducted to simulate and analyze the hypothetical pressure-reduction scenarios. The proposed numerical analysis will include the representation of the salt dome, caverns within the salt dome, overlying caprock and overburden, and surrounding sedimentary basin. The most recent sonar surveys and well gyroscopic surveys for all caverns in the dome will be used to develop the geomechanical model. The pressure histories for Caverns 6 and 7,

measured brine injection flows for Caverns 6 and 7, and any relevant geological data will also be required to complete this study. It is planned for the mechanical properties of the salt to be based on laboratory testing of salt core recovered from Well No. 22, similar to a previous geomechanical study conducted in 2017. Laboratory testing on salt core recovered from Boardwalk Well No. 4 and No. 5 was previously conducted, however, are further away from Cavern 7 than Well No. 22. If permission is obtained to use the Boardwalk data for this study, the test data from Boardwalk Well No. 4 and No. 5 may be reviewed for comparison to the Well No. 22 data. However, because Well No. 22 is closer to Cavern 7, the test data from Well No. 22 salt core may be more appropriate for defining mechanical properties of the salt for the purposes of this study.

A 3D finite difference model will be developed of the Eagle Caverns 6 and 7, and the surrounding caverns. The model will include representation of the entire salt dome boundary, the caprock and overburden, and a simplified representation of the sedimentary basin surrounding the salt dome. Generally, low-pressure conditions in a cavern create a stress perturbation in the surrounding salt, but the spatial influence is typically limited to two or three cavern diameters away from the cavern. Caverns that are sufficiently distant from Caverns 6 and 7 will likely not see any impact from low-pressure conditions in Caverns 6 and 7; therefore, the proposed numerical modeling will be focused on evaluating the effects of low-pressure conditions in Caverns 6 and 7 and the surrounding nearby caverns. The nearby caverns that may potentially see effects from the low-pressure conditions include Sulphur Mines Storage No. A-1, PPG No. 16, the gallery of PPG No. 2, PPG No. 4, and PPG No. 5, Liberty Gas Storage No. 1 and No. 2, Vista No. 1-A, and PPG No. 20. The remaining caverns in the dome will be roughly approximated in the 3D model to capture the general influence of those caverns on the overall stress distribution in the salt dome. The baseline 3D modeling effort will be used to determine if any of the more distant caverns require a more thorough evaluation regarding the low-pressure conditions in Caverns 6 and 7.

The most recent dome contours, cavern sonar surveys, and gyroscopic surveys will be used to fully define the 3D model for this study. The 3D model will be used to estimate the in-situ stress conditions in the salt dome and the surrounding sedimentary basin to initialize the stress state in the model prior to any cavern development. The model will then be used to simulate the historical development and operations of the existing caverns in the salt dome that are included in the model, up until the recent pressure loss event in Cavern 7. The pressure histories and brine flow data from Caverns 6 and 7 will be used to approximate the cavern pressure conditions in Caverns 6 and 7 up to present day to estimate the stress state in the surrounding salt stock in March 2023. The model-predicted stress state in the salt surrounding Caverns 6 and 7 at present day will be analyzed to determine factors of safety with respect to salt dilation to establish a baseline condition of cavern and salt web stability prior to simulating the hypothetical pressure-reduction scenarios. The 3D model will be used to simulate the steady-state creep response of the caverns to gradual pressure reductions. Because the modeling will not account for the transient creep response typically seen during dynamic pressure changes, the model-predicted stresses will not be representative of short-term pressure-reduction conditions. The model will be used to evaluate three hypothetical pressure-reduction scenarios with Cavern 7 at a brine pressure gradient of 0.52 pounds per square

inch per foot (psi/ft) of depth at the casing shoe depth and two other pressure gradients. The pressure histories for Caverns 6 and 7 will be used to estimate correlated pressure reductions in Cavern 6X. The model-predicted stress states with the caverns at the hypothetical reduced pressures will be analyzed to predict dilation factors of safety in the salt surrounding the caverns. The modeling results will provide a comparative analysis of the stress state in the salt webs before and after the cavern pressures are reduced, which can be used to evaluate the potential impact of the low-pressure conditions on cavern stability.

Because of the limited data available for the dome flank and the non-salt rock immediately adjacent to the salt dome, the deformation and strength properties of the non-salt rock and the interface with the salt dome cannot be well defined in the numerical model. The proposed baseline 3D modeling approach will assume that the salt is perfectly bonded to the adjacent non-salt rock formations along the dome flank. This modeling approach has been used historically for evaluating many salt cavern facilities within salt domes in the Gulf Coast region. This modeling assumption may represent artificially higher stiffness and strength for the salt webs between the caverns and the dome flank, which may result in less conservative predictions regarding the stability of the salt webs. Additionally, the leak path from Cavern 7 is undefined, and the model will not represent the presence of a physical void through the salt webs, which may not be a conservative structural representation of the salt webs. Therefore, the proposed analysis will primarily provide a comparative evaluation of the change in stresses at the caverns' surfaces as a result of the cavern pressure being reduced to the hypothetical steady-state conditions.

Additional modeling scenarios may be developed to investigate the assumptions and methods employed in the baseline modeling effort, such as the deformation and strength characteristics of the non-salt formations next to the salt dome, the presence of a depleted reservoir next to the salt dome, the presence of a caprock sheath along the flank of the salt dome, or the effects of a theoretical coalesce of Cavern 6 and 7. These additional scenarios will be scoped based on the findings of the initial modeling effort.

10.2.4.3 Reporting

At the conclusion of the study, a comprehensive technical presentation will be developed that describes the technical approach, assumptions, numerical model, modeling results, and conclusions.

11 Theoretical Failure Mechanisms & Associated Impacts

The following section provides an outline of possible or theoretical failure mechanisms and associated impacts related to Cavern No. 007 and Cavern No. 006 based upon the current geologic, operational, and monitoring knowledge of the caverns and surrounding environment. This discussion is also based upon research completed on cavern integrity failure incidents that have occurred, and with certain examples outlined in *Section 0* of this report. Evaluation and monitoring efforts are ongoing and which may produce a future understanding of a leading cause, failure mechanism, and/or associated impact that is not included within this discussion.

11.1 Continued Loss of Brine to Adjacent Formation

This theoretical mechanism involves continuous brine migration from the current Cavern 7 geometrical space, through a conduit, and into an adjacent formation(s) to the salt dome. The conduit for brine migration is assumed to maintain its integrity, meaning the salt pillar between the dome flank and the cavern would maintain structural integrity, and would have physical characteristics likely of a mixture of salt, sand, anhydrite, and other rock that would allow for a permeability characteristic. It would be presumed that the performance of the conduit is like that of a porous/permeable formation, in that the flow rate capability of the conduit is driven by the pressure differential across it (i.e. Darcy's law). Therefore, in theory, the flow rate through the conduit could be reduced or stopped by achieving a pressure equilibrium between the cavern and the adjacent formation. This failure mechanism is analogous to that of the LOOP 14 integrity failure discussed previously.

11.1.1 Geomechanical Stresses

The fluid pressure in a solution-mined cavern helps support the geologic loads that act on the rock surrounding and overlying the cavern. As the cavern pressure decreases, the loads that must be supported by the surrounding rock increase. If the loads exceed the rock strength, the rock will fail and lose strength. Unlike brittle rock types that fail suddenly, rock salt around a solution-mined cavern will typically begin to fail through micro-fracturing along the grain boundaries, which is a process referred to as dilation (or damage). If dilatant states of stress are maintained, the microfractures will increase and coalesce, which, in turn, reduces the strength of the salt. Salt damage is a progressive process that can lead to the salt spalling from the roof and walls of the cavern and may lead to salt-web failure or roof collapse. It is desirable to design and operate salt caverns in a manner that precludes the onset of salt dilation to maintain cavern stability.

Numerical modeling can be used to predict the stress state surrounding solution mined caverns to assess the potential for salt damage and evaluate the structural stability of the caverns. Currently under development is a three-dimensional numerical model of the Sulphur Mines caverns and salt dome to evaluate the structural effects if low-pressure conditions were to exist in Cavern 6 and 7. The model-predicted stresses will be analyzed to determine the potential for damage to initiate in the salt surrounding the caverns.

As stated previously, this impact and theory is still undergoing evaluation, and as such could produce a future understanding of a failure mechanism and/or associated affect that is not included within this discussion.

11.1.2 Adjacent Mineral Production Impacted

In the event that brine loss continues to migrate into a permeable formation (below the lowermost USDW) adjacent to the salt dome flank, associated oil and gas production could be impacted. The known permeable and stratified formation adjacent to the salt dome is various zones of the Miocene group. The brine influx could displace hydrocarbons currently in place and could impact oil/gas production performance of the formation.

An estimation of this impact is not yet understood, however, theoretically the brine influx into an adjacent permeable zone would tend to flow downwards and away from the salt dome due to the structural dip of the stratified formations immediately adjacent to the salt dome, and due to fluid density drift effects (the density of the saturated cavern brine is higher than that of the native formation fluids). Additionally, based upon the general knowledge regarding the extent and characteristics of the porous/permeable formations adjacent to the dome in this area, formation pressure increase due to the brine influx is unlikely. However, pressure increase of a productive formation could occur if there was a geologic boundary, and therefore would likely improve the production performance of any oil and gas wellbores completed into that formation.

As stated previously, this impact and theory is still undergoing evaluation, and as such could produce a future understanding of a failure mechanism and/or associated affect that is not included within this discussion.

11.1.3 Impact to USDW

With the described theory of this section in mind, theoretically any brine influx into an adjacent permeable zone would tend to flow downwards and away from the salt dome due to the structural dip of the adjacent stratified formations and due to fluid density drift effects (the density of the saturated cavern brine is higher than that of the native formation fluids). Additionally, based upon the general knowledge of the porous/permeable formations adjacent to the dome in this area, formation pressure increase due to the brine influx is unlikely. Therefore, based upon reservoir characteristics and accepted hydrostatic pressure calculations, it is unlikely to have the drive pressure required to move cavern brine up hole through an ancillary conduit (geologic feature or wellbore) and into the USDW. Given this theoretical failure mechanism, affects, and conditional understanding it is unlikely that the USDW would be impacted or contaminated with cavern brine.

As stated previously, this impact and theory is still undergoing evaluation, and as such could produce a future understanding of a failure mechanism and/or associated affect that is not included within this discussion.

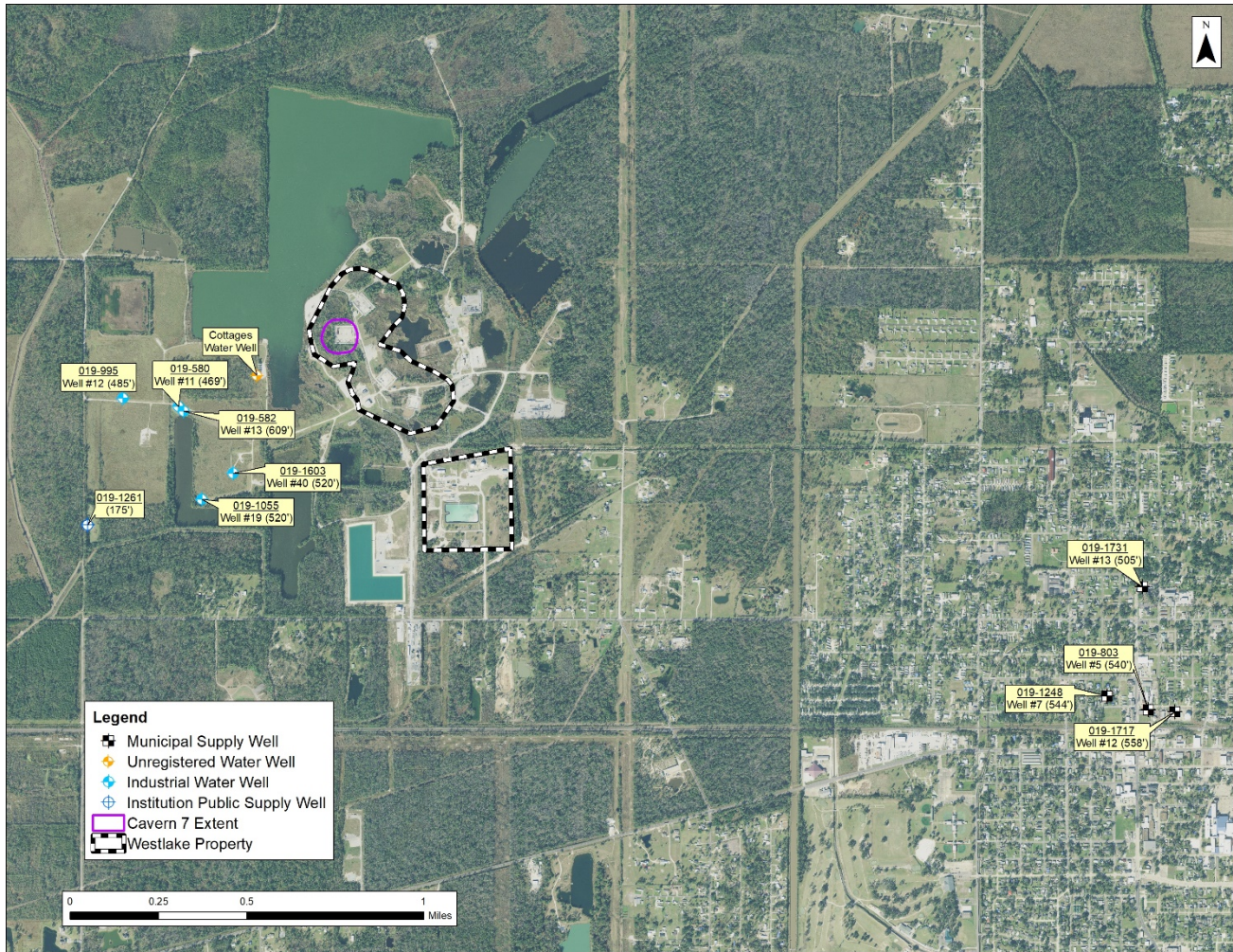


Figure 56 – Known Active Water Well Locations Adjacent to PPG Cavern No. 007

11.2 Cavern Coalescence

When two adjacent salt caverns develop a hydraulic connection through a physical void in the salt web separating the caverns, the resulting salt web may be structurally compromised. The potential near-term impacts on the stability of the salt web depend on the location, size, and shape of the physical void that has developed through the salt web. Typically, if the caverns remain in storage service, they will be operated as a gallery to minimize the pressure differences and fluid transfer between the caverns, to minimize further deterioration of the salt web. If the physical void through the salt web continues to grow, the web will generally become less stable, leading to salt sloughing from the walls of the caverns. As the salt web thins, the potential for progressive salt web failure increases. As the salt web loses load-bearing capacity, the overburden load in the salt web will be redistributed to the remaining salt stock surrounding the caverns. The combined roof span of the coalesced cavern gallery will be substantially increased, which increases the overburden load that must be supported by the roof salt. Very large roof spans can result in high stresses in the roof salt, which can lead to roof falls in the caverns. Roof falls in the cavern will reduce the distance between

the roof and the casing seat, resulting in increased straining of the cemented casing caused by salt creep closure, which can lead to casing failure.

Typically, the coalescence of two salt caverns is a gradual process that can be detected by monitoring of cavern operating conditions. Sonar surveys are generally obtainable and sometimes help characterize the location and extent of the web deterioration over time. These data can be used to develop numerical models for predicting the resulting stress redistribution around the caverns. The model-predicted stresses can then be analyzed to assess the structural stability of the coalesced cavern gallery and predict the potential for cavern instability or casing failure through extensile strain caused by salt creep in the cavern roof.

Caverns 6 and 7 are known to have a small web thickness (approximately 29.4 feet). Based upon the available pressure data and domal salt cavern principles, it is theorized that brine is also migrating away from Cavern 6. A likely theory is that the leak mechanism is via an indefinite, permeable pathway directly into Cavern 7. This pathway may be correlated with the known small web thickness region separating the two caverns. It is theorized that the brine flow rate from Cavern 6 would be dependent on the natural maintenance of an equilibrium pressure relationship with Cavern 7. If the equilibrium condition is satisfied between the caverns it is theorized further that the leak rate from Cavern 6 would be directly proportional to the salt creep closure rate. This same theory could be applicable to Cavern 7 if an equilibrium pressure with the adjacent formation(s) were to be achieved. In this case, Cavern 6 and 7 could be defined as a gallery, and with respect to minimizing salt stresses should be maintained at similar pressures. The most appropriate magnitude for the gallery pressure would need to be determined through geomechanical modeling, however, to achieve a nominal brine migration rate away from the gallery solely due to salt creep closure affects via a Cavern 7 wall conduit to an adjacent formation, the gallery pressure would need to be equalized with the adjacent formation.

As stated previously, this impact and theory is still undergoing evaluation, and as such could produce a future understanding of a failure mechanism and/or associated affect that is not included within this discussion.

11.3 Cavern-To-Flank Pillar Failure with Associated Surface Expression

This theoretical mechanism involves the failure of the salt pillar between the dome flank and a cavern, which would cause the collapse of the pillar into the cavern void space. In continuation of the theory, this would produce the continued collapse of adjacent and shallower formations ultimately leading to the subsidence of the ground surface.

11.3.1 Geomechanical Stresses

Analyzing the potential effects of a cavern collapse near the salt dome flank can be very challenging because of the limited ability to characterize the extent of the collapse and the immediate impact on the surrounding rock mass. Numerical modeling can be used to estimate potential impacts of a

cavern failure. Obtaining downhole pressure data and estimates of the failure extent can aid in the development of modeling scenarios to evaluate. Methods to history match the salt web failure using numerical models can aid in estimating the in-situ strength of the salt. The estimated in situ salt strength can then be used in assessing the remaining salt webs and caverns surrounding the failed cavern. However, salt domes can have anomalous zones within the salt stock that exhibit different strength characteristics that may not be representative of the salt strength in other areas of the dome. Particularly near the salt dome flank, there may be regions of dirty salt that may exhibit considerable heterogeneity in its deformation and strength characteristics. An additional variable can be the presence of abnormal pressures within the stratified formations adjacent to the salt dome flank. If the oil and gas bearing formations adjacent to a salt dome have been heavily produced, there may be an under-pressured condition within those formations in comparison to the native/discovery pressure of the formations.

When a cavern is in close proximity to the salt dome flank, the thin salt web can develop elevated shear stresses that can cause micro-fracturing (damage) in the salt. If damaging states of stress are maintained in the salt web, the salt will progressively lose strength and begin sloughing from the cavern wall. This process can potentially lead to salt web collapse. If salt web failure occurs at the flank of the salt dome, the non-salt rock units outside of the salt dome may also experience failure, which can lead to progressive failure of the overlying units. This type of failure has the potential to migrate upwards in depth and present at the surface as a sinkhole.

The catastrophic failure of a salt cavern near the edge of the salt dome may lead to the cavern being partially backfilled with various rock types, and ground water. This backfilling of material may result in abnormal pressure conditions that may fluctuate over time, until a steady-state condition is reached in the cavern. If fresh water is able to enter the salt cavern, some dissolution of the salt walls will occur, increasing the size of the cavern and reducing the salt webs thickness between any adjacent caverns. Additionally, the failure of a salt web at the edge of the dome will redistribute the overburden load onto the remaining salt surrounding the cavern, increasing the vertical load on the salt webs between adjacent caverns. These conditions can potentially lead to reduced web stability between the failed cavern and neighboring caverns.

As stated previously, this impact and theory is still undergoing evaluation, and as such could produce a future understanding of a failure mechanism and/or associated affect that is not included within this discussion.

11.3.2 Adjacent Mineral Production Impacted

In consideration of this theoretical failure mechanism, a channel of disturbed rock is created from surface down to the depth of the salt pillar collapse. The geometric extent of this sub-surface channel could directly impact oil and gas production in a number of ways.

As stated previously, this impact and theory is still undergoing evaluation, and as such could produce a future understanding of a failure mechanism and/or associated affect that is not included within this discussion.

11.3.3 Impact to USDW

As stated previously, this impact and theory is still undergoing evaluation, and as such could produce a future understanding of a failure mechanism and/or associated affect that is not included within this discussion.

11.3.4 Offset Wellbore Damage / Blowout

In consideration of this theoretical failure mechanism, a channel of disturbed rock is created from surface down to the depth of the salt pillar collapse. The geometric extent of this sub-surface channel could directly impact offset wellbores. The shifted rock could physically damage wellbore casings and could lead to blowouts expressed at surface or underground.

As stated previously, this impact and theory is still undergoing evaluation, and as such could produce a future understanding of a failure mechanism and/or associated affect that is not included within this discussion.

11.3.5 Surface Environmental Impact

As understood and observed from other analogous cavern/salt structure collapses, typically the resultant surface expression is a pond/lake filled with salty water. Figure 57 illustrates a couple examples of surface expressions due to a cavern/salt structure collapse. In addition to the physical effects caused by the sub-surface formation collapses and the surface subsidence expression, the event can cause the release of brine, liquid hydrocarbons, and/or natural gas to the surface.

As stated previously, this impact and theory is still undergoing evaluation, and as such could produce a future understanding of a failure mechanism and/or associated affect that is not included within this discussion.

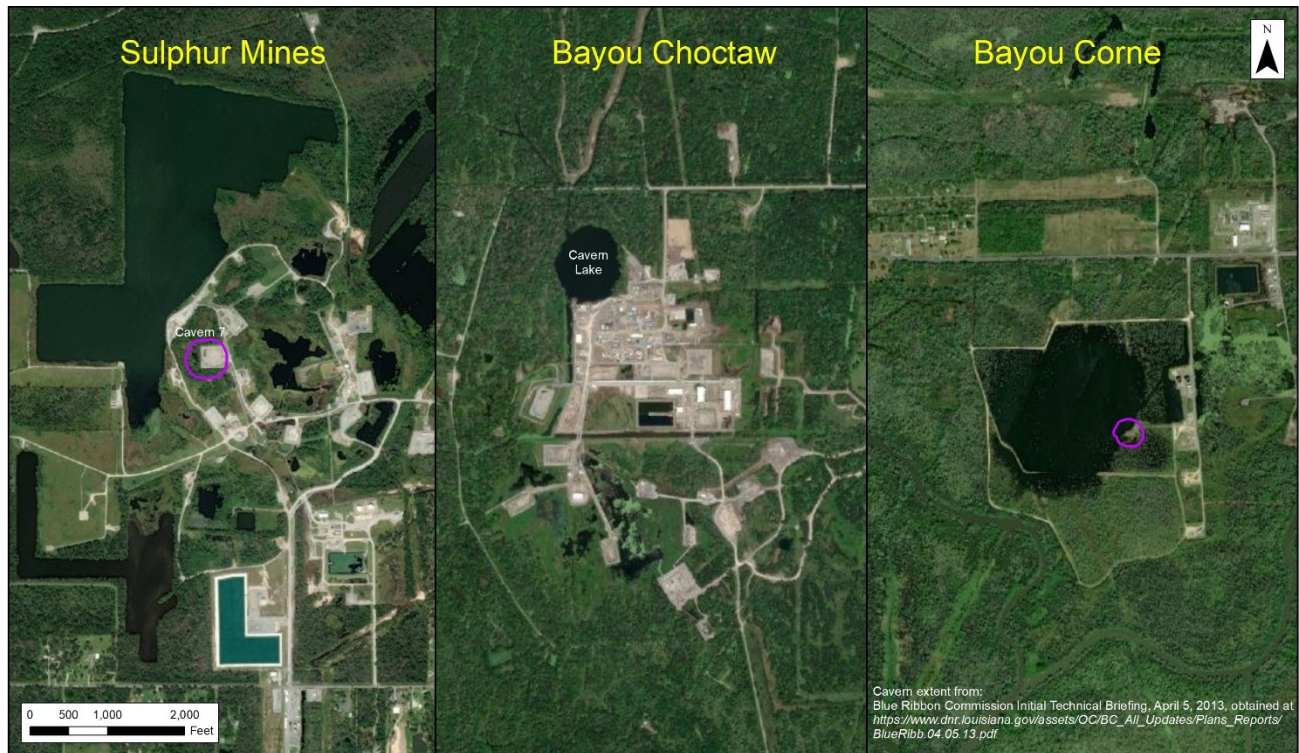


Figure 57 – Example of Cavern Collapse Surface Features

11.3.6 Surface Expression Impact Zone Estimate

Analysis was performed to estimate the size and location of a potential subsidence zone if a cavern-to-flank pillar failure of Cavern 7 were to occur. The sinkhole associated with the collapse of the Oxy 3 cavern at the Napoleonville Dome was analyzed for reference. A major structural failure occurred at Oxy 3 in 2012. This resulted in a transfer of underground material into the cavern and the development of a sinkhole at the surface. A three-dimensional model was created for Oxy 3 which includes salt dome contours, original cavern geometry, and the location and shape of the sinkhole. The analysis of Oxy 3 revealed that the epicenter of the sinkhole formed almost directly above the edge of the salt dome at the point nearest to the cavern. This indicated that disturbed material traveled vertically along the outside edge of the salt dome, originating at the point where the flank is closest to the cavern. The sinkhole initially formed in a funnel shape. As material settled, it became flatter with a larger radius and more shallow center. The cavern geometry, edge of salt, and initial and final sinkhole shapes are shown in Figure 58 and Figure 59 below.

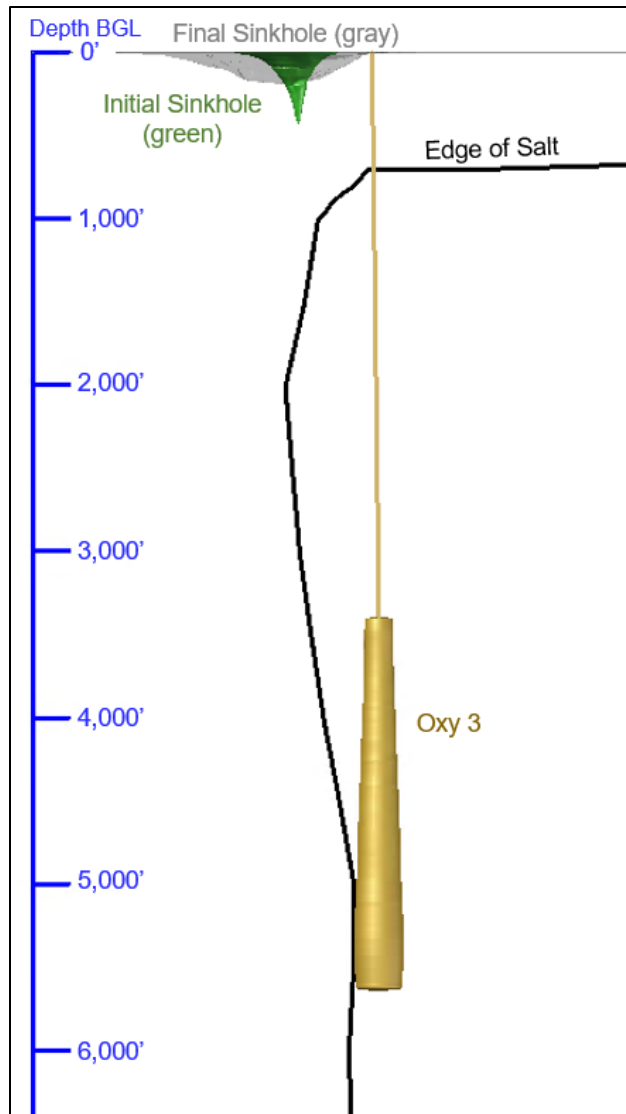


Figure 58 – Side View of Oxy 3

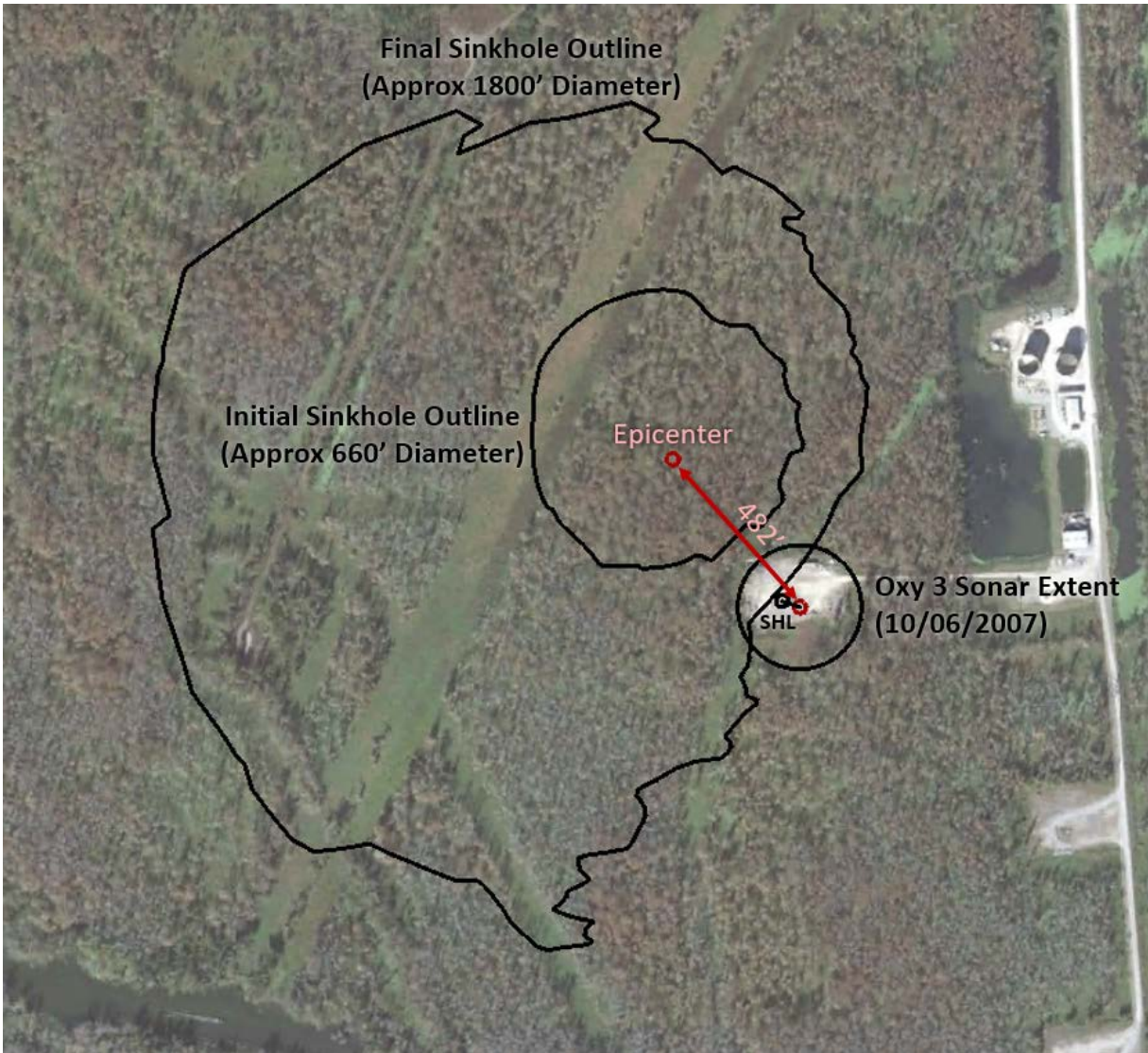


Figure 59 – Top View of Oxy 3

In the same manner as Oxy 3, a 3-D model for Cavern 7 including cavern geometry and salt dome contours was developed. The observations of the Napoleonville event were applied to Cavern 7 to estimate the potential epicenter for subsidence should a similar collapse event occur. Additionally, the diameter of the impact zone was estimated for Cavern 7 through comparison to Oxy 3. It was assumed that the subsidence volume would be proportional to the volume of the associated cavern. This was done for both the initial and final subsidence shapes. The estimated location and areal extent of the impact zones can be seen below in Figure 60 and Figure 61.

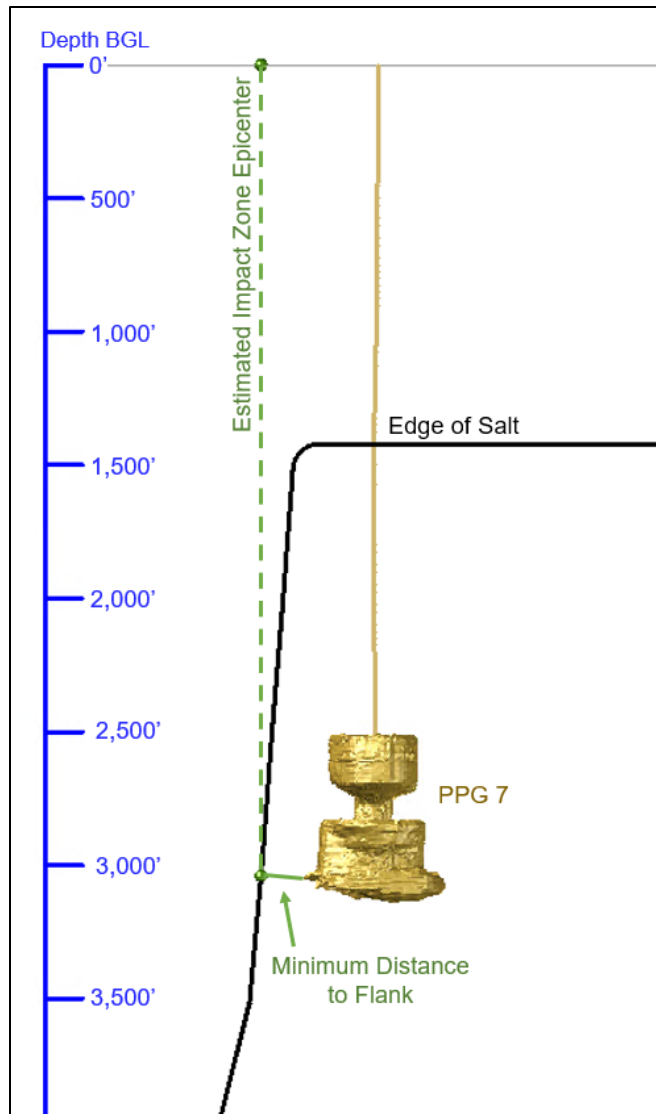


Figure 60 – Side View of Cavern 7

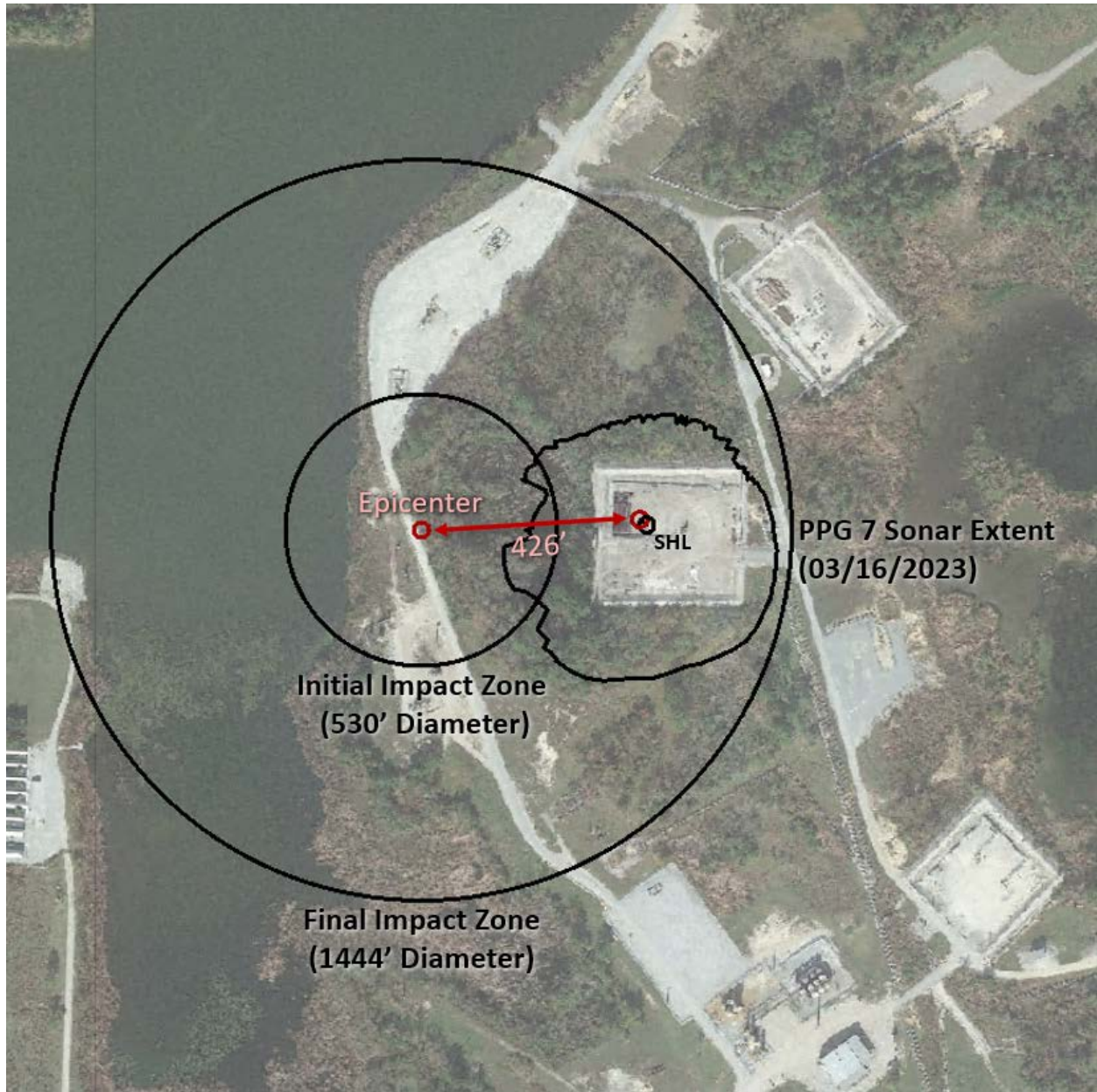


Figure 61 – Top View of Cavern 7 w/ Theoretical Sink Hole Projection

12 Concluding Remarks

The format and contents of this failure analysis report were a novel development and document the history of the Sulphur Mines Salt Dome, Cavern No. 007 and Cavern No. 006, the acute and ongoing pressure loss/integrity failure of those Caverns, the monitoring/evaluation efforts implemented and ongoing, and an assessment of theoretical failure mechanisms that may explain the integrity failure. The primary points that can be established at this time are:

- Cavern No. 007 brine is leaving the known cavern geometry and the point of efflux is not precisely known; however, it is most likely entering a adjacent formation to the salt dome.

Estimated total brine loss from September 1, 2021 through March 23, 2023 was calculated to be 793,046 barrels (inclusive of Cavern No. 006 loss of 63, 449 barrels).

- Cavern No. 006 brine is leaving the known cavern geometry, albeit at a comparably slower rate than Cavern No. 007. The point of efflux is not precisely known; however, it is likely solely flowing into Cavern No. 007 at the known area of minimum web thickness between the Caverns. Additionally, Cavern No. 006 has a distinct pressure relationship with Cavern No. 007 and which would be interconnected with the brine efflux rate of Cavern No. 006.
- Multiple “events” were identified from 2021 through 2023 from analysis of the surface instrumentation pressure and flow rate data that indicated the leakage mechanism of Cavern No. 007 has exhibited different leak rates and exhibited signs of being a pressure dependent leak.
- The current interpretation of the minimum spacing from Cavern No. 007 to the dome flank is 165 feet. The current interpretation of the minimum spacing from Cavern No. 006 to the dome flank is 302 feet. The minimum web thickness between Cavern No. 006 and No. 007 is 29.4 feet.
- No other Eagle operated caverns on the Sulphur Mines Dome have observed anomalous, sustained pressure responses.
- No other cavern operators on the Sulphur Mines Dome have reported anomalous pressure responses with their caverns.
- It was informally reported by the offset oil and gas operator (Yellowrock) that at the time of the December 2021 acute pressure loss event on Cavern No. 007 and No. 006 that one of their wells (Fee No. 1012 [Serial No. 209459]) experienced atypical pressure and production responses.
- No micro-seismic events have been detected proximal to Cavern No. 007 or Cavern No. 006 since the installation of the monitoring system.
- No deviation from established surface subsidence trends has been identified since 2016.
- A change in cavern geometry was identified in Cavern No. 007 based upon an evaluation of the May 2018 sonar survey with sonars performed after the December 2021 acute pressure loss event. There have been no observed geometry changes in Cavern No. 007 from all sonars conducted subsequent to the December 2021 acute pressure loss event. Due to the timing of the sonar surveys it cannot be definitely proven if the geometric changes observed between the 2018 and 2022 data sets are connected to the integrity failure. Additionally, the cavern geometry changes identified between the 2018 and 2022 sonars coincide with similar geometric changes that have occurred over many decades and appear to relate to the collapse of an internal geometric feature of the cavern (a “shelf”). The collapse of a shelf over time is generally a common occurrence for caverns, and that alone is very unlikely to lead to an integrity failure. Also, the cavern geometry changes identified between the 2018 and 2022 sonars showed no apparent reduction to the previously established cavern-to-flank spacing.
- No changes in cavern geometry were observed in Cavern No. 006 via sonar survey analysis when comparing pre-2021 to post-2021 data to date.
- No surface thermal expressions have been identified.

In consideration of the above points and data/analysis completed to date, it is believed that the most likely theory for the failure mechanism is that an anomalous geologic feature is providing the conduit for the Cavern No. 007 brine to leave the observable cavern geometry. The brine is most likely entering an adjacent permeable formation and migrating down dip (away from the salt dome) throughout a regionally extensive sandstone formation. The apparent integrity failure of Cavern No. 006 is most likely due to the minimum web thickness with Cavern No. 007 allowing brine communication between the caverns thereby now being defined as a gallery. Due to the integrity failure of Cavern No. 007, Cavern No. 006 is therefore interconnected by this gallery characteristic. This overall theory aligns most similarly with that of the integrity failure discussion for LOOP Cavern No. 14.

The root cause that initiated the conduit for brine to leak from Cavern No. 007 is still under investigation. Additional evaluation and monitoring efforts are ongoing and which may produce a different or additional understanding that is not included within this report.

13 References

Shemeta, J., 2023, Borehole Microseismic Monitoring at Napoleonville Salt Dome, Louisiana: Nine Years of Microseismicity Associated with Brining and Storage Facilities on a Gulf Coast Salt Dome, USA, abstract submitted for the Solution Mining Research Institute Spring 2023 Technical Conference, to be presented at Detroit, Michigan 23-26 April 2023.

Geomechanical Evaluation of Natural Gas Storage in Starks No. 1, Starks Salt Dome, Louisiana p.3

Stout, S.A. and Wang, Z. (2016) Standard Handbook Oil Spill Environmental Forensics: Fingerprinting and Source Identification. Acad. Press, Cambridge, MA, 1107 p.

Stout, S.A. (2023) Full report – Chemical fingerprinting of oils, Westlake Sulphur Dome Study. NewFields letter report dated March 10, 2023.

Proposed Limited Oil Storage in LOOP Cavern 14, Submitted by LOOP LLC to Louisiana Department of Natural Resources Office of Conservation Injection and Mining Division, March, 2000

McCauley, T.V.; Ratigan, J.L.; Sydansk, R. D.; and Wilson, S. D. (1998) Characterization of the Brine Loss Zone and Development of a Polymer Gel Plugging Agent to Repair Louisiana Offshore Oil Port (LOOP) Cavern 14

Lolan, W. E.; Valadie, R. J.; and Ballou, P. J. (1998) Remote Operated Vehicle (ROV) Design, Cavern Survey and Gel Plugging Agent Application to Repair Louisiana Offshore Oil Port (LOOP) Cavern 14.

Neal, J. T.; Todd, J. L.; Linn, J. K.; and Magorian, T. R. (1993) Threat of a Sinkhole: A Reevaluation of Cavern 4, Bayou Choctaw Salt Dome, Louisiana.

Brouard Benoit, (2016) In-Situ Mechanical Tests in Salt Caverns, SMRI Spring Technical Class “Elements of Rock Mechanics Related to Salt Caverns”, 24 April, 2016, Galveston, Texas

Shircliff, C.; Ashour, M.; Benoit, A.; and Dunn, C.; (2013) Infamous Salt Failures in Louisiana and Subsequent Impacts on the Regulatory Environment, SMRI Spring 2019 Technical Conference, 8-9 April 2013, New Orleans, Louisiana

Whiting, G. H., editor (1981) Strategic Petroleum Reserve (SPR) Geological Site Characterization Report Sulphur Mines Salt Dome, SAND80-7141, printed March, 1981

Beasley, R. R.; (1982) Strategic Petroleum Reserve (SPR) Oil Storage Cavern Sulphur Mines 7 Certification Tests and Analysis, SAND81-2069, May, 1982

Beasley, R. R.; (1982) Strategic Petroleum Reserve (SPR) Oil Storage Cavern Sulphur Mines 6 Certification Tests and Analysis, SAND81-2068, April, 1982

Sulphur Mines Underground Storage Facility Description (1989) DOE/FE-0136, July, 1989

Strategic Petroleum Reserve Sulphur Mines Decommissioning and Big Hills Expansion (1990), DOE/EA-0401, January, 1990